

PENINSULA TECHNIKON



Faculty of Engineering

MECHANICAL ENGINEERING DEPARTMENT

**Laser Cladding Surface Treatment
For Enhancement of Mechanical Properties**

Wen Fu Yang

BSc. (Eng.) (Taiyuan University of Technology, China)

**A Thesis Submitted Towards the Degree of
Master of Technology (M Tech)**

**Supervisor: Prof. Dr. Graeme. John. Oliver,
MSc. (University of Cape Town), PhD (IFTR Warsaw)**

Cape Town, 2003

Acknowledgements

I would like to thank my supervisor and the father of research at Peninsula Technikon, Prof. Dr. Graeme. John. Oliver, for patiently providing me with invaluable advice and insight during the course of this work, noteworthy assistance with the Finite Element Method for calculating the surface temperature distribution, without his constant assistant and encouragement, it is improbable that this work would have been completed.

I would like also to express my gratitude to Professor Qin Jianping, from Taiyuan Heavy Machinery Institute, China, for his comments and suggestions. I express my sincere appreciation to Professor Brian Figaji, Vice Chancellor of Peninsula Technikon, Dr. Oswald Franks, the dean of the Faculty Engineering, Mr. Keith Jacobs, Head of Mechanical Engineering Department, all for their friendly advice and encouragement.

I would like also to express my gratitude to South Africa National Laser Center, for her funding financial support us finish laser-cladding research experiments in CSIR (Council for Scientific and Industrial Research), Pretoria.

I would also like to acknowledge useful discussions with the experts of the staffs in South Africa National Laser Center (Pretoria). They are Mr. Corné van Rooyen and Mr. Ken Labuschagne for their suggestions and cooperation as well as Mr. Thomas du Plooy, who organized the laser cladding experimental visits for us. And Mr. Jan Koster, who operated the CO₂ laser equipment: Triumph, LASERCELL 1005, who assisted us in performing all the laser cladding experiments other some of the powder injection experiments which was assisted by Mr. Corné van Rooyen.

I would like also to acknowledge the financial support received from the Peninsula Technikon.

In addition, I would like to thank my many colleagues, especially Mrs. Wenhui, who encouraged me.

Dedication

I dedicate this modest work to my father and mother for their untiring and patient support and encouragement of my aspirations, to my brother and sisters, and to my wife Xiaoyan Li and my son Guangyu Yang.

Abstract

Systematic laser cladding experiments were performed using a mixture of a Nickel base alloy powder mixed with tungsten carbide powder (percentage contents of tungsten carbide from 10% to 40%) on EN8 steel substrate with pre-placed powder method. Laser cladding of the Nickel base alloy powder + 50% tungsten carbide powder on EN9 steel substrate was performed with powder injection method as well.

A Finite Element Method for calculating the surface temperature distribution was used to help prediction of temperature distribution laser cladding results. Composition of cladding materials was designed; a sticking agent was chosen for the pre-placed powder method. Clad coatings were obtained for different process parameters for laser cladding, and a detailed study of the affects of these parameters has been carried out.

The characteristic microstructure and properties of the clad layers and interface were investigated by using an optical microscope, a micro hardness tester and a makeshift wear test. A comprehensive review is presented on the dilution of the coating and the typical problems experienced with the coating/substrate interface.

The results show that microstructure of clad layers comprise three zones: the cladding layer, bonding zone and heat-affected zone. The results showed that tungsten carbide particles increased the hardness and wear resistance as expected. Wear resistance of laser cladding coating is 3.5 times than that of substrate. The micro hardness range of the cladding layer is from HV 981.5 to HV 1187, which is 2-3 times than that of substrate. The micro hardness varies from cladding coating to transition layer then to heat affected zone and substrate along a gradient. The gradient distributions of microhardness near bonding interface provides a matching between the coating and substrate, which releases stress concentration, avoids the formation of cracks and realizes better metallurgical bonding between the coating and substrate.

The crack formation mechanism was analyzed. The influences of the laser parameters, the technological process parameters, the substrate state and the cladding material on crack behavior were studied and investigated to try and predict cracking. Effective control and preventive methods for cracks were found. It is pointed out that a reasonable matching of the processing parameters can result in no crack, no gas porosity and clad layer with the desired properties. Metallurgical bonding between the cladding layer and substrate material was realized.

It indicated: The formation of cracks in the clad layer is mainly caused by the thermal

stress created by the high thermal gradient produced during the cooling stage. The crack probability for a multi-pass clad, where several adjacent tracks of laser cladding are applied, is higher than that of single-track cladding.

The study and investigation on the solidification features and formation law of the microstructure for laser cladding layer has been carried out.

It indicated: There are different solidification parameters for different position in the cladding layer. The microstructure at the cladding layer bottom was the typical extension growth on a plane basis. The microstructure at the top and middle was the regular pine-tree eutectic crystal and small cell and column crystal respectively. And the crystalline anisotropy was a main factor to influence the crystal growth form.

There are 48 Figures and 22 Tables in this thesis.

Contents

Acknowledgement	ii
Dedication	iii
Abstract.....	iv
Table of the contents	vi
List of Figures	x
List of Tables.....	xii
List of Symbols.....	xiii
1. Introduction.....	1
1.1 Preface.....	1
1.2 Laser cladding technology.....	3
1.2.1 Fundamental concept of laser cladding technology.....	3
1.2.2 Laser cladding technology process.....	4
1.3 Laser cladding technology characteristics and parameters.....	5
1.3.1 Advantages of laser cladding technology.....	5
1.3.2 Technological parameters of laser cladding.....	5
1.3.3 Three kinds of external appearance of laser cladding layer.....	7
1.3.4 Laser cladding coatings materials.....	8
1.4 Introduction of laser cladding ceramic materials.....	10
1.5 Summarize on application of rare-earth element in laser cladding.....	11
1.6 Laser cladding technology appaiiation and prospect.....	12
1.6.1 Industry application of laser cladding.....	12
1.6.2 Present problems in laser cladding technology.....	15
1.7 Background and research subjects.....	15
1.7.1 Background.....	15
1.7.2 Research objectives and research contents of this thesis.....	16
1.8 Research methods and research route.....	16
1.8.1 Research methods.....	16
1.8.2 Research route.....	17
2. Analysis of laser cladding heat transfer process and mathematical of model laser heat flux.....	18
2.1 Introduction.....	18
2.2 Analyses of heat transfer process of laser cladding.....	19
2.2.1 Heat transfer characteristic of pre-placed powder laser cladding.....	19
2.2.2 Heat transfer characteristic of powder injection laser cladding.....	20

2.3	Surface temperature distribution modeling.....	22
3.	Laser cladding experiments with pre-placed powder method.....	30
3.1	Introduction.....	30
3.2	Composition design of Ni-base alloy cladding materials.....	31
3.3	Selection of sticking agent (chemical binding).....	33
3.4	Substrate material and ceramic material.....	35
3.4.1	Selection of substrate materials.....	35
3.4.2	Select ceramic cladding materials.....	35
3.5	Proportion control of tungsten carbide.....	36
3.6	Parameters of Laser cladding with pre-placed powder method.....	40
3.7	Experiment results analysis.....	40
3.8	Conclusions.....	43
4.	Laser cladding experiments with powder injection method.....	44
4.1	Introduction.....	44
4.2	Powder injection method versus pre-placed powder method.....	45
4.3	Powder injection experiments.....	47
4.3.1	Cladding materials.....	48
4.3.2	Substrate material.....	48
4.3.3	Experiment parameters.....	49
4.4	Experiments results.....	49
4.5	Effect of powder injection angle on clad height and quality.....	50
4.6	Powder particles splash and ricochet phenomenon.....	52
4.7	Crack behavior.....	52
4.8	Conclusions.....	54
5.	Study on cladding shape, microstructure characteristics and formation features of solidification microstructure.....	55
5.1	Introduction.....	55
5.2	Effect of laser parameters variation on clad geometrical dimensions.....	56
5.2.1	Effect of laser scanning speed variation on clad geometrical dimension of laser clad layer.....	57
5.2.2	Effect of laser power variation on geometrical dimension of laser clad layer.....	59
5.2.3	Effect of laser beam diameter variation on geometrical dimension of laser clad layer.....	61
5.3	Microstructure characteristics of laser cladding coating.....	63
5.3.1	Solidification modeling of the inside of coating.....	64
5.3.2	Formation features of solidification microstructure for laser clad layer.....	65
5.3.3	Effect of laser scanning speed variation on microstructure.....	67

5.4	Analysis microstructure features near bonding interface.....	68
5.5	Effect of Rare-earth element on microstructure and wear resister of laser clad layer.....	69
5.6	Conclusions.....	70
6.	Analysis on microhardness distribution and wear resistance of laser cladding coating.....	72
6.1	Introducation.....	72
6.2	Distribution of microhardness in laser cladding coating.....	72
6.2.1	Micro-hardness test experiments.....	72
6.2.2	Micro-hardness test results and analysis.....	73
6.3	Wear resistance property of laser cladding coating.....	76
6.3.1	Wear resistance test experiments.....	76
6.3.2	Wear resistance test results and analysis.....	77
6.4	Analysis on wear resistance.....	79
6.4.1	Wear mechanism analysis.....	79
6.4.2	Effects of micro-hardness distributing on wear resistance property of materials.....	79
6.5	Other methods for enhancement of wear-resistance.....	80
6.6	Conclusions.....	80
7.	Study on the influence factors of laser clad crack behavior.....	82
7.1	Introduction.....	82
7.2	Analysis of crake behavior reasons of metal theory.....	83
7.3	Effect of laser system parameters on laser cladding coating crack.....	86
7.3.1	Effect of laser beam diameter on crack of laser cladding coating.....	86
7.3.2	Effect of laser scanning speed on crack behavior.....	87
7.4	Effect conditions of laser technological treatment on laser cladding layer..	87
7.5	Effect of cladding materials on laser cladding crack.....	90
7.6	Effect of substrate materials condition on laser cladding layer crack.....	91
7.6.1	Effect of substrate materials on crack.....	91
7.6.2	Effect of substrate surface condition on laser cladding crack.....	92
7.6.3	Effect of thermal capacity of substrate on crack.....	92
7.6.4	Effect of shape and structure on laser cladding crack.....	93
7.7	Conclusions.....	94
8.	Conclusions and recommendations.....	95
8.1	Conclusions.....	95
8.2	Recommendations for future work.....	98

References.....	99
Appendices.....	106
1. Literature of Substrate and cladding materials.....	106
2. Performed Pre-placed Powder Experiments Process.....	109
3. Geometrical Properties of single Track Samples.....	113

List of Figures

Figure 1.1 Three kinds of external appearance of laser cladding layer.....	8
Figure 2.1 Heat transfer process of pre-placed powder laser cladding.....	20
Figure 2.2 Heat transfer process of powder injection laser cladding.....	21
Figure 2.3 FE Calculated Temperature 3kW, 0.2mm spot.....	27
Figure 2.4 FE Calculated Temperature 3.5kW, 0.2mm spot.....	28
Figure 2.5 FE Calculated Temperature 4kW, 0.2mm spot.....	29
Figure 3.1 Experimental set up laser cladding for the pre-placed powder method...	31
Figure 3.2 Pre-placed powder sample and laser cladding process.....	35
Figure 3.3 Cross-sections of several overlapping tracks.....	41
Figure 3.4 An illustration of increased dilution by apply several adjacent tracks...	42
Figure 4.1 Laser cladding with Powder injection method.....	45
Figure 4.2 Powder feeder (Left side), and a practical process.....	46
Figure 4.3 A sample performed with powder injection method.....	47
Figure 4.4 Clad heights as function of nozzle degree of powder injection.....	51
Figure 4.5 Higher nozzle angle results in a reduced surface quality.....	51
Figure 4.6 Particles splashed and ricocheted from the substrate.....	52
Figure 4.7 A crack sample (crack occurs in overlap area).....	53
Figure 5.1 Typical cross-sections of single-track clad layers.....	56
Figure 5.2 Pre-placed cladding Sample 10-1, (×50).....	57
Figure 5.3 Pre-placed cladding Sample 10-4, (×50).....	58
Figure 5.4 Clad geometrical dimensions as function of the laser scanning speed...	59
Figure 5.5 Lower power sample 6-4 and Higher power sample 5-2.....	60
Figure 5.6 Clad geometrical dimensions as function of the laser power.....	61
Figure 5.7 Sample12-1 and Sample 12-5.....	62
Figure 5.8 Clad geometrical dimensions as function of the laser beam diameter...	63
Figure 5.9 Low times microstructure characteristic of Laser cladding coating.....	64
Figure 5.10 Top of laser cladding layer (×200).....	66
Figure 5.11 Middle region of cladding layer (×200).....	66
Figure 5.12 Bottom of laser cladding layer (×200).....	66
Figure 5.13 Effect of scanning speed on grain size (×200).....	67
Figure 5.14 High times microstructure characteristic of Bonding Interface.....	69
Figure 5.15 Affect of La ₂ O ₃ on the microstructure of nickel base alloy coating....	70
Figure 6.1 Microhardness tester.....	73

Figure 6.2 Points hitting line.....	73
Figure 6.3 Microhardness distribution of sample 2.1.....	75
Figure 6.4 Microhardness distribution of sample 2.5.....	75
Figure 6.5 Microhardness distribution of sample 3.2.....	76
Figure 6.6 Wear testing machine and Precisa XT220A analytical balance.....	77
Figure 6.7 Wear resistance compare.....	78
Figure 7.1 Some crack samples.....	83
Figure 7.2 Crack samples caused by impurity and gas porosity (50×).....	84
Figure 7.3 Sample12, Beam spot =2.0mm, 2.5mm, 3.0mm (200×).....	87
Figure 7.4 Effects of scanning speed on crack behavior.....	87
Figure 7.5 Effect of laser power on crystal grain size.....	88
Figure 7.6 Effect of Re-melting.....	89
Figure 7.7 Sample 22.....	90
Figure 7.8 Pre-heated and heat preservation sample 21 (50×).....	93
Figure 7.9 Microstructure of Pre-heating and heat preservation sample 24, (500×). 93	

List of Tables

Table 1-1 Laser cladding application.....	15
Table 1-2 Research route.....	17
Table 3-1 Chemical components of Nickel-base alloy for pre-placed method.....	33
Table 3-2 Chemical components of EN8 steel.....	35
Table 3-3 Physical properties of the cladding materials.....	36
Table 3-4 Physical properties of cladding materials and substrate.....	37
Table 3-5 Powder components of comparative experiments.....	38
Table 3-6 Mathematical conversions between weight and volume proportion.....	39
Table 3-7 Expansion coefficient and elastic modulus values.....	39
Table 3-8 Data of Single-track sample 3-4 and Multi-pass sample 21.....	41
Table 4-1 Chemical components of alloy powder for powder injection.....	48
Table 4-2 Physical properties of the cladding materials (Powder injection).....	48
Table 4-3 Chemical compositions of EN9 steel substrate.....	48
Table 4-4 The varied process parameters of laser cladding (Powder injection).....	49
Table 4-5 Experiments results of laser cladding with powder injection method.....	50
Table 4-6 The experiment values of 5A, B and 6A, B.....	51
Table 4-7 A statistics of cracks of powder injection laser cladding layers.....	54
Table 5-1 Date of samples from 2-1 to 2-5.....	58
Table 5-2 Date of samples of 2-1, 3-1, 4-1 and 5-1.....	60
Table 5-3 Date of single-track samples from 12-1 to 12-5.....	62
Table 6-1 Micro-hardness experimental results.....	74
Table 6-2 Data of wear resistance experiments.....	78

List of Symbols

A	Absorptivity [-]
D	Diameter of laser spot [m]
D_c	Clad depth [mm], $D_c = T_c - H_c$
E	Specific energy ($E=P/VD$) [Jm^{-2}]
E_c	Elastic modulus of cladding coating
H_c	Clad height[mm]
G_l	Temperature grads of crystal direction
G	Gravitational acceleration [ms^{-2}]
K	Thermal conductivity [$\text{Wm}^{-1}\text{K}^{-1}$]
κ	Thermal diffusivity [Wm^{-2}]
m	Mass [kg]
P	Laser power [kW]
R	Solidification speed
S_c	Cross-section area of clad layer
S_s	Cross-section area of substrate
T	Time [s]
T_c	Total clad height [mm]
T_s	Substrate depth
T	Temperature [K]
T_0	Initial temperature [K]
T_{max}	Maximum temperature [K]
$q(x,y)$	Power of point source [W]
V	Laser scanning speed [m/min, or mm/s]
V_c	Cooling speed
V_s	Solidification speed
W_c	Clad width [mm]
ρ	Material density [kgm^{-3}]
τ	Thermal time constant [s]
θ	Contact angle
θ_w	Wetting angle
η	Dilution rate, $\eta = D_c / T_c$
α_c	Thermal expansion coefficient of cladding coating
α_s	Thermal expansion coefficient of substrate
σ_c	Thermal stress of clad

Abbreviation

<i>CVD</i>	Chemical vapor deposition
Ce_2O_3	Cerium oxide
La_2O_3	Lanthanum oxide
<i>PRMMCS</i>	Particle Reinforced Metal Substrate Composites
<i>TiC</i>	Titanium carbide
<i>WC</i>	Tungsten carbide

Chapter 1

Introduction

1.1 Preface

The invention of the laser was one of the most important scientific research achievements in the 1960's. In fact, laser is just an abbreviation of "Light amplification by stimulated emission of radiation". A laser is a kind of device, which transmits an extremely narrow and coherent beam of electromagnetic energy in the visible light spectrum. Compared with other ordinary heat sources, a laser has a number of special features. It can be used to do many kinds of surface heat-treating.

Laser heat treatment technology is a relatively new form of surface strengthening and surface modification technology available only for decades. The development direction of laser heat treatment mainly focuses on four aspects: laser hardening, laser cladding, laser surface alloying and industrial applications of laser heat treatment.

The new surface strengthening and surface modification technology dates back to the mid 70's. In 1976, D.S.Gnanamuthu, who worked in an American company AVCO Everett invented laser cladding technology and gained a patent. And by the 1980's, laser cladding technology had already been a front line topic in surface engineering

[Boas M, 1990, Abbas G, 1991].

The current development of laser-cladding technology is in the area of special alloys for particular performance and use for Ceramic / Metal composite coatings, and even for pure ceramic coatings.

In this new surface modification technology, the high-density energy of laser is used to clad alloy powder onto the surface of the substrate material. Metallurgical bonding between the cladding layer and substrate material is realized. The cladding layer has the same excellent performance as that of the alloy powder materials. Their mechanical properties are enhanced. Including hardness, resistance against wear and corrosion, fatigue properties etc. The purpose of surface modification and surface repair is accordingly achieved. Thus, particular requirements for the material surface were satisfied without using large quantities of expensive metals. This means that laser cladding technology will have a very wide application.

It is known that to improve the surface properties of metallic mechanical parts, such as the resistance against wear and corrosion, several other thermal surface treatments are available; for instance, flame spraying, plasma spraying and arc welding are established techniques. What characterizes all of these techniques is the application of a surface layer with the required properties on top of a cheap material lacking the desired properties.

In addition, other traditional surface modification technologies such as electro plating, intermittent element infiltration, chemical vapor deposition (CVD) etc. are also available established techniques, but due to their low equilibrium solubility, or due to the limitations of low solid state diffusivity, or due to the weak bonding strength between cladding layer and substrate they are not as good. The required surface modification effect is not necessarily achieved.

Depending on the application technique, common problems are a combination of poor bonding of the applied surface layer to the base material, the occurrence of porosity, the thermal distortion of the work piece, the mixing of the surface layer with the base material and the inability to apply a very localized treatment.

One of the techniques that overcome these problems is laser cladding. Compared with ordinary coating technology, laser-cladding technology has lots of advantages: Owing to the high energy density laser beam, the heat source is more focused. Heating and cooling rates are more rapid. Cladding layer has good remelting performance. Less distortion happened on work pieces. The heat-affected zone is narrower. The surface is more bright and clean (depending on the alloy used).

And after laser cladding treatment, or laser cladding repair on the surface of the main parts of the work piece, their performance, working life, work reliability and value will

be greatly increased. In addition, laser cladding technology is also highly adaptable, has high precision, and controllable dilution rate, resulting in a fine microstructure and/or metastable phases, low porosity with metallurgical bonding via a compound interface is, and the process is easy to automate. It is possible to economize on energy and material with no pollution etc. So by adopting laser-cladding technology, people will realize low input, high output resulting in increased economic value. This has led to laser cladding technology developing very quickly in recent years.

Current laser cladding research mostly focus on: (1) Opening up the applications and developing techniques, (2) To investigate different cladding layer materials, (3) the problem of rapid solidification microstructure in the melting area. (4) Bonding interface state and performance test between base-material and clad layer. Because laser-cladding technology is still a new surface modification technique, much research is still required to perfect it in theory and practice.

At present, there are still a number of reasons preventing laser cladding from realizing extensive industrial application. The variation in the quality of the cladding layer is the most important reason. Defectives such as cracks, gas porosity and variation in microstructure and chemical constituent uniformity tend to occur. This is especially true for thicker layers and for large areas. These defectives are more common for some special cladding materials and for large work pieces with complex shapes.

1.2 Laser cladding technology

1.2.1 Fundamental concept of laser cladding technology

Laser cladding has been defined as “A process which is used to fuse with a laser beam another material which has different metallurgical properties on a substrate whereby only a very thin layer of the substrate has to be melted in order to achieve metallurgical bonding with minimal dilution of added material and substrate in order to maintain the original properties of the coating material” [Komvopoulos, 1990].

Laser cladding consists of two essential parts: supply of cladding material to the substrate followed by melt pool formation and fusion by a moving laser beam. Under the irradiation of a laser beam an alloy powder layer and a small part of the substrate surface layer is melted. After a rapid cooling and solidification process, metallurgical compounds appear in the bonding zone between the clad layer and substrate. The dilution rate of the surface cladding layer is low compared to other processes. Thus the properties desired of a cladding process such as a localized effect, hardness, wear resistance, corrosion resistance and improvement of contact fatigue life will be produced. Laser cladding technology is especially suited for the rehabilitation of an expensive work-piece.

1.2.2 Laser cladding technology process

The goal of laser cladding is to achieve good quality clad layers. In this context, a good quality clad layer means no cracks, no porosity, a good bonding to the substrate and a low dilution of the coating material by the substrate.

An important part of the laser surface cladding process, is the supply of cladding material to the substrate. At present, various methods are available, but the most common method is the application of powder. We can distinguish two powder coating methods: placement prior to the process: pre-placed powder, or during the process: powder injection.

The different kinds of additional cladding material and placement methods not only affect the amount of energy transferred and metallurgical reactions, but also affect the quality of the laser cladding layer. The pre-placed powder laser cladding and powder injection laser cladding are shown in Figure 3.1 and Figure 4.1.

The powder may be pre-placed by plasma spraying, flame spraying, electroplating and electro deposition etc, or to directly use a sticking agent to a pre-conglutinate alloy powder onto the substrate surface. A laser beam is then scanned over the clad layer to cause the cladding materials and substrate to fuse and bond by the formation of metallurgical compounds.

These pre-placed powder methods were widely adopted due to their relatively simple technology and relatively convenient method of operation. But these methods also have shortcomings as shown below: When cladding with pre-placed powder the melt pool is formed on top of the cladding material and proceeds downwards to the substrate. Only when the substrate has been melted can a clad layer be formed. So it is difficult to control the depth of the melt pool. So, in general, the dilution is relatively high. This will debase the quality and mechanical properties, ultimately affecting the performance of the cladding layer.

Another method is to adopt the powder injection method. In the case of laser cladding with powder injection, special powder feeding equipment has to be used. Powder particles are transported by a gas stream and injected into the melt pool. Currently Helium gas or Argon gas are used as the shielding gas. The powder injection method starts with the formation of a melt pool in the substrate in which cladding powder is being fed.

But before alloy powder particles were fed into melt pool, the powder particles absorb laser energy on their way through the laser beam. They were heated into a glowing and flaming state by the laser beam, therefore; they are preheated on arrival in the melt pool. In the melt pool, they exchange heat and mix with the elements already present. The powder particles might also affect the laser power density. After laser beam

scanning, it rapidly solidifies. Thus a clad layer is formed almost instantaneously.

In the process of laser cladding with powder injection, different metallurgical compounds could be produced by regulating the velocity of powder flow, nozzle stand off and other parameters. In addition to increasing the utilization rate of the laser energy, it also ensures that the powder has already melted before it comes into melt pool. Bonding through metallurgical compounds forming between the cladding layer and substrate zone is realized while avoiding excessive melting of the substrate. The main shortcoming of this method is the percentage utilization of the alloy powder, which is low, while the powder feeder equipment is comparatively complex.

For big samples or work-pieces it is necessary to make several adjacent tracks to treat the larger areas. Most laser cladding processes requires the use of a shielding gas to avoid corrosion of the treated area.

1.3 Laser cladding technology characteristics and parameters

1.3.1 Advantages of laser cladding Technology

In general, the use of a laser beam in surface treatments offer several advantages over conventional heat sources [Webber, 1987; Konig, 1989; Oberlander, 1992]: the energy supply can be well controlled; a very local treatment is possible; the total heat input is low, resulting in minimal distortion; the heating and cooling rates are high, resulting in a fine microstructure and metastable phases; the treatment is a non-contact process. There is no wearing of tools, nor any mechanical forces acting on the workpiece; the process depth is well defined.

Atamert [1989], Cai [1990], Li [1994], Monson [1990] and Oberlander [1992] describe some more advantages of laser cladding over conventional coating techniques. The combination of a controlled minimal dilution of the substrate by the coating material and nevertheless a very strong fusion bond between them, is a unique feature of laser cladding. Porosity in the coating can be prevented entirely and a homogeneous distribution of elements can be achieved.

1.3.2 Technological parameters of laser cladding

The most important technology parameters of laser cladding are as: laser power, laser beam spot diameter, laser scanning speed or the speed of relative movement of the work-piece, pre-placed powder layer thickness, powder feeding rate, nozzle angle and stand off etc. In addition, the powder placement method as described in last section can be considered as a parameter. In addition, the specific energy and dilution are two important parameters, which have to be controlled.

Specific energy:

Some scholars' research results [Blake, 1985; Chen, 1989; Engstrom, 1988; Kar, 1988, 1989; Komvopoulos, 1990; Molian, 1988; Singh, 1985] relate laser cladding results to the specific energy E :

$$E = P/DV. \quad (Jm^{-2}) \quad (1.1)$$

Where P is the laser power, V is the feed rate of the workpiece, and D is the diameter of the laser beam spot.

After introducing the concept of Specific energy, we have an overall assessment method of how the leading technology parameters affect the quality of the laser-cladding layer.

Dilution rate:

It is known that laser cladding requires the achievement of a strong fusion bond between the cladding material and the substrate, which requires the formation of a melt pool in the substrate. So that the depth of this melt must be as small as possible in order to obtain a pure surface layer, which is not diluted by the base material. The dilution of the produced clad layer by elements of the substrate is used to characterize the clad quality.

In order to reduce the influence of the substrate on the cladding alloy components, and in order to achieve the metallurgical bonding between cladding layer and substrate, we introduce a very important concept: dilution rate η . When a laser beam irradiates both the cladding layer and substrate, elements of the substrate infuse the cladding layer, and cause cladding component change. The degree of the change is the dilution rate η . Dilution rate η can be approximately calculated by two ways [Bruck, 1987]. One method is based on the clad layer geometry, namely, measuring the cross sectional area of cladding layer. The dilution is then defined as the ratio of the cross section area of substrate over the cross section area of clad layer. The formula is as below:

$$\text{Dilution rate } (\eta) = S_s / (S_c + S_s) \quad (1.2)$$

Where, S_s is cross section area of substrate, S_c is cross section area of clad layer.

The scale of substrate melting layer depth and cladding layer total depth can also approximately calculate dilution rate. Abbsa [Abbsa, 1991] found the simple dilution rate calculate method by experiments.

The geometrical dilution is then defined as the ratio of the clad depth (D_c) in the substrate over the total clad height (T_c) as shown in Figure 5.1. This geometrical

approach assumes a homogeneous distribution of elements over the clad cross-section. The formula is as below:

$$\text{Geometrical dilution rate } \eta = D_c / T_c \quad (1.3)$$

This method is quite easy to use, and the absolute error is within 5%. Research results show that dilution rate, on the one hand controlled by laser treatment parameters, and on the other by cladding materials, such as the alloy powder's granularity, melting point, chemical composition and the substrate's wettability, etc. Laser cladding technology, is practicable when the dilution rate is between 5% and 10% or so. By this, the expected designed cladding layer properties can be realized, as well as the production of fine metallurgical compounds between the cladding layer and substrate. Optimisation is based on producing both fine metallurgical compounds and the appropriate dilution degree as far as possible.

1.3.3 Three kinds of external appearance of laser cladding layer

[Weerasinghe V M, Steen W.M., 1983] investigated the process of powder injection laser cladding, pointed out that when the foreside of melt pool on substrate melts, sprays alloy powder into melt pool immediately, could get metallurgical compounds. When using the synchronous injection powder feeding method, the appearance of a single-channel sequential scanning cladding layer were affected by many factors as shown in Figure 1.1 showing the cross-section external appearance of single-track sequential scanning cladding layer.

By adopting a relatively high powder feeding rate and a relatively low energy density, the external appearance A as shown in Figure 1.1 is obtained. The characteristics are as below: due to insufficient melting, binding strength decreases, contact angle θ is less than 90° , and the laser cladding coating could easily detach from the substrate; greatly decreasing the operating life of the coating.

By adopting the appropriate technology parameters, the external appearance B as shown in Figure 1.1 is obtained. The characteristics are: a very good liquid-solid Phase combination. And the contact angle θ is bigger, with better wettability.

By adopting relatively low powder feeding speed and relatively high energy density, the external appearance C as shown in Figure 1.1. is obtained. This results in undesirable compounds being formed within the clad layer, additional dilution and a large heat affected zone. This will decrease the microhardness and wear resistance of the cladding coating. Overheating also increases the distortion and residual stresses, which may cause micro-cracking in the clad.

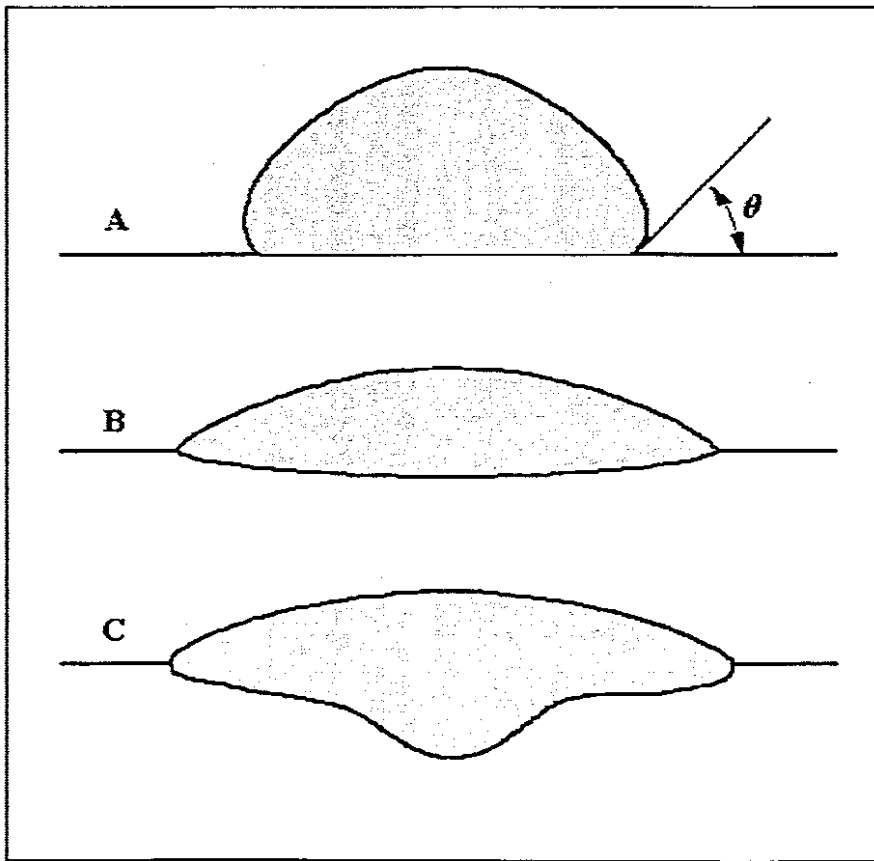


Figure 1.1 Three kinds of external appearance of laser cladding layer

A: higher powder injection rates and lower energy density,

B: Appropriate technology parameters.

C: Low powder feeding speed and relatively big energy density

1.3.4 Laser cladding coatings materials

Since the new Laser cladding technology emerged, it was widely used by international researchers to improve the material's surface properties, to enhance material surface wear resistance and oxidation-resistance. The earliest used cladding materials are Fe-based alloy, Co-base alloy, and nickel-based alloy that are widely use in plasma and flame spraying technology. They are also suitable for use in laser cladding, because the intended functional properties are the same. The reasons for adopting the above-mentioned materials are due to the good wettability of these alloys to various carbon steel, alloy metals, stainless steel and various nonferrous alloy metals.

Some of the current research being done is aimed at enhancing properties and usability of the cladding process for some special work pieces. Researchers have even added various granular ceramics with high-melting points to the alloy powder, using laser-cladding technology to synthesize Particle Reinforced Metal Substrate Composites (abbreviation PRMMCS). At present, a lot of scientists make ceramic wear resistance cladding layers [Liu, 1994], erosion-resistant [Wang, 1993],

oxidation-resistant coating, and heat barrier coatings via laser cladding technology [Pei, 1995]. Some research and development concerning coating materials is presented in the next section.

Alloy powder can be classified into three kinds:

The first kind is the nickel-base alloys. Nickel base alloys are suited to applications with parts that are exposed to an aggressive atmosphere at elevated temperatures. They have a good high temperature corrosion and oxidation resistance. Nickel based alloys can also be used as a substitute for cobalt. This may be important in the future, because cobalt is a relatively rare and expensive element, whereas nickel is widely available and much cheaper.

Elements that are commonly mixed with nickel are chromium, boron, carbon, silicon and aluminium. The formation of hard borides and silicon carbide improves the wear resistance and hardness.

Aluminium can be added in nickel base alloys to further increase the hardness. The hardness increase is due to the formation of intermetallic phases (NiAl_3 and Ni_2Al_3) [Grunenwald, 1996; Marsden, 1990] or an oxide layer (Al_2O_3).

The second kind is the Cobalt base powders. Cobalt base superalloys (namely Stellites) are very popular with regard to the improvement of the wear resistance of mechanical parts, especially in hostile environments [de Hosson, 1996]. Those powders are mixtures of cobalt and other elements like nickel, chromium, tungsten, carbon and molybdenum. Chromium is added to form carbides and to provide strength to the cobalt matrix as well as to enhance the resistance against corrosion and oxidation. Tungsten and molybdenum have large atomic sizes and give, therefore, additional strength to the matrix. They also form hard brittle carbides. Nickel is added to increase the ductility.

The predominant carbide found in Stellites is of the chromium rich M_7C_3 (where M = metal) type. These carbides (2200 HV) are responsible for the hardness of the clad (550 HV) and for the wear resistance. In low-carbon alloys other carbides such as M_6C and M_{23}C_6 are abundant [de Hosson, 1996].

If the wear properties of a given cobalt-base powder mixture is not sufficient, then hard particles, such as carbides, nitrides and borides, can be added directly to this mixture [Gassmann, 1992; Nowotny, 1994]. Those hard particles usually have a high melting temperature. The flow in the melt pool must ensure that they are uniformly mixed with the other elements and become embedded in the matrix provided by the molten cobalt-base material.

Gassmann [1992] described the addition of tungsten carbide ($\text{WC}/\text{W}_2\text{C}$) to a Stellite

powder in order to enhance the abrasive wear resistance. Tungsten carbide is distinguished by a minimal plastic deformation capacity, a low thermal expansion and a high wettability by molten metals, especially cobalt. Due to the low free formation enthalpy tungsten carbide is dissolved in the solid state by molten cobalt. The dissolution increases with the temperature of the melt and the interaction time. Depending on the carbon concentration in the melt, dissolved tungsten carbide recrystallises either to WC, or with low carbon concentrations, to W₂C or brittle phases such as Co₃W₃C and Co₆W₆C. It is therefore important to keep the temperature in the melt as low as possible. This not only results in low carbide dissolution, it also ensures a dense coating with lower tensile stresses.

The third kind is the Iron base alloys: Although the selection of an iron base alloy for improving surface properties of an iron base substrate may not be the most obvious choice, some research has been done in this subject.

It has been reported that a mixture of iron, chromium, carbon and manganese or tungsten has superior wear properties compared to Stellite 6 [Choi, 1994; Eiholzer, 1985; Komvopoulos, 1994]. The elements that are added to iron ensure the formation of carbides, contribute to the oxidation and corrosion resistance and promote the solid solution strengthening. The main carbide type found in this kind of clad layer is M₆C instead of the M₇C₃ type found in Stellite 6.

Others have reported on the application of austenitic corrosion resistant steel layers on top of ordinary low carbon steels [Fouquet, 1994; Jasim, 1989]. The corrosion resistance of those layers can be further improved by increasing the molybdenum content in it [Huang, 1995].

1.4 Introduction to laser cladding ceramic materials

At present, there are two main kinds of laser cladding using powder. One kind, is metal powder, such as chrome, nickel and cobalt-base, nickel-base and Fe-base alloy powder. Another kind is ceramic powder, such as WC, SiC, TiC, Al₂O₃ and ZrO₂ etc.

Because there is not too much of a difference of properties between metal alloy powder and the substrate, it is relatively easy to realize laser cladding of metallic powder onto a substrate. According to the different applications, people select different metal powders to satisfy the requirements such as wear resistance, erosion-resistance and oxidation-resistance. In contrast, properties of ceramics and metals are quite different, so, it is relatively difficult to laser clad ceramic materials onto a metal substrate.

Metal materials have high intensity, toughness and outstanding technology performance. But ceramic materials have distinguishing properties that metals cannot compare with, such as wear-resistance, heat resistance and erosion-resistance and

chemical stability. When a metal substrate is clad with a ceramic layer the material will possess both the superior properties of metals and ceramics.

An essential aspect of laser cladding is the achievement of a strong fusion bond over the entire interface between the substrate and the clad layer. Good wetting between the coating material and the substrate is therefore required. But the heat conduction rate, thermal expansion coefficient between metal and ceramic are quite different. And because of the poor wettability of ceramics to metals, it is very difficult to clad ceramics on to a metal substrate [de Hosson, 1995].

But people have great interest in laser ceramic cladding technology all the same. Commonly, when ceramic is clad on to metal some metal powder or alloy powder is added in the coating layer. In this way it is easy to produce a good compound between cladding layer and substrate, and the ceramic phase will be protected as well.

In 1979, D.S.Gnanamuthu [Ayers J.D., 1984] did a laser cladding experiment with a powder mixture of large particles (0.5mm) of tungsten carbide (WC) and iron powder (44 μ m), onto AISI 1018 mild steel substrate, with no sticking agent used. The thickness of powder layer was 1mm, width was 19mm and tungsten carbide powder was covered by iron powder to decrease decomposition during laser beam irradiation. The laser's power was 12.5kW. The laser beam size was 12 \times 12mm² and the scanning speed was 5.5mm/s. The cladding process was shielded by helium gas. After laser cladding, the average hardness of cladding layer was HV1100, in contrast, peripheral substrate hardness was HV870. Around every tungsten carbide particle, there was an obviously different area considered to be as a result of laser cladding action.

In 1981, Ayers J.D. [Ayers J.D., 1981] used the powder injection feeding method to successfully clad titanium carbide (TiC) on to a 5052Al aluminum alloy substrate, obtaining a fine surface quality cladding layer, with no cracks occurring. This might have been possible due to the lower levels of stress generated in the aluminium substrate compared to steel.

A literature research is presented as appendix: 1. It shows laser cladding substrate and cladding materials.

1.5 Summary of applications of rare-earth element in laser cladding

There is an 80 yearlong history of Research into applications for rare-earth elements in the area of metals. Rare-earth elements have the functions of cleansing, metamorphosing and surface alloying. They also improve metallurgic behaviour, molten behaviour, heat machining performances, mechanical behaviour (tenacity, toughness, lower temperature brittleness), surface performance, wear-resistance, corrosion resistance, oxidation-resistance, welding performance and material's high temperature performance. So rare-earth elements were named the penicillin of the

steel.

In the recent two decades, the United States of America, Japan and some European countries engaged in research and development with an emphasis on the new rare-earth element materials used in new and high technology. Now, rare-earth elements are generally accepted as the strategic elements in the new-tech revolution, the growing point of high tech, the treasure house of new materials. [Du Ting, 1997]

Cerium is widely used in the Chemical heat-treatment of steel, flame spraying, and electro plating fields. Cerium is a kind of surfactant; its function is to decrease the surface tension, decrease the critical mass of nucleus to come into being. But cerium was less used in laser surface modification technology. It had been reported [Wang Kun-lin, 1998] by some scholars for the use in laser cladding powder.

Wang Kunlin [Wang Kun-lin, 1999] added different contents of lanthanum oxide (La_2O_3) powder with nickel-based alloy powders, then laser cladded these powders onto steel substrates. The results were compared with those of the coatings without La_2O_3 addition. The comparison indicates that the addition of La_2O_3 can refine and purify the microstructure of the clad coating, reducing the dilution of clad material from substrate, decrease the lattice constant of solid solution. Moreover, the friction coefficient of the clad coating with the addition of La_2O_3 is reduced and the wear resistance of the clad coating with La_2O_3 addition is enhanced.

1.6 Laser cladding technology application and prospects

1.6.1 Industry application of laser cladding

Laser cladding can enhance surface properties by changing the material composition in the surfaces. It is a technique used to produce hard wear resistant and/or corrosion resistant surface layers in industry. The technique is used to produce high quality surface layers on top of industry work piece. At present, of all laser heat treatment technologies, laser cladding is one of the most promising surface modification technologies.

Now, by using laser cladding technology, not only excellent performances such as wear-resist and corrosion-resist materials are available, but also high temperature-resistant, oxidation-resistant and good electrical conductivity performances materials are available.

By using laser-cladding technologies, a high-performance and high quality-working surface can be made on low-cost materials saving valuable and rare metals. So the technology has been developing rapidly in a number of countries in recent years [Ariely S, 1995, Hu. C, 1996]. Laser-cladding technology has been used for repair on the surface of the work piece. This kind of application has caused people to pay more

attention to laser cladding making it more prominent in engineering. At present, a large number of laser cladding applications focus on realizing a partial wear-resistant cladding layer on the surface of the work piece. In some countries, laser-cladding technology has already realized a considerable area of application.

Considering the history of laser cladding industry applications we can see that laser cladding has established itself using trial and error methods. Americans did a lot of pioneering work on laser cladding industry applications [Ayers J.D., 1984]. They clad silver on copper to be used as a contact electrode using less material causing extensive interests worldwide. Another advantage of using the technology is that conventional methods use poisonous chemical electro plating materials, which can be eliminated with benefits for the environment. These advantages made the technology have a huge economic value and greatly accelerated its commercial progress.

The high-quality surface layers that can be produced by laser cladding only, make it a strategic technique. Laser cladding technology has already been put into use in cladding relatively smaller work pieces obtaining obvious economic benefits. Other well known applications include the improvement of the wear resistance of diesel engine exhaust valves, the enhancement of the corrosion resistance of gas turbine blades and the repair of dies and inserts. Pratt & Whitney and Rolls Royce Corporation began to use the technology for the surface strengthening of blades of gas turbines from 1982, and a laser cladding station was established with an annual output of tens of thousand of work pieces. [R.M.Macintyre, 1983]

A literature survey is presented as Table 1-1 below. It shows laser-cladding materials with applications.

Cladding Materials And Substrate	Application	Information Source
Al-bronze	Extruder screw plastic machinery (steel 1.4541)	[Wolf, 1995]
AISI 410	Valve seat	[Bruck, 1988]
CrC, Cr, Ni on cast iron	Parts of off-shore drilling heads	[Eboo]
Co-alloy	Valve parts (Cr18Ni12Mo2Ti)	[Fu Geyan, 2000]
Co-Cr-W-C	(14CrMoV6 9) Moulding die (45NiCr6)	[Fischer, 1996]
Co-alloy	Nuclear Valve Parts	[Zhang Chunliang]
Fe-C-Si-B	on the cast iron substrate	[Tan Wen, 2000]
FCo-05 alloy	Chemical Industry Valve (0Cr18Ni12Mo3Ti Austenitic stainless steel)	[Li Biwen, 2000]
LC2.3B (Ni-base)	Extruder screw plastic	[Schneider, 1995]

	machinery	
Ni-Cr-Al-Y	Extruder screw plastic machinery	[Gasser, 1996]
Ni-alloy +WC	Parts of Pump	[Li Guohua, 1999]
Ni-Cr alloy	Compressor blade (Ti-6Al-4V)	[Konig, 1992]
Ni 21 alloy	Exhaust Valve of automobile	[Li Chunhua, 2000]
on cast iron	Cylinder and valve	Fiat [Eboo, 1983]
Stellite, Triballoy T-800	Automotive parts	GM [Eboo, 1983]
Stellite, Colmonoy	Aerospace	Rockwell [Eboo, 1983]
Stellite 6, Stellite SF	Turbine blade	Westinghouse [Eboo, 1983]
Stellite 6	Turbine blade, plough blade	[Bruck, 1987]
Stellite 6	Diesel engine valve	[Lubbers, 1994]
Stellite SF6	Deep drawing tool (cast iron GGG60)	[Haferkamp, 1994]
Stellite 6	Drainage plough blade	[Weerasinghe, 1987]
Stellite 6	Leading edge steam turbine blade	[Amende, 1990]
Stellite 6	Aircraft engine turbine blade Z-notch Leading edge turbine blade in industrial	[Blake, 1985]
Stellite 6	Deformation tool	[VandeHaar, 1988]
Stellite 6	Stainless steel seal runner	[Bruck, 1988]
Stellite; induction heating	Stainless steel gate valve	[Bruck, 1988]
Stellite 6,F	Leading edge steam turbine blade	[Ritter, 1991]
Stellite 21	Valve in combustion engine (X45CrSi9)	[Gasser, 1996]
Stellite 6	(NiCr20AlTi ~ DIN 2.4952)	[Lang, 1994]
Stellite	Blowing mould Extruder screw plastic machinery	Pratt&Whitney [Duhamel, 1986]
Stellite 6, Colmonoy 5	Jet engine turbine blade notch (PWA Alloy 1455). Die for production of glass bottles components of nuclear plants (AISI 304)	[Bergmann, 1994] [Corchia, 1987]
Triballoy on	High pressure gas turbine blade	Rolls Royce

Nimonic	shroud.	[Macintyre, 1983]
Triballoy T-800	Valve in combustion engine (X45CrSi9)	[Kupper, 1990] [Blake, 1985]

Table 1-1 Laser cladding application

1.6.2 Present problems in laser cladding technology

Being a new applied technology, the development of laser cladding technology faces some difficulties. The following aspects need to be researched [Pei Yutao, et al.1994], (1): Development of high power lasers and dedicated optical systems suits for roboticised manufacturing production. (2): Development of rapid solidification theory and research of the structure of interface. (3): the stability and feedback control during processing. (4): quality monitoring and defect control.

Many researchers [Zhang Guangjun, 2000] indicate that in the melt-solidification layer, there exist tensile stresses. When the local tensile stress is more than the material's limit then a crack will come into being. Cracks appear mostly at the interface of dendrites, at gas porosity sites, at impurities and other areas of weakness.

Another problem is due to the different coefficient of expansion between the cladding layer alloy and substrate material. When the coefficient of expansion is too big, tensile stress will come into being. When the tensile stress exceeds the utmost limit of tensile resistance at that temperature, a crack will appear [Li Biwen, 2000].

In addition rapid heating and cooling occurs in the laser cladding layer (10^4 - 10^6 K/s) as the life of the weld pool is very short. This always means that oxides; sulfides and other impurities have not enough time to be emitted. They are retained in the cladding layer. They can become the crack fountainhead. In addition, after the laser beam moves away, instantaneous solidification and crystallization occurs as the cladding layer is formed, it is easy to cause a disturbance of the crystal interface, increasing the crystal vacancy count. Also hot-shortness (red brittleness) increase, the ductility degree (Plasticity and Toughness degree) also decreases, crack susceptibility then as a result increases. The thicker the cladding layer the more the above-mentioned situation becomes observable.

1.7 Background and research subjects

1.7.1 Background

Energy resources and natural resources are limited in the world. The research is done to open up the application and development of laser cladding technology, which will

allow for the use of low-price materials while retaining outstanding service performance. The adoption of laser cladding technology will provide the superior quality and superior properties of the alloy coating. Even a pure ceramic material layer can be deposited on a low-price base metal. Another benefit is the replacement of more expensive metal alloys in service with low-price metals with localized changes in only those areas subject to wear. This technology is especially suited to applications where only a part of the work piece needs to be resistant to corrosion, wear and oxidation.

Alternatives to the application of the technology are the use of quality alloy materials throughout. This method greatly increases the manufacturing cost in terms of formability and cost of material.

Another method is to repair the surfaces in service with welding technology. The dilution rate is relatively high using welding technology and the microstructure is coarser and more prone to hot cracking. Sometimes, the repair-welding layer of the repaired work pieces could very easily detach from the substrate greatly decreasing the operating life of the coating.

The above problems could be avoided by adopting the laser cladding technology. On the premise of guaranteed service performance the consumption of the high-level alloy materials would be greatly decreased. The production cost would decrease so laser cladding technology offers very good economy benefits.

1.7.2 Research objectives and research contents of this thesis

The study mainly includes: the design of the composition of cladding materials, the choice of sticking agent, and definition of laser processing parameters. By means of an optical microscope, micro-hardness tester and wear-resistance testing machine, analysis of the shape of the cladding coating, microstructure, distribution of micro-hardness, properties of wear-resistance and integration of interface between cladding and substrate, dilution of alloying elements and an analysis of the crack behaviour and prevention was undertaken. Solidification features and the formation of the microstructure were studied in the cladding layer. Some features in the solidification process of pool under laser will also be analysed.

1.8 Research methods and research route

1.8.1 Research methods

1. Theoretical analysis: choosing benchmark problems, choosing cladding materials, choosing cladding process parameters, choosing experimental equipment.
2. Experimental research: Laser cladding experiments. Machining samples.
3. Microstructural analysis.
4. Analysis of the relationships between process parameters and bond strength,

penetration, distortion, dilution, hardness, wear-resistance and cracking.

1.8.2 Research route

In this thesis, the author adopted theoretical analysis, and an experimental study of microstructure, micro-hardness, wear-resistance, and crack analysis. The research route the author used is listed in the Table below.

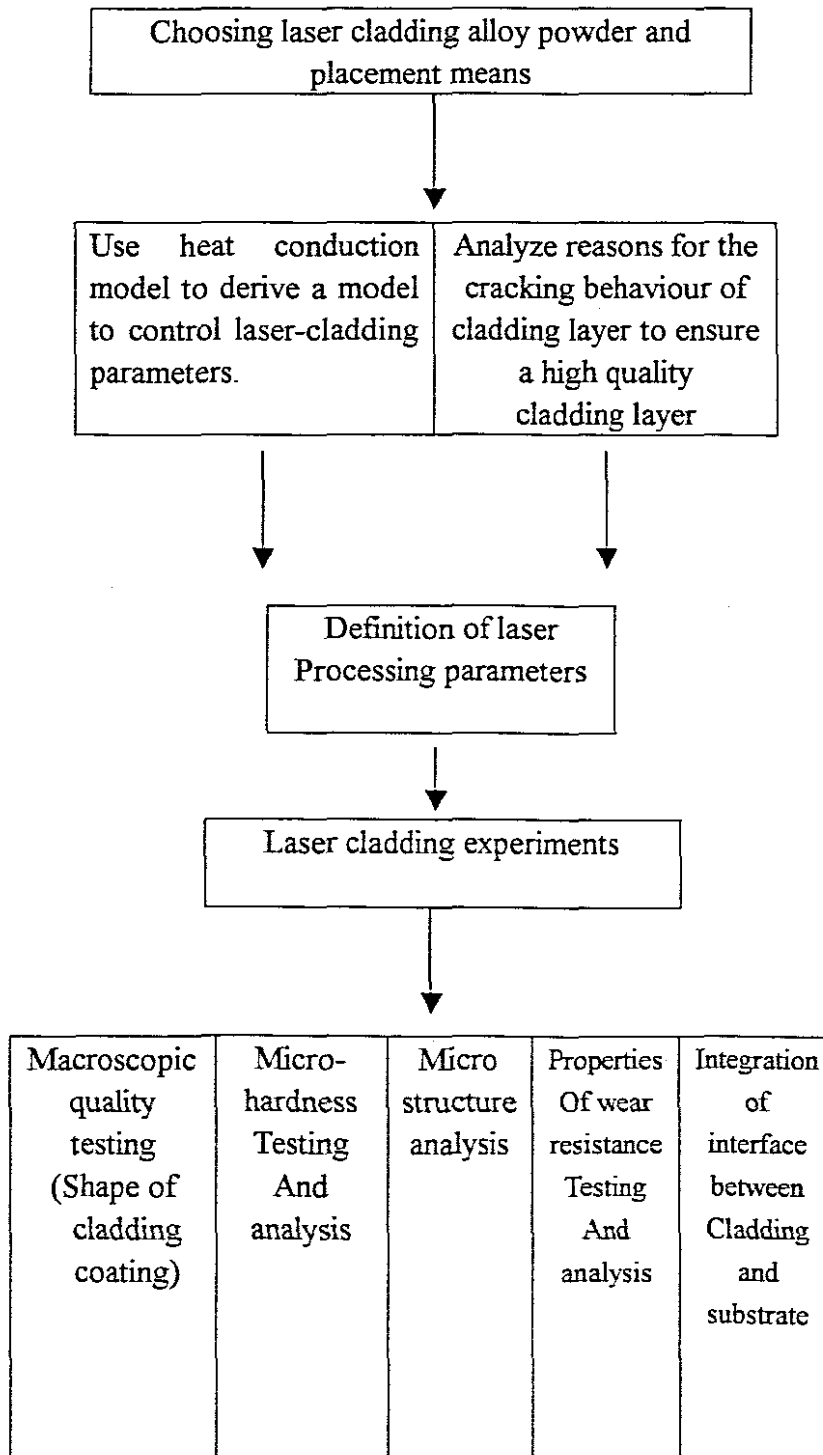


Table 1-2 Research route

Chapter 2

Analysis of the laser cladding heat transfer process and mathematical model of laser heat flux

2.1 Introduction

During the laser cladding process, it is important to control the laser energy distribution and the resulting temperature distribution over the surface. The temperature distribution of the melt pool must be reasonably controlled. If the temperature in the melting pool is too high, it will result in undesirable compounds being formed within the clad layer, additional dilution and distortion of the substrate and a large heat affected zone. It will also result in the hard elements such as tungsten carbide being transformed to a less desirable form, and the elements, within the coating, will be deeply diluted by the substrate material. This will decrease the microhardness and wear resistance of the cladding coating. Overheating also increases the distortion and the residual stresses, which may cause microcracking in the clad.

In addition, very higher temperatures in the molten pool will also result in a higher rate of burning damage of the chemical elements. Critical grain sizes will be coarser as well; therefore the advantages of laser cladding will be lost.

In contrast, if the temperature in melts pool is too low; substrate will not melt sufficiently, or even no substrate melting is possible. Thus, the intermediate metallurgical compounds which need to be formed between the substrate and laser cladding coating will not come into being. This will obviously decrease the bond strength between laser cladding coating and substrate; the laser cladding coating could detach from the substrate greatly decreasing the operating life of the coating.

As we all know, during the laser cladding process, the temperature distribution of melt pool greatly depends on laser parameters. Consequently, it is necessary to match the technology parameters to the required structure. We need to calculate and predict the temperature in the melt pool to be able to enhance the quality and properties of clad layer. There is also a need to optimize the chemical components of laser cladding alloy in terms of the mixture of metallurgical powders to achieve a given hardness, which is not characterized by microcracking.

In this chapter an analysis of the heat transfer process of laser cladding was performed. (Including heat transfer characteristic of pre-placed powder laser cladding and heat transfer characteristic of powder injection laser cladding). Some numerical solution and analytical solutions for the distribution of temperature are introduced. A Finite Element Method for calculating the surface temperature distribution was used to help predict the temperature distribution resulting from laser cladding.

2. 2 Analysis of heat transfer process of laser cladding

Laser cladding technology is one of the laser surface treatments. The effects of laser cladding are based on a change of the material composition of the surface layer due to a thermal cycle, which is induced by a moving laser source.

The laser cladding treated area is heated by absorption of energy delivered by the laser beam. The heat input due to a high power laser is a well-confined narrow and very intense beam. Therefore, heating rates in the surface layer are high. The heated layer is self-quenched after the passing of the laser beam by diffusion of heat to the cold bulk. The high heating and cooling rates in the surface layer result in grain refinement and in the formation of metastable phases and altered microstructures.

The process of laser cladding involves the formation of a melt pool to which material is applied. A very distinguishing characteristic of laser cladding is the generation of a surface layer that hardly contains elements of the substrate on top of the base material. Enough mixing is allowed to achieve strong bonding so the material properties of clad layer entirely depend on the applied coating material.

During the process of laser cladding with pre-placed powder, firstly, the laser beam must melt the pre-placed layer, then a melt pool is formed on top of the cladding material and proceeds downwards to the substrate. Only when the substrate has been melted can a clad layer be formed. The following Figure 2.1 shows the heat transfer process of pre-placed powder laser cladding.

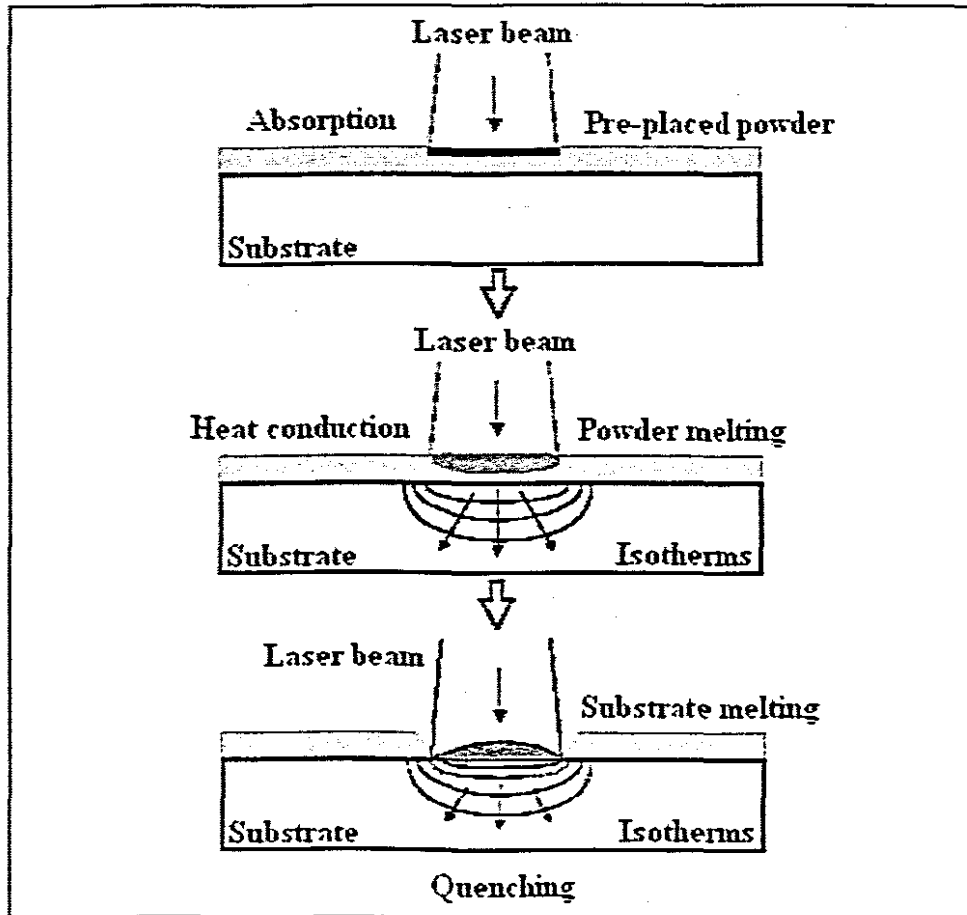


Figure 2.1 Heat transfer process of pre-placed powder laser cladding

2.2.2 Heat transfer characteristic of powder injection laser cladding:

For powder injection laser cladding the heat transfer process characteristics are quite different from that of pre-placed powder laser cladding. The formation of a very shallow melt pool in the substrate is the first stage in laser cladding with the powder injection process. At the same time, injected powder particles are transported from the feeder to the process area by the powder feeder and trapped in this melt pool, and the formation of a clad layer on the substrate surface starts.

The melt pool is formed due to absorption of laser power. During the powder injection process, not all the laser energy can reach the surface due to attenuation by the powder cloud. The attenuated energy is responsible for the heating of the particles in the powder cloud. Depending on their temperature on arrival in the melt pool, they

either extract or add energy to the melt pool.

The following Figure 2.2 shows the heat transfer process of powder injection laser cladding.

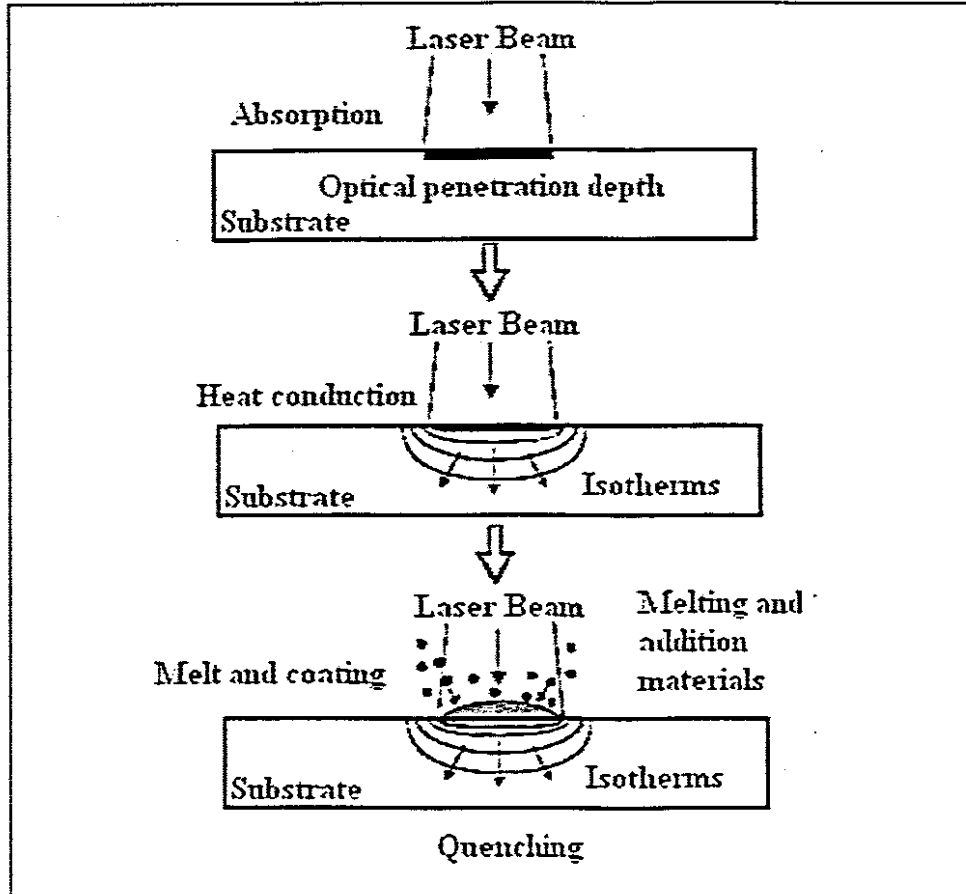


Figure 2.2 Heat transfer process of powder injection laser cladding

The formation of a melt pool in the substrate is not only affected by the total power absorbed in the surface, but also affected by the intensity profile of the laser beam.

In a word, during the laser cladding process, the heating and the cooling process, which follows all acts in a very thin layer and in a very short time. The heat input must be well controlled to prevent deep melting of the substrate and which would result in severe dilution on the one hand, and to achieve a strong fusion bond on the other hand. But to measure this directly is very difficult and almost impossible. Commonly, after certain simplified hypothesis, people can use mathematical modeling to calculate the technology parameters.

In this chapter some methods are presented to calculate the temperature induced on the surface of a semi-infinite solid by a laser source. In general, almost no exact analytical solutions for this problem can be found. Therefore, the equations describing

the surface of a semi-infinite solid by a laser source. In general, almost no exact analytical solutions for this problem can be found. Therefore, the equations describing this problem must be discretised and solved numerically. However, people can still use the analytical solution to help predict the temperature distribution resulting from laser cladding.

2.3 Surface temperature distribution modeling

Whether adopting the pre-placed powder or powder injection laser cladding method, the first stage of all laser cladding starts with the absorption of laser radiation in the pre-placed layer or substrate material. Laser energy absorption occurs in a very thin surface layer, where the optical laser energy is converted into heat.

The absorbed heat diffuses into the surrounding bulk material by conduction. The diffusion equation for a linear heat flow in a homogeneous isotropic medium is:

$$\rho c_p \frac{\partial T}{\partial t} = k \nabla^2 T \quad (t > 0) \dots\dots\dots (2.1)$$

The laser beam can be considered as a moving heat source with a certain power density distribution that imposes a boundary condition on the substrate surface.

The classical approach to the modeling of the heat flow induced by a distributed heat source moving over the surface of a semi-infinite solid, starts with the solution of the heat diffusion equation for a point source [Carslaw, 1959; Elshof, 1994]. The temperature field is connected to a Cartesian coordinate system moving with a velocity v along the x -axis. For time $t \rightarrow \infty$ a steady state solution is obtained for a semi-infinite body, which is valid for a point source coming from $-\infty$:

$$T(x, y, z) = \frac{q(x, y)}{2\pi k \sqrt{x^2 + y^2 + z^2}} e^{-\frac{v(\sqrt{x^2 + y^2 + z^2} - x)}{2\kappa}} + T_0 \dots\dots\dots (2.2)$$

Where κ is the temperature independent thermal diffusivity, $q(x, y)$ is the power in the point source; z is the depth, y is the co-ordinate along the surface perpendicular to the direction of movement and, T_0 is the initial temperature. The solution of the heat diffusion equation for the moving point source is integrated over the entire laser spot to obtain a solution for an arbitrarily shaped source. The temperature, as a result of the laser spot with boundaries $x_s, x_e; y_s, y_e; z_s, z_e$, is:

$$T(x, y, z) = \frac{1}{2\pi k} \int_{z_1}^{z_2} \int_{y_1}^{y_2} \int_{x_1}^{x_2} \frac{q(x', y') e^{-v(\sqrt{(x-x')^2+(y-y')^2+z^2}-(x-x'))}}{\sqrt{(x-x')^2+(y-y')^2+z^2}} dx' dy' dz' + T_0. \quad (2.3)$$

The surface ($z = 0$) temperature of a semi-infinite body moving past an arbitrarily shaped heat source is thus given by:

$$T(x, y, 0) = \frac{1}{2\pi k} \int_{y_1}^{y_2} \int_{x_1}^{x_2} \frac{q(x', y') e^{-v(\sqrt{(x-x')^2+(y-y')^2}-(x-x'))}}{\sqrt{(x-x')^2+(y-y')^2}} dx' dy' + T_0 \dots\dots\dots (2.4)$$

Analytical solutions of the type of integral in equation 2.4 are only known for some special cases [Elshof, 1994]. In general, numerical methods are needed to solve this type of integrals. The integral was solved numerically by [Bos, 1993]. First, it was transformed to a series expansion on a grid with step size h . The temperature on a grid point $(x_i, y_j) = (x_0 + ih, y_0 + jh)$ can be written as:

$$T(x_i, y_j) = \frac{1}{2\pi k} \sum_{k=0}^{n_x} \sum_{l=0}^{n_y} K_{ijkl}^{hhhh} q_{kl} + T_0 \dots\dots\dots (2.5)$$

With

$$K_{ijkl}^{hhhh} = \int_{x_m}^{x_p} \int_{y_m}^{y_p} \frac{d(y-y')d(x-x')}{\sqrt{(x-x')^2+(y-y')^2}} e^{-\frac{v(\sqrt{(x-x')^2+(y-y')^2}-(x-x'))}{2\kappa}} \dots\dots\dots (2.6)$$

An analytical expression does not exist for this surface integral and numerical calculation is very time consuming. Fortunately, [Bos, 1993] was able to apply an exact reduction of this surface integral to a line integral, which, apart from exponential integrals, consists of finite integrals only. Polynomial as well as rational approximations exists for the exponential integral. This integral reduction results in the following expression:

$$\begin{aligned}
 K_{ijkl}^{hhhh} = & y_m \left[E_1 \left(v(\sqrt{x_m^2 + y_m^2} - x_m) \right) - E_1 \left(v(\sqrt{x_p^2 + y_m^2} - x_p) \right) \right] \\
 & - y_p \left[E_1 \left(v(\sqrt{x_m^2 + y_p^2} - x_m) \right) - E_1 \left(v(\sqrt{x_p^2 + y_p^2} - x_p) \right) \right] \quad \dots (2.7) \\
 & - \int_{y_m}^{y_p} \left(\frac{e^{vx_m - v\sqrt{\xi^2 + x_m^2}} \xi^2}{\sqrt{\xi^2 + x_m^2} (-x_m + \sqrt{\xi^2 + x_m^2})} - \frac{e^{vx_p - v\sqrt{\xi^2 + x_p^2}} \xi^2}{\sqrt{\xi^2 + x_p^2} (-x_p + \sqrt{\xi^2 + x_p^2})} \right) d\xi
 \end{aligned}$$

Where E_i is an exponential integral of the form:

$$E_1(x) = \int_x^\infty \frac{e^{-t}}{t} dt \quad (x > 0) \dots\dots\dots (2.8)$$

Compared with a differential equation, an integral equation needs a great amount of calculation time. Integration over the entire domain is required to calculate one single point. [Brandt, 1984], [Lubrecht, 1989] and [Venner, 1991] developed an algorithm (multi-level multi-integration) for fast evaluation of an integral. They showed that if the kernel K has certain smoothing properties, the complexity of the evaluation of an integral could be reduced without loss of accuracy. This algorithm was subsequently applied to solve equation 2.5.

This is a numerical solution. Li Hengde [Li Hengde, Xiao Jimei, 1990] has a simple analytical solution to help predict the temperature distribution laser cladding results. The modeling of the laser cladding temperature field established with this hypotheses is as follows:

1. Physical property of materials does not change with temperature.
2. To neglect crystalline latent heat, to neglect phase change latent heat.
3. The cladding surface receives laser irradiation neglecting heat loss caused by convection and radiation.
4. The initial temperature of the material is 293K (20 °C)
5. To treat the base material as semi-infinite solid.
6. During the course of laser cladding, some heat loss is caused by convection and radiation.

When the width of the melt pool is obviously bigger than the depth of the melt pool, the material can be considered as a 1-dimensional semi-infinite solid. This is a 1-dimensional modeling after adopting the above-mentioned hypothesis. The heat conduction equation, boundary conditions, and initial conditions are listed as follows: [Li Hengde, Xiao Jimei, 1990].

$$\frac{\partial T(z,t)}{\partial t} - \alpha \frac{\partial^2 T(z,t)}{\partial z^2} = \frac{q\delta(z-0)\eta(\tau-t)}{c \cdot \rho} \dots\dots\dots (2.9)$$

$$\frac{\partial T(z,t)}{\partial z} = 0, \quad (z=0) \dots \dots \dots (2.10)$$

$$T(z,0) = T_0, \quad 0 \leq z < \infty \dots \dots \dots (2.11)$$

The solution of the above equations gives the temperature distribution of the melt pool while heating:

$$T(z,t) = T_0 + \frac{q_0}{k} \left\{ \sqrt{\frac{4\kappa t}{\pi}} \cdot \exp\left[-\left(\frac{z}{\sqrt{4\kappa t}}\right)^2\right] - z \cdot \operatorname{erfc}\left(\frac{z}{\sqrt{4\kappa t}}\right) \right\} \dots \dots \dots (2.12)$$

The temperature distribution of the melt pool while cooling:

$$T(z,t) = T_0 + \frac{q_0}{k} \left\{ \begin{array}{l} \left[\sqrt{\frac{4\kappa t}{\pi}} \cdot \exp\left[-\left(\frac{z}{\sqrt{4\kappa t}}\right)^2\right] - \sqrt{\frac{4\kappa \gamma}{\pi}} \exp\left[-\left(\frac{z}{\sqrt{4\kappa \gamma}}\right)^2\right] \right] \\ - z \left[\operatorname{erfc}\left(\frac{z}{\sqrt{4\kappa t}}\right) - \operatorname{erfc}\left(\frac{z}{\sqrt{4\kappa \gamma}}\right) \right] \end{array} \right\} \dots \dots \dots (2.13)$$

In the above equations (from 2.9 to 2.13):

$T(z, t)$ is temperature [K],

z is the distance from surface [mm],

t is time.

T_0 is the initial temperature of material [K].

$\gamma = t - \tau$, $\tau = D/V$,

τ is the interaction time between laser and material[s].

D is the diameter of laser beam mm.

V is the laser sweep speed mm/s,

q is the theoretical laser beam power density [kW/mm^2].

q_0 is the effective power density used on heating [kW/mm^2],

$q_0 = Aq = 0.5q$, A is the power absorptivity, here, we suppose $A = 0.5$,

k is thermal conductivity [$Wm^{-1}K^{-1}$],

κ , is thermal diffusivity [Wm^{-2}],

c is specific heat,

ρ is density [kgm^{-3}].

$\delta(x)$: delta function.

$\eta(x)$: Heaviside function.

$\operatorname{erfc}(x)$: error function complement.

Where, A is the absorptivity of energy. During the course of laser cladding, some heat loss is caused by convection and radiation. In order to make the model to close to

practical situation, can reduce the absorption coefficient of energy to $0.5A$ or so.

The maximum temperature of cladding layer surface can be obtained from the above formula (2.12),

$$T_{\max}(t) = T_0 + \frac{q_0}{k} \sqrt{\frac{4\kappa t}{\pi}} \dots\dots\dots (2.14)$$

During this project, we use the Finite Element Method (FEM) to do a numerical experimental investigation to calculate and predict the temperature in the melt pool.

The finite element equations used to solve a transient nonlinear finite element analysis [Bathe, 1982] are given below:

$${}^t K^k \Delta \theta^{(i)} = \left(\sum_m \int_{V^{(m)}} B^{(m)T} {}^t k^{(m)} B^{(m)} dV^{(m)} \right) \Delta \theta^{(i)} \dots\dots\dots (2.15)$$

$${}^t K^c \Delta \theta^{(i)} = \left(\sum_m \int_{S_c^{(m)}} {}^t h^{(m)} H^{S(m)T} H^{S(m)} dS^{(m)} \right) \Delta \theta^{(i)} \dots\dots\dots (2.16)$$

$${}^t K^r \Delta \theta^{(i)} = \left(\sum_m \int_{S_r^{(m)}} {}^t \kappa^{(m)} H^{S(m)T} H^{S(m)} dS^{(m)} \right) \Delta \theta^{(i)} \dots\dots\dots (2.17)$$

$${}^{t+\Delta t} C^{(i)} = \sum_m \int_{V^{(m)}} H^{(m)T} {}^{t+\Delta t} C^{(m)(i)} H^{(m)} dV^{(m)} \dots\dots\dots (2.18)$$

$${}^{t+\Delta t} Q^c{}^{(i-1)} = \sum_m \int_{S_c^{(m)}} {}^{t+\Delta t} h^{(m)(i-1)} H^{S(m)T} \left[H^{S(m)} ({}^{t+\Delta t} \theta_e - {}^{t+\Delta t} \theta^{(i-1)}) \right] dS^{(m)} \dots\dots\dots (2.19)$$

$${}^{t+\Delta t} Q^r{}^{(i-1)} = \sum_m \int_{S_r^{(m)}} {}^{t+\Delta t} \kappa^{(m)(i-1)} H^{S(m)T} \left[H^{S(m)} ({}^{t+\Delta t} \theta_r - {}^{t+\Delta t} \theta^{(i-1)}) \right] dS^{(m)} \dots\dots\dots (2.20)$$

$${}^{t+\Delta t} Q^k{}^{(i-1)} = \sum_m \int_{V^{(m)}} B^{(m)T} \left[{}^{t+\Delta t} k^{(m)(i-1)} B^{(m)} {}^{t+\Delta t} \theta^{(i-1)} \right] dV^{(m)} \dots\dots\dots (2.21)$$

Equations 2.15-2.18 are the L.H.S stiffness matrix contributions for the conductivity, convection, radiation and heat capacity respectively. Where k is the conductivity, h is the convection coefficient, κ is the radiation coefficient. Equations 2.19-2.21 are the R.H.S thermodynamic force type terms for convection, radiation and the iterative corrections for the conductivity calculations respectively.

The complete system that is solved to give the temperature, θ , at any time increment is:

The heat source model used in the FEM is presented below:

$$q_v = \frac{\phi \eta VI}{2\pi\sigma_x\sigma_y\sigma_z} \exp\left(\frac{-(x_0 - x)^2}{2\pi\sigma_x}\right) \exp\left(\frac{-(y_0 - y)^2}{2\pi\sigma_y}\right) \exp\left(\frac{-(z_0 - z)^2}{2\pi\sigma_z}\right) \dots\dots\dots (2.23)$$

$$x_0 = x_s + v_x t \dots\dots\dots (2.24)$$

$$y_0 = y_s + v_y t \dots\dots\dots (2.25)$$

$$z_0 = z_s + v_z t \dots\dots\dots (2.26)$$

Where:

$P=VI$ is the laser power used.

σ_x (P, R) are empirical distribution parameters and are a function of the power and laser spot sized used.

ϕ, η are parameters accounting for efficiency and surface absorptivity.

x,y,z are distances from the center of the heat source.

The center of the heat source (x_0, y_0, z_0) travels with a given velocity and is thus a function of time.

The following Figures are some results obtained using this FEM method.

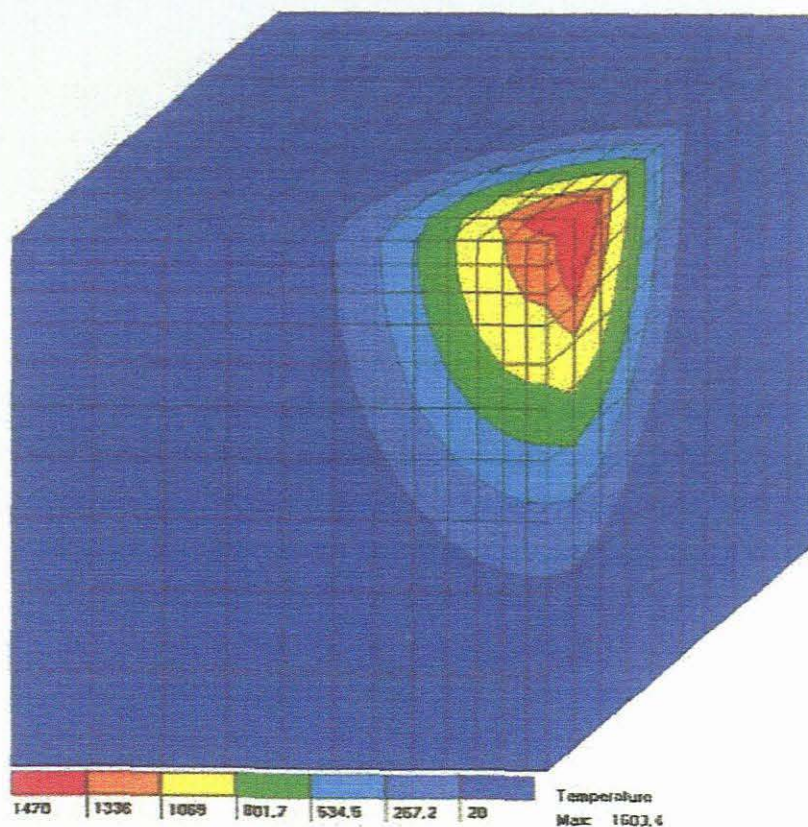


Figure 2.3 FE Calculated Temperature 3kW, 0.2mm spot

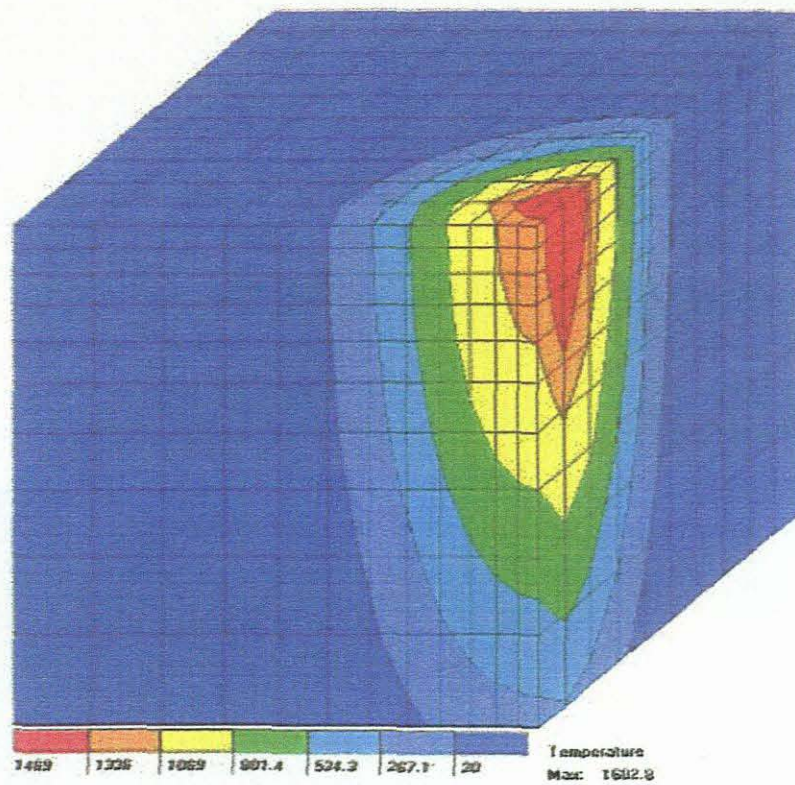


Figure 2.4 FE Calculated Temperature 3.5kW, 0.2mm spot

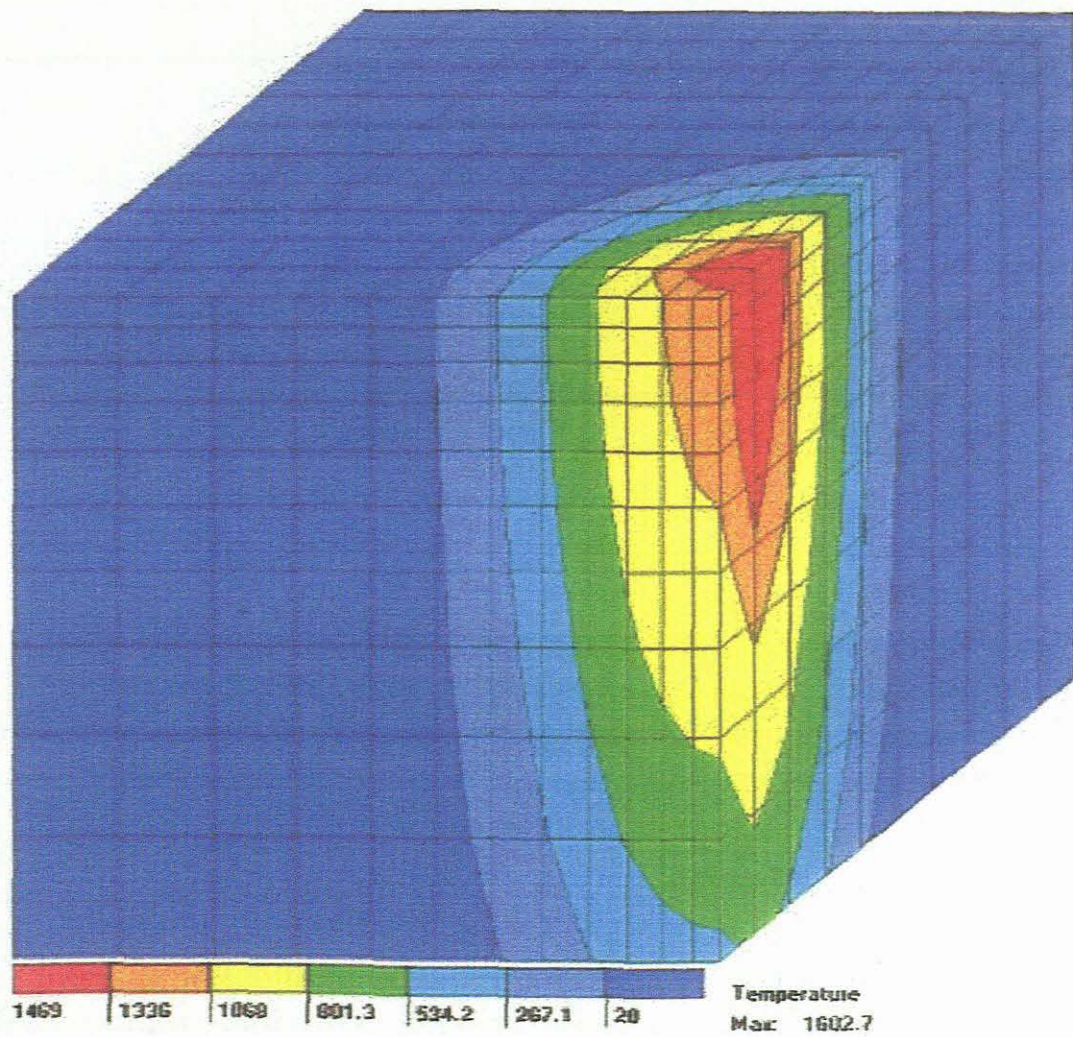


Figure 2.5 FE Calculated Temperature 4kW, 0.2mm spot.

Chapter 3

Laser cladding experiments with Pre-placed powder method

3.1 Introduction

In this chapter, laser-cladding experiments using the pre-placed powder method were designed and performed. A 5 kW CO₂ laser TRUMPF LASERCELL 1005 was used as the laser heat source. Single track clad layers were produced. Larger areas samples were treated as well by applying several adjacent Multi-pass laser-cladding tracks. Several machining parameters were varied. Those parameters include the scanning speed, the laser power, and the laser beam spot diameter.

A number of different percentage compositions (by mass) of tungsten carbide (WC) powder in a nickel base were used to produce samples. The percentage composition was varied from 10% to 40%. Samples series 1 to 13 are single track cladding; samples 14 to 24 are adjacent multi-pass over lapping laser cladding. Argon was supplied to the processing area to prevent the clad layers from oxidising and to protect the optical system. The experimental set-up is shown in figure 3.1.

Remelt treatment technology methods were adopted on some samples (sample 19, 22, 23 and 24). Preheating before laser cladding and heat preservation after experiments were adopted on sample 21 and 23.

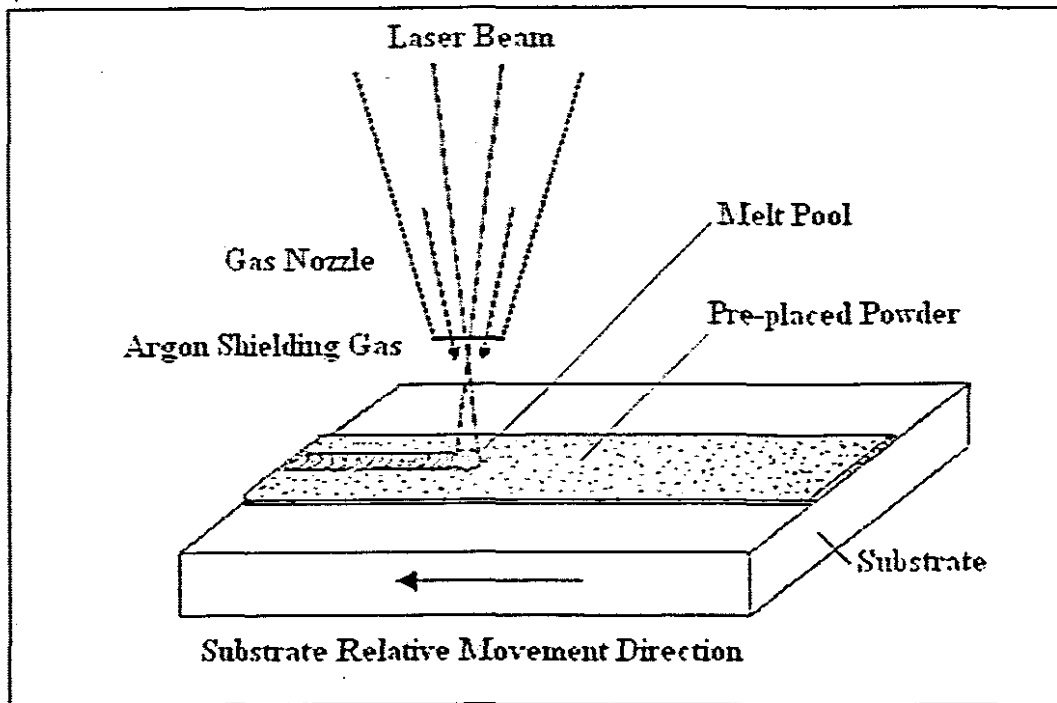


Figure 3.1 Experimental set up laser cladding with pre-placed powder method; the sample performs a relative movement to the laser beam. The area exposed by the laser beam is treated. Applying several adjacent tracks can treat samples with larger areas.

3.2 Composition design of Ni-base alloy cladding materials

At present, there are not too many special and commercial alloy powders for laser cladding materials conveniently available for us to use. The applied powders are the same as those used in flame and plasma spraying. Most of the experimental laser cladding research also adopts these kinds of alloy powder. Commonly, people choose their cladding alloy materials based on the application request and the state of the substrate. Cladding materials are mostly composed of fusible Hyper-eutectic alloy powders, which have high flexibility.

When selecting coating materials, the melting point of the substrate must preferably be higher than that of the coating material. If this is not the case, then it is possible that during solidification and subsequent cooling of the clad layer, the substrate region just underneath it can be heated to a temperature over the melting point. This region will subsequently lose its strength. Under the effect of the stress of the clad above, hot tearing will occur along this region [Li, 1992]. Such a situation will in any case result in porosity along the interface.

Fusible hyper-eutectic elements currently are boron and silicon. Nickel-base alloy powders for plasma and flame spraying contain a high proportion of boron and silicon. The addition of boron and silicon improves the wetting behavior so that smooth surfaces can be achieved [Wolf, 1995].

It is known that the addition of elements of boron, silicon and carbon will create a hard phase. The formation of hard borides and silicon carbide improves the wear resistance and hardness. This will increase the hardness of the cladding layer. However, a large presence of these hard phases makes the coating very brittle [Arlt, 1994; Grunenwald, 1992] and decreases plasticity, and increases the crack opportunity as well. A lot of research experiments indicate, the higher the proportion of boron, silicon and carbon the harder the clad layer while the likelihood of cracking increases.

In addition, boron and silicon have the benefits of deoxidizing, improving slagging, wetting the interface and resisting the appearance of gas porosity. But the solubility of boron in Fe and Ni is almost zero. So they separate out easily and congregate at the crystal interface causing cracks. Silicon elements in alloy powders with high a contents of Nickel always tend to segregate, so the hot cracking tendency will increase.

According to metal theory, high carbon content can increase hardness. But with the increasing of carbon content, brittleness will increase as well. The probability of crack formation will increase too. On the other hand, it is possible that chemical combination of carbon and chromium will form chromium carbide. This will decrease the chromium content in the cladding layer reducing corrosion resistance of the laser-cladding layer.

In fact, high-energy laser heat source has a special function to produce various strengthening effects. Some scholars who did a lot of experiments proved that for the same powder, the hardness of the laser-cladding layer would increase 20%–40% compared to a thermal-spray welding layer. [Shi Shihong, 1999] So, there are various benefits in decreasing the carbon content in laser cladding powder.

Based on the literature survey and the above analysis, the laser cladding alloy powder the author chose for the pre-placed powder laser cladding experiments was Nickel alloy powder-SM505. Its chemical composition is listed below. (The Nickel-base alloy's chemical components percentage is based on weight.)

Percentage of Nickel-base alloy's chemical components are based on weight					
Cr (Chromium)	B (Boron)	C (Carbon)	Si (Silicon)	Fe (Iron)	Ni (Nickel)
14.25 %	3.5 %	0.6 %	2.0 %	4.0 %	75.65%

Table 3-1 Chemical components of Nickel-base alloy for laser cladding experiments with pre-placed powder method

3.3 Selection of the sticking agent (chemical binding)

In the experiments of this chapter, laser cladding with pre-placed powder were performance as shown in Figure 3.2 right side. Laser cladding with pre-placed powder is the most common cladding method. The powder must be mixed with a chemical binder to ensure that it will stick to the substrate during the process. It has to be given enough structural strength to withstand forces imposed by gas flows or gravitation [Arlt, 1994]. The chemical binder evaporates during the process. This can result in some porosity in the clad layer.

Laser cladding with pre-placed powder, when compared to powder injection method, has a slightly lower heat conductivity and increased energy requirements. It is the most convenient and economical method though especially for lab experiments.

In order to prevent the remnant melted sticking agent from infusing the alloy coating and influencing the quality and designed performance of the alloy coating the sticking agent has to have specials chemical characteristics. It must be provided with a high volatility, and cannot damage and influence the performance of the cladding layer. In addition, a very important requirement is the absence of water.

Based on current and actual experiments many of sticking agents can be selected. Generally, people select varnish, silicate glue, soluble glass, oxo-cellulose ether, cellulose acetate, alcohol-rosin solution, hydrocarbon solution, epoxy resin, acetone-borax solution, isopropyl alcohol, and even ordinary paste [Wang Jiajin, 1992].

Some research results [Yan Yuhe, 1994] show that silicate glue and soluble glass are dilatible, and this will result in the sedimentary layer detaching from the substrate. On the other hand, during the laser cladding process, due to the high power laser and the resulting high temperature, most of the sticking agent will burn, and after a decomposition reaction carbon black will come into being. This may be result in alloy powder splashing from the pre-placed layer and periodically shielding laser radiation. This will result in a cladding coating with an unequal clad height, and a decrease of alloy element content.

When using cellulose type sticking agents, the above-mentioned problems will not occur, because under the irradiation of a high-energy laser beam, the cellulose-sticking agent quickly burns up and decomposes resulting in few solid granules remaining. Alloy powder is not ejected and it also ensures that the pre-placed powder layer has a relatively nice absorption coefficient for the laser beam.

Cellulose acetate comes from the following chemical reaction: mix cellulose, acetic-anhydride and acetic acid together, and after an esterification, reaction the result is cellulose acetate. After a partly hydrolytic action of cellulose acetate, cellulose diacetate (CDA) comes in to being. Cellulose dilacerate can be dissolved in an acetone solvent. Cellulose dilacerate-acetone solution characterizes quick-drying and outstanding pellicle intensity [Liu Renqing, 1985].

After mixing the cellulose diacetate-acetone solution with alloy powder, it is quite difficult to paste the powder onto the substrate uniformly due to the higher volatility of acetone. The pasted powder layer shrinks after it dries; a characteristic of cellulose will always cause the pasted layer to curl and detach from the metal substrate. However if a medium volatility organic solvent is added this problem is solved. So, in the pre-placed powder experiments, the author selected an absolute-ethanol to mix with acetone.

Based on the above-mentioned study and comprehensive analysis: if we are able to get the pre-placed powder layer to have a flat surface with moderate volatility, then we will obtain a laser cladding layer of high quality. The cellulose acetate-acetone solution mix with absolute ethanol was selected to be the sticking agent in our experiments. The proportions are as below: the concentration of the cellulose acetate-acetone solution was 5%; the proportion of acetone and ethanol was 3:2. The addition of the sticking agent was controlled within 10% to 25% of the gross weight of all powder and sticking agent. The best-optimized proportion was based on practical experiments.

The use of a chemical binder prevents the powder from being blown away by the shielding gas during processing. Before the laser cladding experiments a chemical binder was first prepared to mix the powders into powder mud. Using a specially made small aluminium mould to place the powder mud onto substrates. Figure 3.2 (left) shows a pre-placed powder sample. After the ethanol and acetone evaporates for several hours, or after putting these samples into a heat treatment kiln with the temperature of the kiln kept between 100°C -200 °C degrees for 1-2 hours to dry the samples, a dry powder layer was obtained that adheres to the substrate.

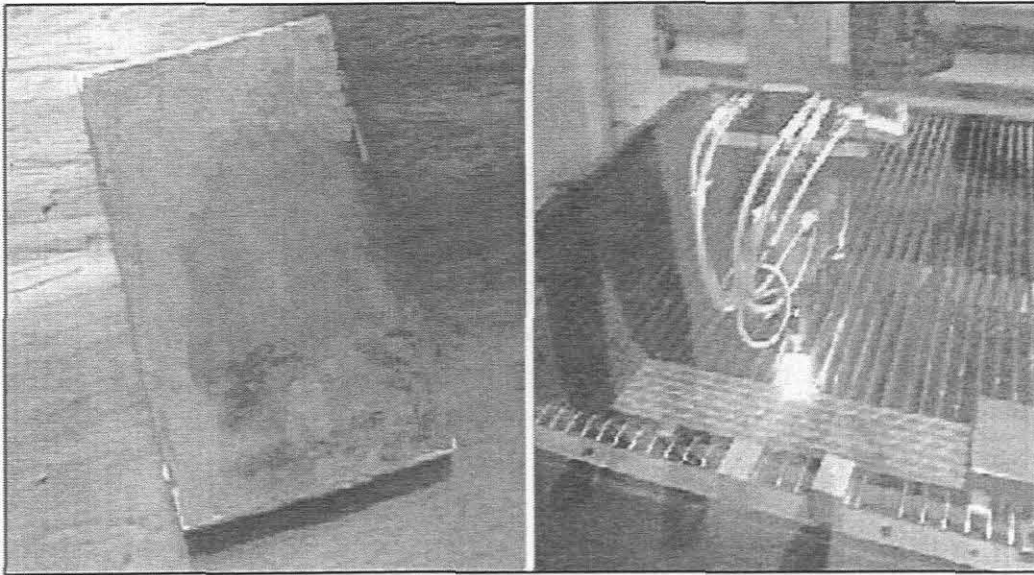


Figure 3.2 Pre-placed powder sample (Left side)
And the laser cladding process at the South African NLC.

3.4 Substrate material and ceramic material

3.4.1 Selection of substrate materials

The substrate material selected for the laser cladding experiments with pre-placed powder method was EN8 mild steel. The chemical components of EN8 mild steel are listed Table 3-2 below:

EN8 Steel	C %	Si %	Mn %	Ni %	Cr %	Mo %	S %	P %
Percentage	0.35-0.45	0.05-0.35	0.6-1.0	-	-	-	0.06 Max	0.60 Max

Table 3-2 Chemical components of EN8 steel

After machining the EN8 steel into some 80mm length \times 50mm width \times 8mm thickness plates and the surface grinding and rust cleaning process, the specimen are degreased with acetone and dried ready for use.

3.4.2 Select ceramic cladding materials

According to the literature of chapter 1, ceramic materials have distinguishing properties that other metal cannot compare with, such as wear-resistance, heat resistance and erosion-resistance and chemical stability. There are a lot of ceramic powders available, such as WC, SiC, TiC, Al₂O₃ and ZrO₂ etc. These powders were developed for the use in plasma and flame spraying. They are also fit for use in laser

cladding because of the same intended functional properties.

But there are thermal stress created by the high thermal gradient built up during the cooling stage. And the thermal expansion coefficients are difference between materials. This is the reason for the formation of cracks in the clad layer [Zhang, 1994; Zhou, 1991]. Layers that are characterized by the presence of hard and brittle particles, such as carbides (tungsten carbide etc.), are especially prone to cracking. Ceramic layers are also vulnerable to cracking, because of their limited ductility combined with the difference in thermal expansion coefficients compared with metals [VandeHaar, 1988].

Tungsten carbide (WC) is a kind of ceramic material that has distinguishing properties that other metal cannot compare with, such as wear-resistance, heat resistance and erosion-resistance and chemical stability. The following Table 3-3 below shows the physical properties of the cladding materials:

	Density (g/cm^3)	Melting point (K)	Hardness HV (Kg/mm^2)
Tungsten carbide	15.8	2873	1800
Ni-base alloy	7.68-7.8	1323-1423	—

Table 3-3 Physical properties of the cladding materials

From the above table, we know that the density of tungsten carbide (WC) is much higher the than density of the Ni-base alloy. Actually, what we want to get is an identical distribution density of tungsten carbide in the cladding coating so we can use the density differences between tungsten carbide and Ni-base alloy. We know that the melt pool has the characteristic of fast flow and the no-uniformity of speed field property, this will accelerate tungsten carbide and the Ni-base alloy to float up and sink down. This makes them have the different distribution density in the cladding coating layer. So in our experiments, we select a mixture of tungsten carbide and Ni-base alloy, the granularity size of the Nickel-base alloy granule is 50-100 μm . and the granule size of tungsten carbide (WC) is 50-150 μm .

3.5 Proportion control of tungsten carbide

Because of the obvious differences of thermal expansion coefficient and elastic modulus between the Nickel based alloy and tungsten carbide (the detailed values are listed in Table 3-4 below) thermal stress, air holes and cracks could be created in the cladding layer.

Cladding Materials And Substrate	Density (g/cm ³)	Melting Point (K)	Thermal Conduction Coefficient k [Wm ⁻¹ K ⁻¹]	Linear Expansion Coefficient (10 ⁻⁶ /k)	Elastic Modulus E_c (Gpa)
Tungsten carbide	15.8	2873	121	4.5	651
Ni-based alloy powder	7.69	1323~1423	21.5	20.7	90
EN8 Steel	7.8	1673	36.7	13.2	206

Table 3-4, Physical properties of cladding materials and substrate

Analysis thermal stress in clad layer:

According to [Jiang Yongqiu, 1993], we can adopt the following formula to solve thermal stress σ_c

$$\sigma_c = E_c \cdot (\alpha_c - \alpha_s) \cdot \frac{\Delta T}{(1 - P_c)} \quad (3.1)$$

In the above Formula (3-1), where

E_c is Elastic modulus of cladding layer, GPa.

α_c is thermal expansion coefficient of cladding layer, (10⁻⁶/k).

α_s is thermal expansion coefficient of substrate, unit is (10⁻⁶/k).

ΔT is the temperature difference between cladding layer's melting point and room temperature.

P_c is the Poisson ratio of cladding layer.

From the formula (3-1) it can be seen that large differences in thermal expansion coefficients leads to large thermal stresses being created in the cladding layer. Let us suppose that powder materials of the cladding layer are absolutely well mixed, and absolutely proportioned and uniformly distributed. According to He Guanhu's formula, [He Guanhu, 1987], the thermal expansion coefficient of the cladding layer A_c , can be calculated by the simple principle of superposition.

$$A_c = \sum A_i \cdot V_i / V \quad (3.2)$$

In the Formula (3-2), A_i and V_i are the thermal expansion coefficient and volume of one material, and V is the total volume of materials. So we can expediently solve for

every thermal expansion coefficient A_c when we select different proportions of tungsten carbide.

In a similar way, the elastic modulus of the cladding layer E_c can also be solved out via the above method, namely

$$E_c = \sum E_i \cdot W_i / W \quad (3.3)$$

The Nickel-base alloy design was 70% of weight of total cladding powder weight in order to ensure both that there is enough tungsten carbide component in the cladding layer and that there is enough liquid state (formed by melting the Nickel-base alloy component) in the molten pool during the laser cladding process. This also avoids the cladding layer being affected by surface tension, which causes distortion and warping in the opposite direction. In order to do some comparative experiments, the author designed several percentage contents of tungsten carbide (WC). Samples were varied from 10% to 40%, as shown in following Table 3-5.

Group	Tungsten carbide powder	Ni-based alloy powder
1	10% tungsten carbide	+90% Ni-based alloy
2	20% tungsten carbide	+80% Ni-based alloy
3	30% tungsten carbide	+70% Ni-based alloy
4	40% tungsten carbide	+60% Ni-based alloy

Table 3-5 Powder components of comparative experiments

The above Formula 3.2 for calculating thermal expansion coefficient is based on the volume proportion in alloy powder. But in our practical experiments, it is not easy to expediently and accurately measure the powder volume proportion. Thus, we need to change the volume proportion to weight proportion to ease our calculation. The following table 3-6 is the result of the mathematical conversion between weight proportion and volume proportion.

Group	Weight proportion	Corresponding volume proportion
1	10% tungsten carbide + 90% Ni-based alloy	5.13% tungsten carbide + 94.87% Ni-based alloy
2	20% tungsten carbide + 80% Ni-based alloy	10.85% tungsten carbide + 89.15% Ni-based alloy
3	30% tungsten carbide + 70% Ni-based alloy	17.26 % tungsten carbide + 82.74% Ni-based alloy
4	40% tungsten carbide + 60% Ni-based alloy	24.5% tungsten carbide + 75.5% Ni-based alloy

Table 3-6 Mathematical conversions between weight proportions and volume proportion

Based on the material data of the cladding materials in Table 3-4, Formula (3.2) and Formula (3.3), the thermal expansion coefficient and Elastic modulus of the powder was calculated for tungsten carbide and the Nickel-base alloy in different proportions. The calculated results are listed in Table 3-7 below.

Group Number	Powder Components of tungsten carbide and Ni-based alloy	Linear Expansion Coefficient A_c ($10^{-6}k$)	Elastic Modulus E_c (Gpa)
1	10% tungsten carbide +90% Ni-based alloy	19.87	146.1
2	20% tungsten carbide +80% Ni-based alloy	18.94	202.2
3	30% tungsten carbide +70% Ni-based alloy	17.9	258.3
4	40% tungsten carbide +90% Ni-based alloy	16.73	314.4

Table 3-7 Expansion coefficient and Elastic modulus values based on different percentage components of tungsten carbide

The calculated results in Table 3-7 shows that with the increase of tungsten carbide percentage component in the cladding alloy from 10% to 40%, the thermal expansion coefficient A_c decreased from $19.87 \times 10^{-6}k$ to $16.73 \times 10^{-6}k$. The decrease is not too big.

But in contrast, calculated results show that with the increase of tungsten carbide percentage component in cladding alloy from 10% to 40%, the Elastic modulus E_c increased from 146.1 GPa to 314.4 GPa. And the increase is very big.

Table 3-4 shows that linear expansion coefficient of EN8 steel is $13.2 \times 10^{-6}k$, Elastic modulus of EN8 is 206 GPa.

Based on the above data, with the increase of the tungsten carbide percentage component, the expansion coefficient difference between the substrate and cladding layer will decrease, but the difference is not big. So in our experiments, the expansion

coefficient difference factor is not so important. In contrast, with the increase in tungsten carbide percentage component, the Elastic modulus difference between substrate and cladding layer greatly increased. The crack sensitivity will also accordingly increase. So, the Elastic modulus difference greatly affects our alloy components design.

So, for the above reason, when we select the tungsten carbide and Nickel-base alloy mixture, in order to ensure a lesser crack tendency, the components of the cladding materials we designed are 70% Nickel based alloy + 30% tungsten carbide. In order to do some comparative experiments, we also chose some groups of contradistinctive experiments as Table 3-5 shown. By analysis the contradistinctive experimental results, we will study relationships between powder components and wear resist property, and study relationships between powder components and crack properties as well.

3.6 Parameters of Laser cladding with pre-placed powder method

In chapter 2, the author already studied the characteristics of the heat transfer process of pre-placed powder laser cladding. During the process of laser cladding with pre-placed powder, the laser beam must melt the pre-placed layer first. After a melt pool is formed on top of the cladding material it proceeds downwards to the substrate until the substrate is melted so that a clad layer can be formed.

Based on above study in this chapter and analysis calculation in chapter 2, there approximately exists an optimum of components of alloy powder and technology parameters. The experiments that follow were done using the above-mentioned chemical components of alloy powder to do contradistinctive experiments to observe how the change of laser treatment parameters affects performance of laser cladding coating.

The performed experimental procedures are listed in Appendix 2. (Samples 1 series to 13 series are single-track cladding; samples 14 to 24 are adjacent Multi-pass laser cladding with an over lap; Shielding gas used was Argon)

3.7 Experiment results analysis

A variation of the laser power from 1000 W to 1800 W; a variation of the laser beam diameter from 1.5mm to 3.5mm; and a variation of laser scanning speed from 0.1m/min to 1.0m/min showed that a minimum power of 1000 W is required to achieve a smooth single track that is flows out over the substrate. Lower power levels result in the formation of clad layers that are not smooth, narrow or even winding. Poor clads can be higher than the thickness of the applied coating and do not have a fusion bond to the substrate.

The results of laser cladding experiments using the pre-placed power method are listed in Appendix 3. A study of the effects of different laser parameters on the geometrical dimensions of the clad layer will be presented in chapter 5. In the following section, an analysis of the dilution of the laser cladding layer produced using the pre-placed method is given.

Analysis of high dilution;

The pre-placed power methods are particularly useful for workpiece parts or samples that can be treated using one single track. It is of course possible to apply several adjacent overlapping tracks. The following Figure 3.3 shows the cross-sections of several overlapping tracks produced by means of the pre-placed powder method. Overlapping results in increased dilution.

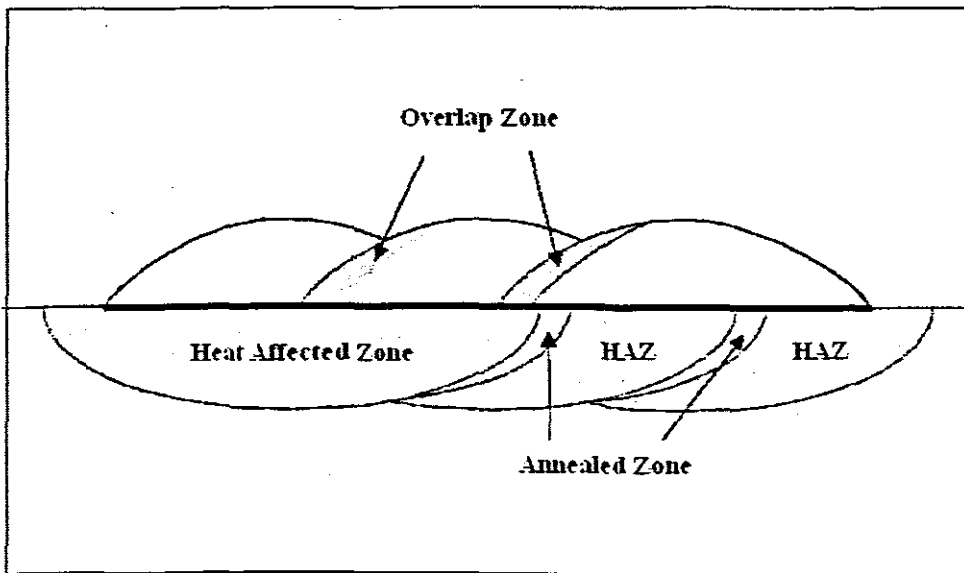


Figure 3.3 Cross-sections of several overlapping tracks produced by means of the pre-placed powder method.

For instance, compare the single-track sample 3-4 with the several adjacent tracks of sample 21, their experiment date list in following Table 3-8.

	Power (kW)	Scanning Speed (m/min)	Beam Spot (mm)	Pre-placed Thickness (mm)	WC %	Dilution %
Single-track Sample 3-4	1	0.2	2.5	0.6	30%	10.3%
Multi-pass Sample 21	1	0.2	2.5	0.6	30%	21.3%

Table 3-8 Data of Single-track sample 3-4 and Multi-pass sample 21

Their substrate condition and powder condition are the same (30% tungsten carbide powder +70% Nickel base alloy powder), and their treatment parameters were also the same but the dilution rate of sample 3-4 is 10.3%; in contrast, the dilution of sample 21 is up to 21.3%.

Dilution results from the requirements of the cladding process. Firstly, the process of pre-placed power laser cladding starts with the formation of a melt pool in the surface of the coating material. Then the melt pool propagates to the interface with the substrate. At this moment, continued heating ensures that the melt pool is extended to the substrate and that a strong fusion bond is achieved. Laser heat input must be well controlled to prevent deep melting of the substrate and the therefrom-resulting severe dilution on the one hand, and to achieve a strong fusion bond on the other hand.

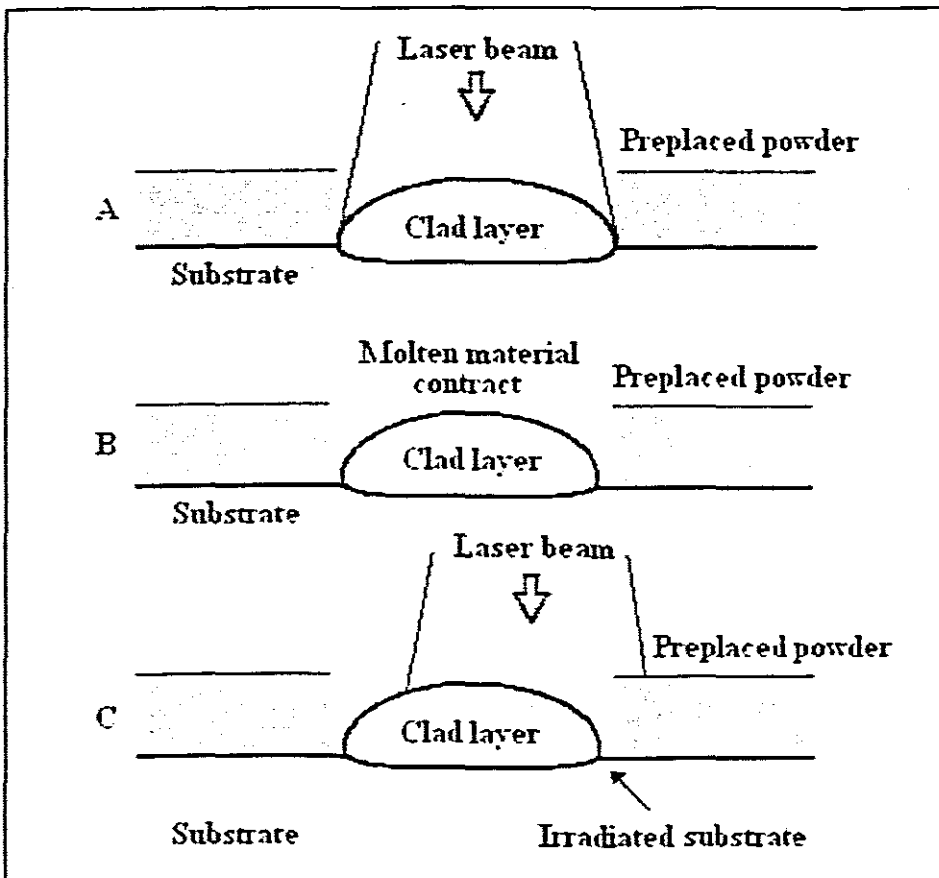


Figure 3.4 An illustration of increased dilution for several adjacent tracks A: First clad track produced. B: Molten material contracts during the solidification. C: application of the next track, the substrate next to the clad layer is exposed to the laser beam.

The above Figure 3.4 illustrates this process. Before the first clad track is produced, the pre-placed material covers the whole area of sample. The laser beam melts a part

of the coating. After the laser beam passes the molten material contracts due to surface tension. Therefore, the substrate area directly next to the produced clad layer is not covered with pre-placed powder material anymore. When the next track is made, the laser beam directly irradiates the non-covered part of the substrate. Deeper melting of the substrate occurs in this area.

3.8 Conclusions

In this chapter, laser-cladding experiments with pre-placed powder method were designed and performed.

The applied powders for laser cladding are the same as those used in flame and plasma spraying. A composition design for cladding materials must obey the following principle: to choose cladding alloy materials based on the application requested and the condition of the substrate. Components of cladding materials should be selected to be a fusible hypereutectic alloy powder, which is highly flexible. The proportion of boron, silicon and carbon can increase the hardness of the clad layer but the probability of cracks forming will increase. There are various benefits of a suitably decreased carbon content in the clad powder.

The choice of the sticking agent, must obey the following principle: It must be provided with a high volatility, be non-hydrous and should not damage the performance of the cladding layer.

The proportion of tungsten carbide also needs to be controlled. From calculations we see that in order to prevent cracking while enhancing the hardness of the clad layer, the optimal components of cladding materials are a 70% Nickel based alloy + 30% tungsten carbide.

Applying several adjacent tracks using a pre-placed powder method will result in a relatively increased dilution phenomenon, because after laser beam passes, the molten material contracts due to surface tension. Therefore, the substrate area directly next to the produced clad layer is no longer covered with pre-placed powder. When the next track is made, the laser beam directly irradiates the non-covered part of the substrate. Deeper melting of the substrate occurs in this area. So a relatively increased dilution occurs.

Chapter 4

Laser cladding experiments with Powder injection method

4.1 Introduction

In this chapter, laser-cladding experiments with powder injection method were performed. A 5 kW CO₂ TRUMPF LASERCELL 1005 laser was used as a heat source. A Powder feeder (GTV Lucken Back) was used for the powder supply for the directly injected powder experiments conducted.

A mixture of 50% Nickel alloy powder and 50% tungsten carbide (WC) powders was applied as the cladding material. The powder was transported from the feeder to the process area by powder feeder. Powder was supplied to the melt pool by means of a powder nozzle with a diameter of 2.0 mm. Nozzle stand off was 10mm and 13mm. Nozzle degree was 45 and 60 degree. The substrate material is EN9 steel. It was polished and degreased before experiments.

Single track clad layers were performed (Samples 10A, 10B, 10C and 10D). Larger areas samples were treated as well by applying several adjacent tracks (From Sample

1A to 9B). Several machining parameters were varied. Those parameters include the laser power (from 2kW to 5kW), the laser scanning speed (from 0.3m/min to 1.2 m/min), the laser beam spot size (from 3.5mm to 5mm), and the resulting specific energy (from 34 Jm^{-2} to 200 Jm^{-2}). Argon was used as the shielding gas for the protection of the samples from oxidation as well as the carrier gas for the injected powder. The nozzle angles used were 45 degrees and 60 degrees. The powder injection angle was measured with respect to the horizontal.

The relationship between the powder injection angle and the clad height was studied and a conclusion was drawn. The crack behavior of the laser-clad layer performed by powder injection method was quantified and studied, and conclusions were drawn.

The experimental set-up is shown in the following Figure 4.1.

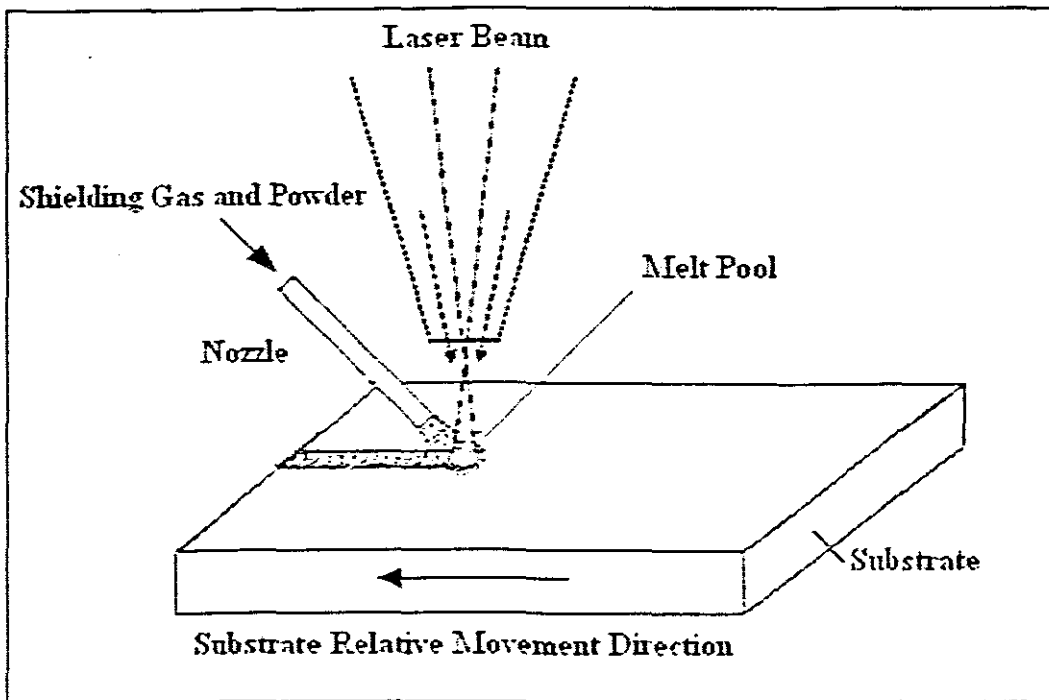


Figure 4.1 Laser cladding using the Powder injection method, the sample performs a relative movement to the laser beam. Argon acts as shielding gas for the protection of the samples to oxidation as well as the carrier gas for the injected powder.

4.2 Powder injection method versus pre-placed powder method

In chapter 3, the author designed a pre-place powder method to do laser cladding experiments. The pre-placed powder method is the most straightforward one to use; the powder is applied as a paste (mixture of binder and powder) on the substrate. So no special equipment is required. It is very easy to achieve. But the pre-placed powder method is not suitable for the cladding of larger areas or for large work-pieces where several adjacent partly overlapping tracks are required.

The powder injection method requires the use of a dedicated powder delivery system and a powder nozzle to direct the powder to the desired position. The literature research showed that laser cladding is predominantly performed by powder injection, because that method is more flexible and easier to control. It is a difficult and environmentally hazardous operation to check and adjust the powder injection.

Laser cladding with powder injection did result in some good quality clad areas. The powder injection process starts with the formation of a melt pool in the substrate. Simultaneously, powder particles of the coating material, are injected as a powder stream into the laser generated melt pool and melts straightway; a strong fusion bond between the coating material and substrate is achieved immediately. In addition, as mentioned in chapter 1, a preheating phenomenon exists in the process: The particles are preheated during their flight through the laser beam, melting of the particles starts after they enter the melt pool.

The following Figure 4.2 shown a powder feeder (left side) and a practical process of laser cladding using powder injection (right side). Aluminium foil is used to prevent reflected laser light damaging the feed tubes.

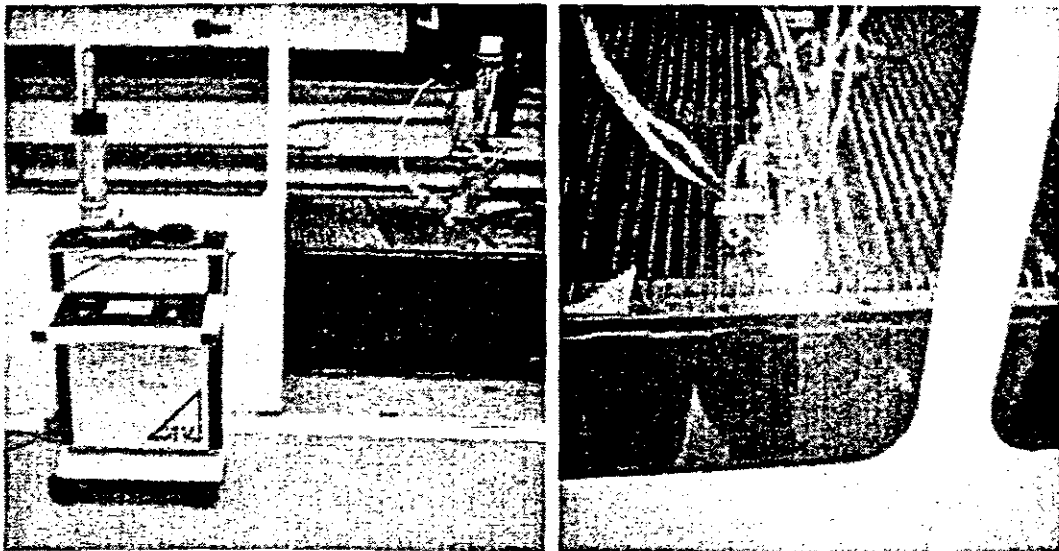


Figure 4.2 Powder feeder (Left side), and a practical process of Laser cladding using powder injection (Right side)

The powder injection laser cladding process has several other advantages over the pre-placed powder laser cladding process: (1) For larger areas, which require the application of several adjacent tracks, the clad can be produced with less dilution. Contraction of the clad layers on cooling down still occurs, but because material is fed to the substrate next to the previous track no part of the substrate is irradiated unnecessarily; (2) the coating thickness can be varied by controlling the material feed

rate; (3) products with a complex geometry can be treated, because material is fed continuously to the interaction zone. The flowing out of the molten material by gravitation is no longer a problem because of this.

But a survey of the available literature reveals that the powder injection method has poor powder efficiency. Less than 30% of the injected powder was utilized for the building of a clad track. The literature also reveals that laser cladding is not a mature technique yet.

A lot of research is being done on how to improve the powder utilization of the powder injection laser cladding process. Liu Ximing studied the factors which influencing the effective utilization rate of cladding materials [Liu Ximing, 2000]. The study indicated that a reasonable matching of powder feeder device and the processing parameters could result in an optimum effective utilization rate of the coating materials. In the future better powder feeder equipment will be needed to satisfy this application.

In order to allow the cladding of products by non-academic personnel and, an effective transfer of results from laboratory to production environment, dedicated powder injection equipment, special optical systems and accurate process control systems are required.

The following Figure 4.3 is a sample performed with the powder injection method by applying several adjacent tracks.

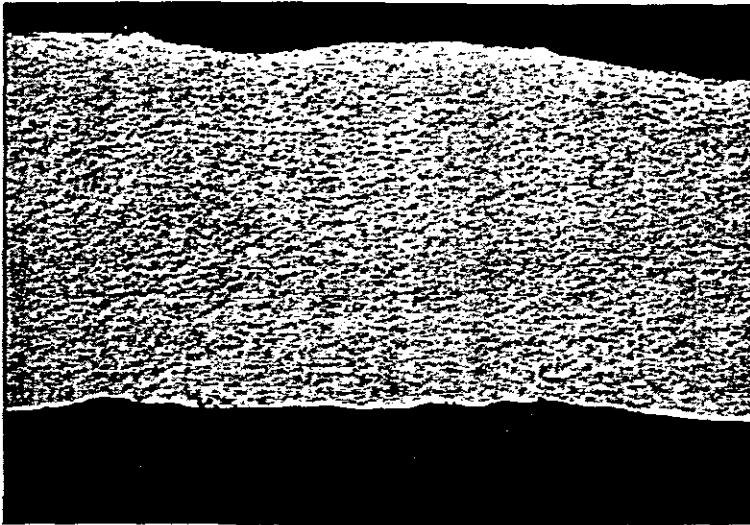


Figure 4.3 A sample performed with the powder injection method
By applying several adjacent tracks

4.3 Powder injection experiments

4.3.1 Cladding materials

The cladding material selected for the powder injection method experiments is a mixture of Nickel-base alloy powder and tungsten carbide powder (50% Nickel based alloy powder + 50% tungsten carbide powder). It was supplied to the melt pool by means of a powder nozzle. And the nozzle angles used were 45 and 60 degrees.

The grain size of the Ni-base alloy granule is 50-110 μm . and the granule size of tungsten carbide is 50-150 μm . Chemical components of the Nickel based alloy powder is listed as below in Table 4-1. (Percentage is based on weight).

Nickel-base alloy's chemical components' percentage is based on weight					
Cr (Chrome)	B (Boron)	C (Carbon)	Si (Silicon)	Fe (Iron)	Ni (Nickel)
17.5 %	3.5 %	1.0 %	4.0 %	4.0 %	70.5%

Table 4-1 Chemical components of Nickel base alloy powder
For powder injection method

	Density (g/cm^3)	Melting point (K)	Grain size (μm)
Tungsten carbide	15.8	2873	50-150
NI-base alloy	7.7	1297	50-110

Table 4-2 Physical properties of the cladding materials (Powder injection)

4.3.2 Substrate material

The substrate material for laser cladding experiments with powder injection was an EN9 equivalent steel, BENNOX. Before the cladding experiment, the steel was cut and machined into some 120mm length \times 50mm width \times 8mm thickness plates. They were sandblasted and degreased with acetone.

In total 10 plates of EN9 steel were prepared for our experiments. The chemical components of the EN9 steel substrate are listed in Table 4.3.

EN9 Steel	C %	Si %	Mn %	Ni %	Cr %	Mo %	S %	P %
Percentage	0.5- 0.6	0.05- 0.35	0.5- 0.8	-	-	-	0.06 Max	0.06 Max

Table 4-3 Chemical compositions of EN9 steel substrate

4.3.3 Experiment parameters

In total 21 experiments were performed. During each experiment 5-8 adjacent, partly overlapping tracks were applied with a beam diameter of 2.5 mm, 3.5 mm and 5.0 mm. The step overs were: 1, 1.5, 2 and 2.5. Several process parameters were varied. The varied process parameters are shown in Table 4-4.

No.	Power (kW)	Speed (m/min)	Spot (mm)	Argon (L/min)	Feed Rpm	Step Over	Nozzle (Degree)
1A	2	0.3	2.5	6	5	1.5	45
1B	2	0.3	3.5	6	5	1.5	45
2	5	1.2	5	4	10	1	60
3A	2	0.3	3.5	4	2	1.5	45
3B	2	0.3	3.5	4	5	1.5	60
4A	2	0.6	3.5	4	5	1.5	60
4B	2	1.0	3.5	4	5	1.5	60
5A	2	0.6	3.5	4	10	1.5	45
5B	2	0.6	3.5	4	10	1.5	60
6A	2.5	0.6	3.5	4	10	1.5	45
6B	2.5	0.3	3.5	4	10	1.5	60
7A	2.5	0.6	3.5	4	10	1	60
7B	2.5	0.6	3.5	4	10	2	60
8A	5	0.3	5	4	10	2.5	60
8B	5	0.6	5	4	10	2.5	60
9A	5	1.2	5	4	10	2.5	60
9B	5	0.45	5	4	10	2.5	60
10A	5	1.2	5	4	10	Single	Fail 60
10B	5	0.3	5	4	10	Single	60
10C	5	0.45	5	4	10	Single	60
10D	5	0.6	5	4	10	Single	60

Table 4-4 The varied process parameters of laser cladding with the powder injection method

4.4 Experiments results

The experimental results are shown in the following tables. Because it is difficult to measure the size of several adjacent tracks samples the following data are not complete. So the study of the effect of the variation of laser parameters on clad geometric dimensions and dilution in chapter 5, will be based on the data of cladding sample produced with the pre-placed powder method of chapter 3.

Sample Number	Clad Width (W_c) [mm]	Total clad height (T_c) [mm]	Clad Height (H_c) [mm]	Clad depth (D_c) $D_c = T_c - H_c$ [mm]	Dilution	Special Energy $E = P/DV$ [Jm ⁻²]
1A	---	---	---	---	---	160
1B	---	---	---	---	---	114.3
2	---	---	1.02	---	---	50
3A	---	---	---	---	---	114.3
3B	---	1.13	---	---	---	114.3
4A	---	0.51	---	---	---	57.1
4B	---	0.28	---	---	---	34
5A	---	0.7	---	---	---	57.1
5B	---	1.0	---	---	---	57.1
6A	---	1.16	---	---	---	71.43
6B	---	1.37	---	---	---	142.86
7A	---	1.81	---	---	---	71.43
7B	---	1.01	---	---	---	71.43
8A	---	1.97	---	---	---	200
8B	---	1.25	---	---	---	100
9A	---	0.65	---	---	---	50
9B	---	1.77	---	---	---	133
10A	5.34	0.89	0.66	0.23	25.8	50
10B	5.14	1.59	1.43	0.18	12.59	200
10C	5.36	1.08	0.81	0.27	25	133.3
10D	5.32	0.91	0.66	0.25	27.4	100

Table 4-5 Experimental results of laser cladding with powder injection method

4.5 The effect of the powder injection angle on clad height and quality

During powder injection laser cladding, the powder nozzle angle is also an important parameter; the author arranged some samples to study the effect of powder nozzle angle on the size of the clad layer. The following Table 4-6 and Figure 4.4 are data and curves of the effect of the powder injection angle on the clad height.

No.	Power (kW)	Feed (Rpm)	Nozzle (Degree)	Clad Height
5A	2	10	45	0.7mm
5B	2	10	60	1.0mm
6A	2.5	10	45	1.16mm
6B	2.5	10	60	1.37mm

Table 4-6 The experiment values of 5A,B and 6A,B.

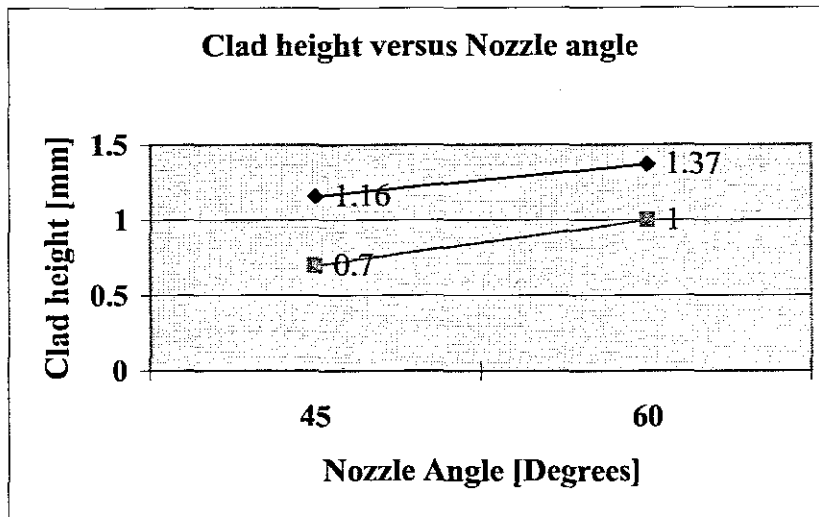


Figure 4.4 Clad heights as function of nozzle degree of powder injection.

Figure 4.4 shows the effect of the powder injection angle on the clad height. The author found that an increase of the powder injection angle results in a higher clad layer; because higher nozzle degrees will result in more powder particles entering into the laser generated melt pool and straightway melts. Author also found that less glowing particles move away from the melt pool area if adopted higher nozzle degree. This phenomenon can also contribute to increase the thickness of clad layer.

But the author also found that after adopting a higher powder nozzle angle, the surface quality of the laser clad decreased. The following Figure 4.5 shows different nozzle angles resulting in different surface quality. For a practical laser cladding process, where the quality of the clad layer is the most important factor, the powder injection angle must be limited to 45°.

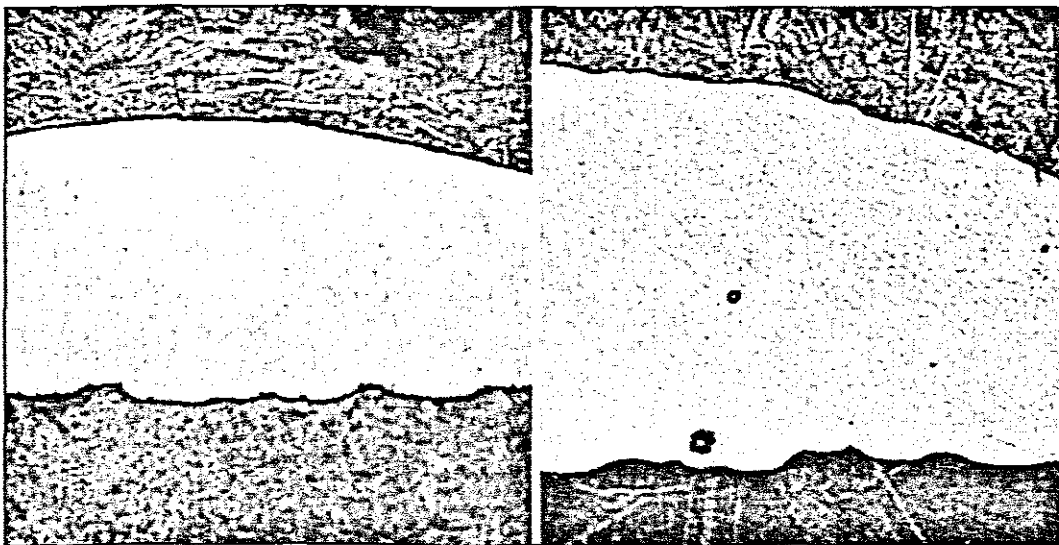


Figure 4.5 Higher nozzle degree results in a reduced surface quality.
Sample 5A (Left side, 45degree), Sample 5B (Right side 60degree)

4.6 Powder particles splash and ricochet phenomenon

During the powder injection method experiments, the author found some glowing powder particles move away from the melt pool area. It indicated that those particles that have splashed and ricocheted from the substrate are exposed to laser radiation long enough to absorb laser energy to start glowing. This phenomenon is one reason that the powder efficiency was very poor.

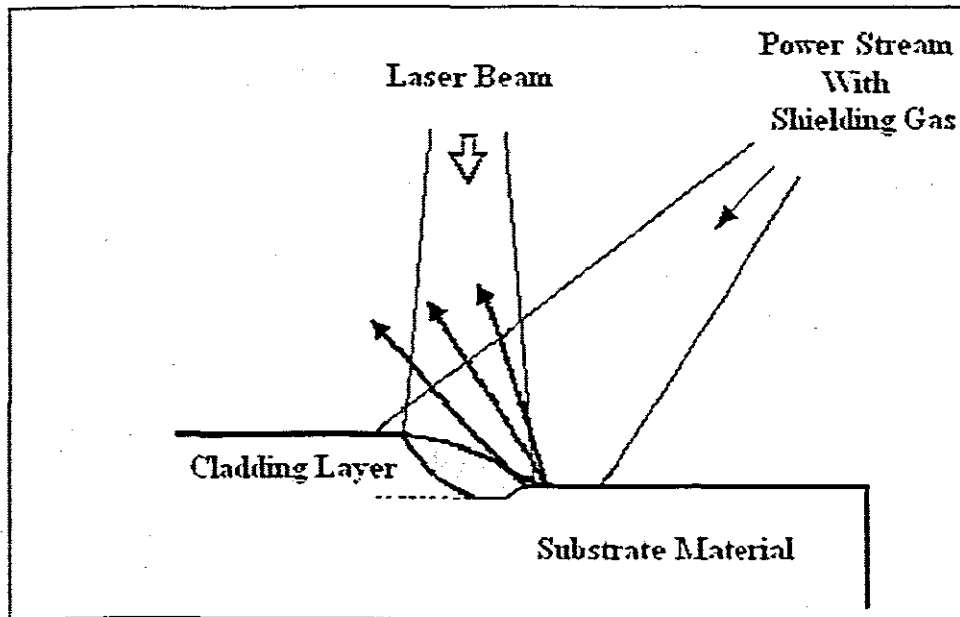


Figure 4.6 Particles splashed and ricocheted from the substrate
Are exposed to laser radiation start glowing

4.7 Crack behavior:

Crack behavior is a big problem during laser cladding process. In the powder injection experiments of this chapter, the crack behavior of the clad layer produced with the powder injection method was investigated. The author found no cracks in layers of single-track samples (from 10A-10D), but for the samples with several adjacent tracks cracks appeared in the overlap area and some other types of cracks also occurred.

The following Figure 4.7 shows a crack in the overlap area.

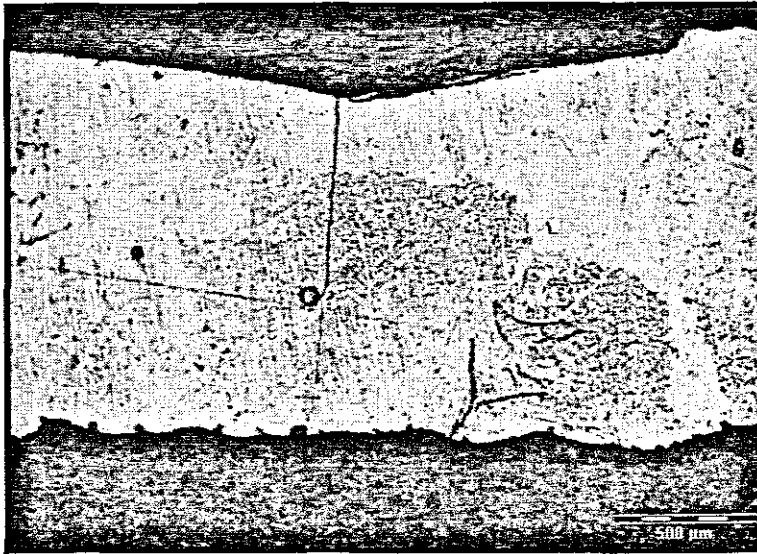


Figure 4.7 A crack sample (crack occurs in overlap area)

The following Table 4-7 provides the statistics of cracks

No.	Power (kW)	Speed (m/min)	Spot (mm)	Crack numbers	Occur Area
1A	2	0.3	2.5	No crack	
1B	2	0.3	3.5	No crack	
2	5	1.2	5	No crack	
3A	2	0.3	3.5	1 small	clad layer middle
3B	2	0.3	3.5	2 big	Clad layer middle
4A	2	0.6	3.5	No crack	
4B	2	1.0	3.5	1 big	Overlap area
5A	2	0.6	3.5	1 big	Overlap area
5B	2	0.6	3.5	1 big	Overlap area
6A	2.5	0.6	3.5	2 big	Overlap area 1, middle 1
6B	2.5	0.3	3.5	1 big	Overlap area
7A	2.5	0.6	3.5	3 big	Edge of clad layer
7B	2.5	0.6	3.5	1 big Porosity	
8A	5	0.3	5	1 slight	Clad surface
8B	5	0.6	5	1 big	Overlap area
9A	5	1.2	5	No crack	
9B	5	0.45	5	1 slight	Clad surface
10A	5	1.2	5	No crack	---
10B	5	0.3	5	No crack	---
10C	5	0.45	5	No crack	---
10D	5	0.6	5	No crack	---

Table 4-7 A statistics of cracks of powder injection laser cladding layers

A Study the above Table indicates: Most of the cracks occur in the overlap area. There are no cracks occurring in single-track samples. May be due to the fact that there are only 4 single-track samples. But it means the crack probability of multi-pass laser cladding is much higher than that of single-track cladding.

Further study and investigation of crack behavior will be presented in chapter 7.

4.8 Conclusions

Laser cladding is predominantly performed by powder injection, because this method is more flexible and easier to control. Controlling the material feed rate can vary the coating thickness and products with a complex geometry and large area can be treated. But laser cladding using this method is not a mature technique yet. The powder efficiency was very poor due to the low utilization rate of the injected powder.

An increase of the powder injection angle results in a higher clad layer but also results in the decreased surface quality of the laser-clad layer.

During the process of laser cladding with the powder injection method, some of the particles that splash and ricochet from the substrate are exposed to laser radiation long enough to absorbed laser energy and start glowing. This phenomenon is one reason for poor efficiency.

During powder injection laser cladding, most of the cracks appear in the overlap areas. The crack probability of multi-pass laser cladding is much higher than that of single-track cladding.

Chapter 5

Study of cladding shape, microstructure characteristics and formation features of solidification microstructure

5.1 Introduction

The goal of the laser cladding experiments was to achieve good quality clad layers. In this context, a good quality clad layer means no cracks, no porosity, a good bonding to the substrate and a low dilution of the coating material by the substrate.

During the laser cladding process, clad layer properties are influenced by the process parameters. The study of the effect of laser parameter variation on the clad layer enhances the knowledge and prediction of laser cladding results, such as clad width, clad height, dilution, hardness, crack behavior etc.

In this chapter, the author studied and evaluated the effect of laser parameter variation on clad geometry. These parameter variations include laser-scanning speed, laser power and laser beam spot diameter. This study yielded some results, figures and conclusions. In order to conveniently measure the geometry of the samples, the author used single track samples produced by laser cladding with the pre-placed powder

method.

The characteristics of the microstructure of the laser cladding coating and the bonding interface were studied and analyzed. Some features of the solidification microstructure were studied yielding some results. The effect of the laser scanning speed on the crystal grain size was studied as well.

5.2 Effect of laser parameter variation on the clad geometry

During the laser cladding process, the clad layer shape, properties, quality, and microstructure are all influenced by the laser parameters. One purpose of the experiments on laser cladding with pre-placed powder and powder injection was to study the effect of the parameter variation on the clad results and to check and determine the parameters, which are most suitable.

After laser cladding the single tracks samples were cut transversely. The clad width, clad height, total clad height, and wetting angle θ were respectively measured and calculated. The value of clad depth is the total clad height minus clad height. The geometrical dilution of the single track samples were calculated with formula 1.3, i.e. $\eta = D_c / T_c$. Results are listed in appendix 3.

Figure 5.1 describes the cross-section of a single track clad layer with the definition of the geometry: clad height (H_c), clad width (W_c), total clad height (T_c), clad depth $D_c = T_c - H_c$, and wetting angle (θ).

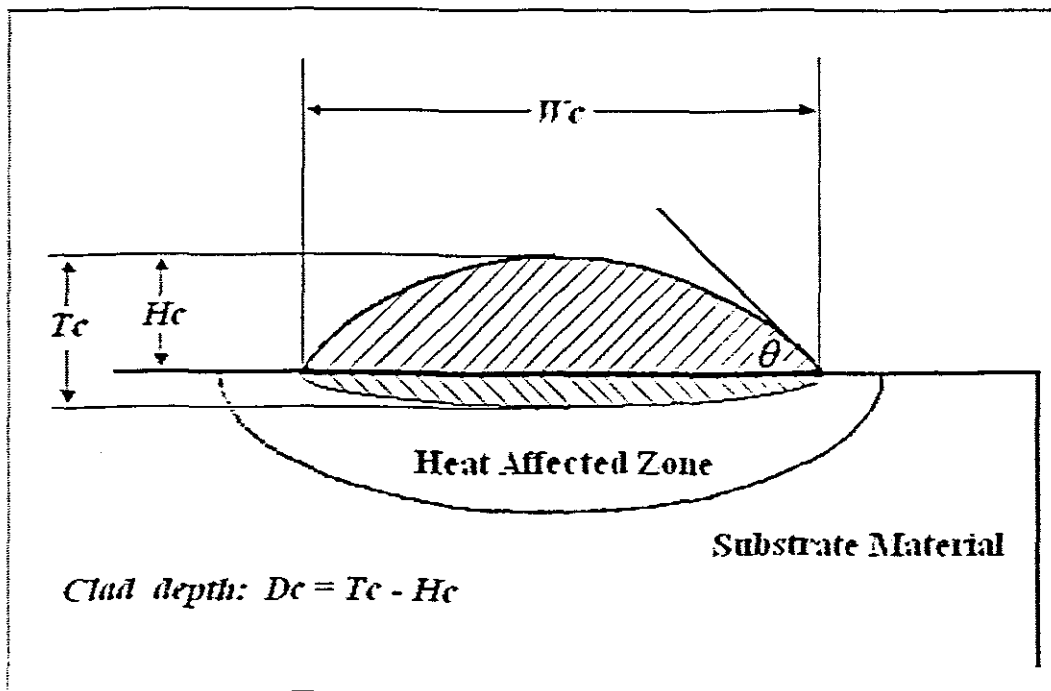


Figure 5.1 Typical cross-sections of single-track clad layers

Produced by means of the pre-placed powder method.

5.2.1 Effect of laser scanning speed variation on geometrical dimension of laser clad layer

The scanning speed is a very important parameter that affects the size of the laser clad layer. Laser scanning speed is one of the factors affecting energy distribution as well. In this section, the author only studies the effect of the laser scanning speed on the shape and geometrical dimension of the laser-clad layer.

The laser scanning speed was varied from 0.1m/min to 1.0m/min for cladding experiments using the pre-placed powder method. The experiments were performed for fixed laser power, laser beam spot diameter, and thickness of pre-placed powder to isolate the effect of scanning speed.

The following figures: Figure 5.2 and Figure 5.3 are two different shapes of clad layer when the scanning speed $V=0.15\text{m/min}$ and $V=0.6\text{m/min}$. Their shape and size are quite different.

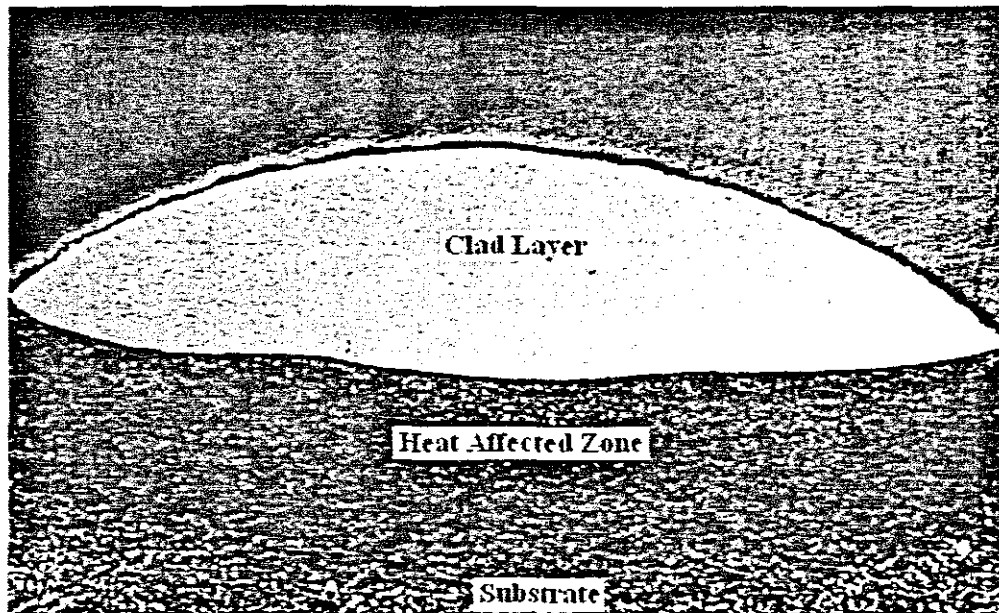


Figure 5.2 Pre-placed cladding Sample 10-1, ($\times 50$), Power 1.0 kW, Beam diameter 2.5mm, $V=0.1\text{m/min}$.

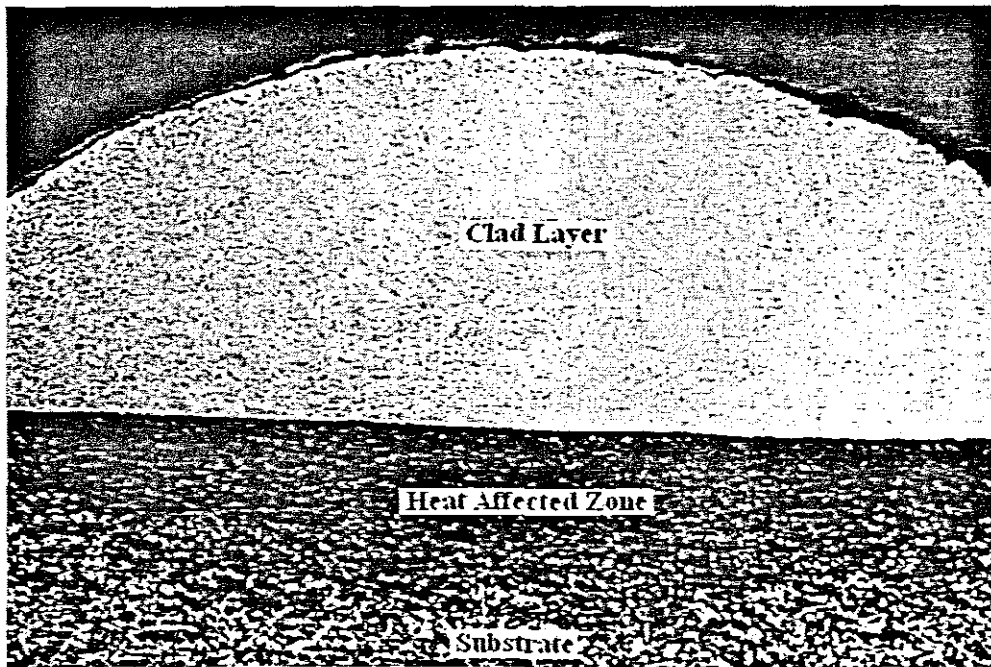


Figure 5.3 Pre-placed cladding Sample 10-4, ($\times 50$),
Power 1.0 kW, Beam diameter 2.5mm, $V=0.18\text{m/min}$.

The author selected 5 different laser scanning speeds, $V_1=0.2\text{ m/min}$, $V_2=0.4\text{m/min}$, $V_3=0.6\text{ m/min}$, $V_4=0.8\text{ m/min}$ and $V_5=1.0\text{ m/min}$ to study. The effect of the laser scanning speed on the single-track clad geometrical dimensions is shown in Table 5-1 and Figure 5.4.

No.	Clad Width (W_c) [mm]	Total Clad height (T_c) [mm]	Clad Height (H_c) [mm]	Clad depth (D_c) [mm]	Geometrical Dilution	Energy Per area [Jm^{-2}]
2-1	2.56	0.66	0.51	0.15	22.7 %	144
2-2	2.53	0.61	0.54	0.07	11.5 %	72
2-3	2.54	0.65	0.6	0.05	7.7 %	48
2-4	2.50	0.66	0.61	0.05	7.6 %	36
2-5	2.45	0.69	0.65	0.04	5.8 %	28.8

Table 5-1 Data of samples from 2-1 to 2-5.

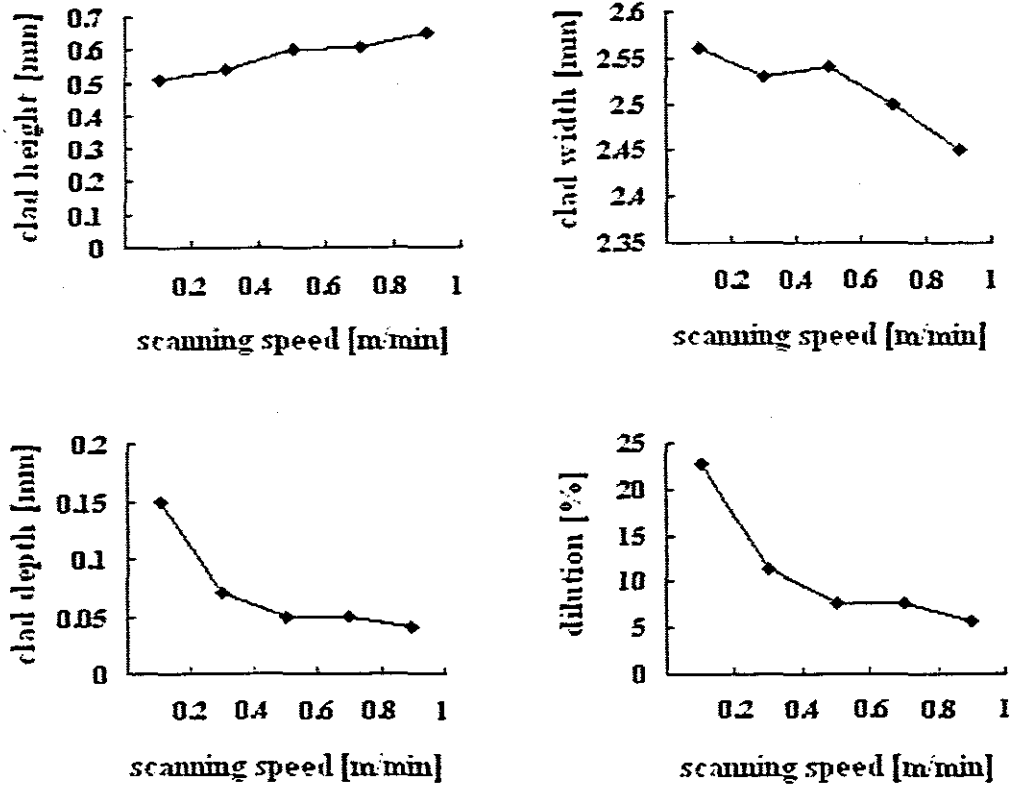


Figure 5.4 Clad geometrical dimensions as function of the laser scanning speed.
(Sample 2-1, 2-2, 2-3, 2-4, 2-5)

The above Table 5.1 and Figure 5.4 indicate that the clad height, clad width, clad depth and dilution rate are a function of the laser scanning speed. The clad height increases with the laser scanning speed, but in contrast the clad width, clad depth and dilution rate decreased (Experiments sample 2-1, 2-2, 2-3, 2-4, 2-5, appendix 2).

The author also found that the variations of the clad width (W_c) were very small, they were approximately close to the diameter of the laser beam (D_l), though scanning speed changed from 0.2m/min to 1.0m/min. It indicates that the clad width (W_c) depends on laser beam spot diameter.

5.2.2 Effect of laser power variation on the geometric dimensions of the clad layer

Laser power is also a very important parameter that affects the size of the laser clad layer and distribution of energy. So it is necessary to describe effect of power variation on the shape and dimension of the laser-clad layer.

Variations of the laser power from 1.0kW to 1.8kW were performed during the laser cladding experiments using the pre-placed powder method. In order to exactly study how the laser power variation influences geometry samples were produced for fixed

laser scanning speed, laser beam spot diameter, and thickness of pre-placed powder.

The study indicates that lower power levels result in the substrate not melting sufficiently. Even no melting of the substrate can occur resulting in the formation of clad layers that are not smooth, narrow or even crooked and intermittent. Low power results in poor metallurgical bonding between the substrate and the cladding coating. Cladding layers formed in this way can be higher than the thickness of the applied coating and do not have a fusion bond to the substrate.

Too high a temperature results in undesirable compounds being formed within the clad layer, additional dilution and distortion of the substrate and a large heat affected zone. The following, Figure 5.5, shows shapes of clad layers with laser powers of 1kW and 1.8kW. Their shape and size are quite different.

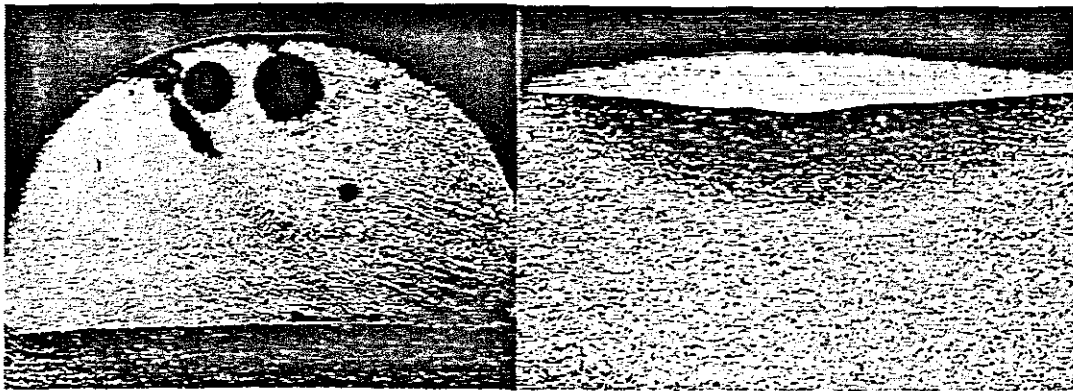


Figure 5.5 Lower power sample 6-4, Power=1.0kW (Left side)
Higher power sample 5-2, Power =1.8kW (Right side)

The effect of the laser power on the single-track clad is shown in Table 5-2 and Figure 5.6.

No.	Clad Width (W_c) [mm]	Total Clad height (T_c) [mm]	Clad Height (H_c) [mm]	Clad depth (D_c) [mm]	Geometrical Dilution	Energy Per area [Jm^{-2}]
2-1	2.56	0.66	0.51	0.15	22.7	144
3-1	2.60	0.67	0.50	0.17	25.3	156
4-1	2.73	0.7	0.48	0.22	31.4	180
5-1	2.76	0.68	0.45	0.23	33.8	216

Table 5-2 Data of samples of 2-1, 3-1, 4-1 and 5-1.

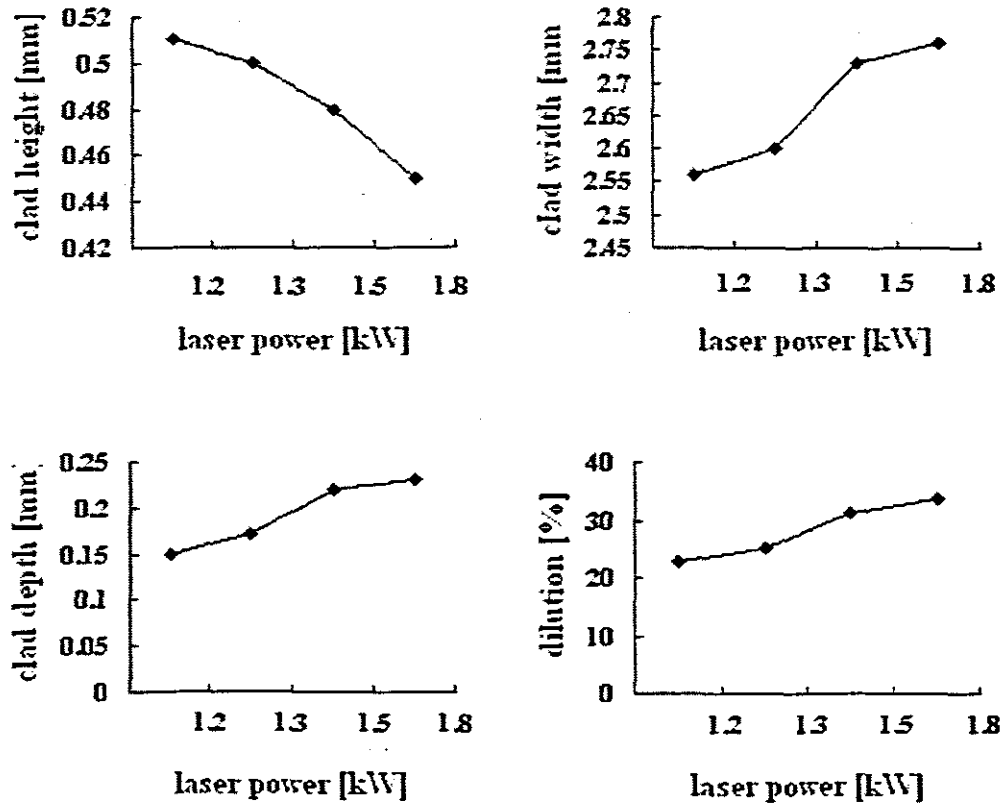


Figure 5.6 Clad geometrical dimensions as function of the laser power.
(Sample 2-1, 3-1, 4-1, 5-1)

A study of the above tables, Table 5-2 and Figure 5.6, indicates: that the clad height, clad width, clad depth and dilution rate are a function of the laser power. The clad width, clad depth and dilution rate increases with the laser power, but the clad height in contrast decreases. (Experiments sample 2-1, 3-1, 4-1, 5-1, Appendix 2). It indicates that the pre-placed powder layer and substrate will absorb more energy, and more fusion area will occur.

The author also found that the clad width (W_c), was approximately the same as the diameter of the laser beam (D_l), though the laser power gradually changed from 1.0kW to 1.8kW. It indicates that the clad width (W_c) mostly depends on the laser beam spot diameter. The effect of laser power on the clad width was not significant.

5.2.3 Effect of laser beam diameter variation on the dimension of the laser clad layer

During the laser cladding process another parameter that influences the geometry of the laser clad layer and the distribution of energy is the laser beam spot diameter.

Variations of the laser beam spot diameter from 1.5mm to 3.5mm were performed for

laser cladding experiments using the pre-placed powder method. Laser scanning speed, laser power, and the thickness of the pre-placed powder were kept constant to study the effects of beam spot size.

The following Figure 5.7, shows shapes of two laser clad layers in which the laser beam diameter are $D_l=1.5\text{mm}$ (Left side) and $D_l=3.5\text{mm}$ (Right side). Their shape and size are quite different.

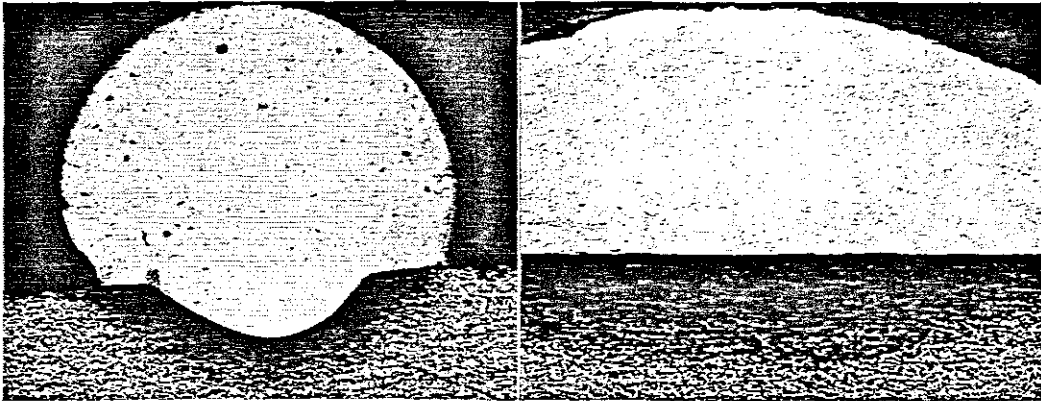


Figure 5.7 Sample 12-1 (Left side, beam diameter 1.5mm)
Sample 12-5 (Right side, beam diameter 3.5mm)

The effect of the laser beam diameter on the single-track clad dimensions is shown in the following Table 5-3 and Figure 5.8.

No.	Clad Width (W_c) [mm]	Total Clad height (T_c) [mm]	Clad Height (H_c) [mm]	Clad depth (D_c) [mm]	Geometrical Dilution	Special Energy [Jm^{-2}]
12-1	1.58	0.67	0.55	0.12	17.9	266.7
12-2	2.08	0.63	0.57	0.06	9.5	200
12-3	2.52	0.63	0.58	0.05	7.01	160
12-4	3.0	0.66	0.62	0.04	6.1	133.3
12-5	3.52	0.65	0.62	0.03	4.6	114.3

Table 5-3 Data of single-track samples from 12-1 to 12-5

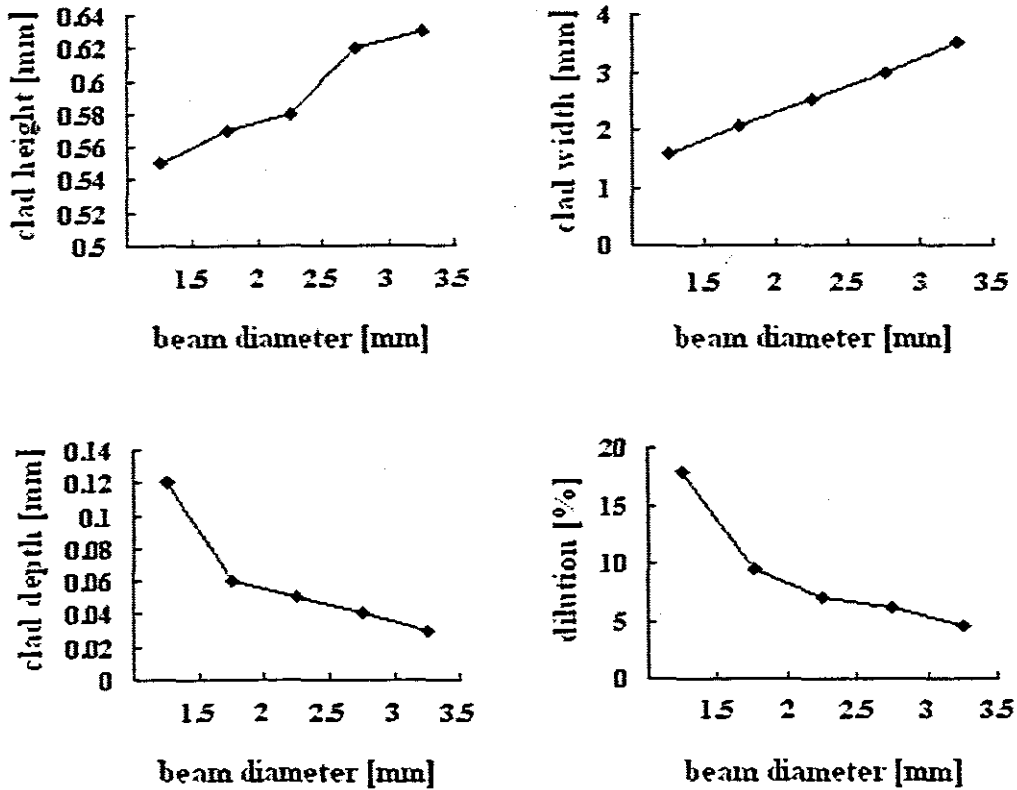


Figure 5.8 Clad dimensions as function of the laser beam diameter.
(Sample 12-1,12-2, 12-3, 12-4, 12-5)

The analysis of the above Table 5-3 and Figure 5.8, indicates that the clad height, clad width, clad depth and dilution rate are functions of the laser beam diameter. The clad height and clad width increases with the laser beam diameter, but in contrast, the clad depth and dilution rate decreases. (Samples 12-1, 12-2, 12-3, 12-4, 12-5, Appendix 2).

With a decrease of laser beam diameter, the energy density will increase. The pre-placed powder layer and substrate will absorb more energy, and this will cause more fusion of clad and substrate. The dilution rate will increase. The clad layer will flow.

Larger beam diameters decrease the energy density. This will result in a lower dilution rate and may result in the substrate not melting sufficiently with possibly no fusion of substrate. It can result in poor metallurgical bonding between the substrate and the cladding coating.

5.3 Microstructure characteristics of laser cladding coating

Compared with other surface strengthening and surface modification technology, the most outstanding feature of laser cladding technology is the formation metallurgical

bonding achieved with a relatively low dilution rate. This ensures outstanding performance of the laser cladding coating. So, it is very important to study microstructure of the cladding coating.

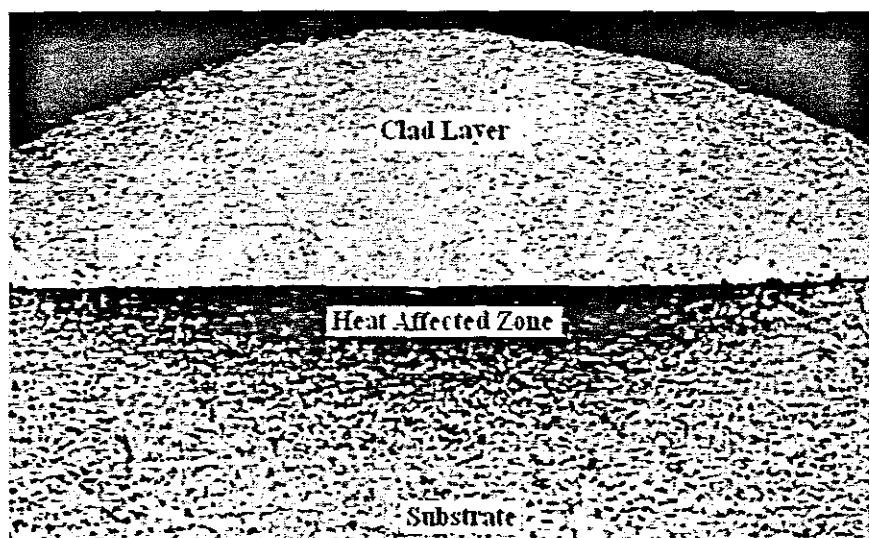


Figure 5.9 The microstructure of the laser cladding coating under low magnification: Sample 2-3 ($\times 50$).

The above Figure 5.9 is a Figure of the microstructure of the laser cladding coating under low magnification. As shown the microstructure of clad layers comprises three zones: cladding layer, bonding zone and heat affected zone.

5.3.1 Solidification modelling of the inside of coating

The laser cladding process is a rapid melting and solidification process.

Some research has been done on the solidification characteristics during the laser treat process [Chen J C.1991; Abboud J H.1992; Shafristen G. 1991; Leach P W.1992; Lugscheider E.1991]. It indicated that when using different cladding parameters, for a single-phase solidification microstructure, the morphology of the solidification structure can be planar, cystiform and dendritic. There are various eutectic crystal microstructure morphologies for the multiphase solidification microstructure.

Ding Peidao [Ding Peidao, 1995] indicated that after the laser beam passes, that due to the effect of forced cooling by substrate, solidification firstly occurs nearby the solid / liquid interfaces at the bottom of melt pool. It then develops in an upward direction to the surface of melt pool. When solidification finishes, in the surface melt that is not solidified yet, a mass of new solidification cores come into being. These cores grow in a perpendicular direction to the melt pool surface center.

Solidification in the laser melt pool tends to start from the bottom and ends at the

surface. In the bottom and middle part of the melt pool, solidification proceeds in the direction perpendicular to the melt pool. Therefore we would expect that the solidification of the laser melt pool has some directional resulting in crystal grains having a similar tropism.

5.3.2 Formation features of solidification microstructure for laser clad layer

We now study the features of the solidification microstructure of the laser cladding layer. The ratio of temperature grads and solidification speed (G_l/V_s) is a controlling factor for the growth morphology of the solidification structure [Kurz W, 1989]. In the melt pool-substrate interface, the solidification speed (V_s) tends to zero, and the temperature gradient (G_l) value is a maximum so the ratio of temperature gradient to solidification speed (G_l / V_s) is very high. With the increase of solidification speed V_s , the ratio of temperature gradients to solidification speed will decrease and the cystiform/dendritic transformation will occur.

In different areas of the cladding melt pool the ratio of G_l / V_s is different. So the final formed microstructures are different.

The morphology of the microstructure is jointly a result of solidification speed and temperature gradients in the crystal direction. Microstructure morphology is not only related to the temperature grads (G_l) and solidification speed V_s , but is also related to the chemical components [Li Qiang, Lei Tingquan, 1999].

During the laser cladding process, there is a difference of concentration between coating components and substrate components. Atomic diffusion will make these components tend to uniformity. Laser cladding is a rapid melting and solidification process, and different atoms have different diffusivity, as a result, components contents in cladding coating and bonding interface are not uniform.

The following Figures 5.10, 5.11 and 5.12 shows the features of the different microstructures of the different regions: the top of the laser cladding layer, the middle region of the cladding layer and the bottom of the cladding layer.

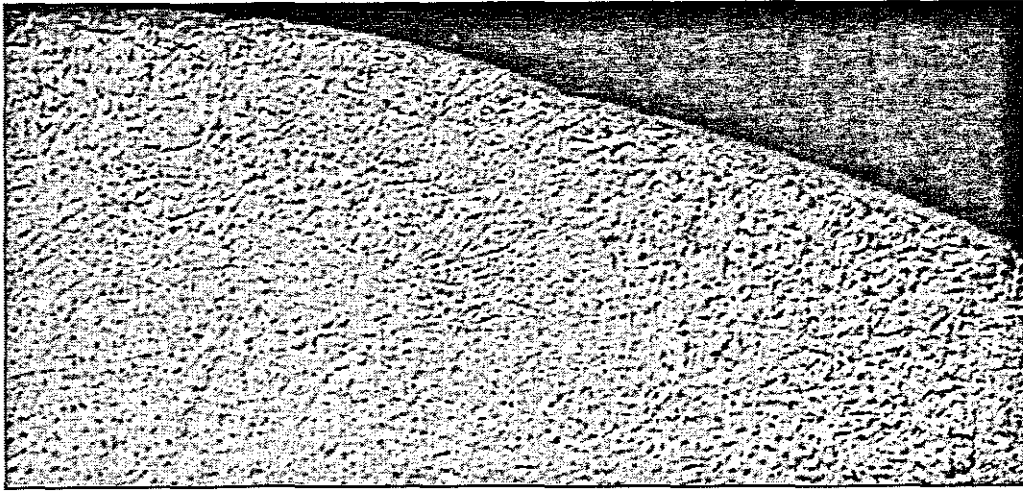


Figure 5.10: Top of the laser cladding layer ($\times 200$)

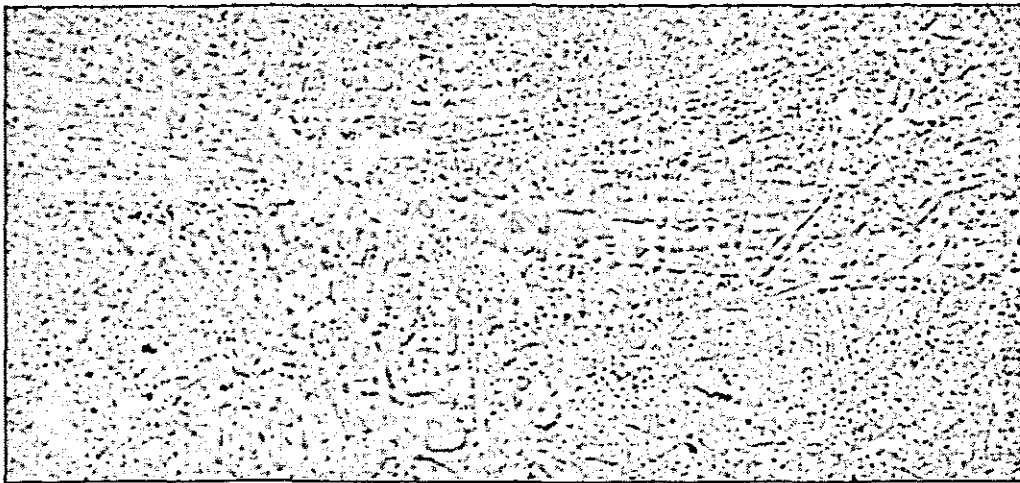


Figure 5.11: Middle region of the cladding layer ($\times 200$)

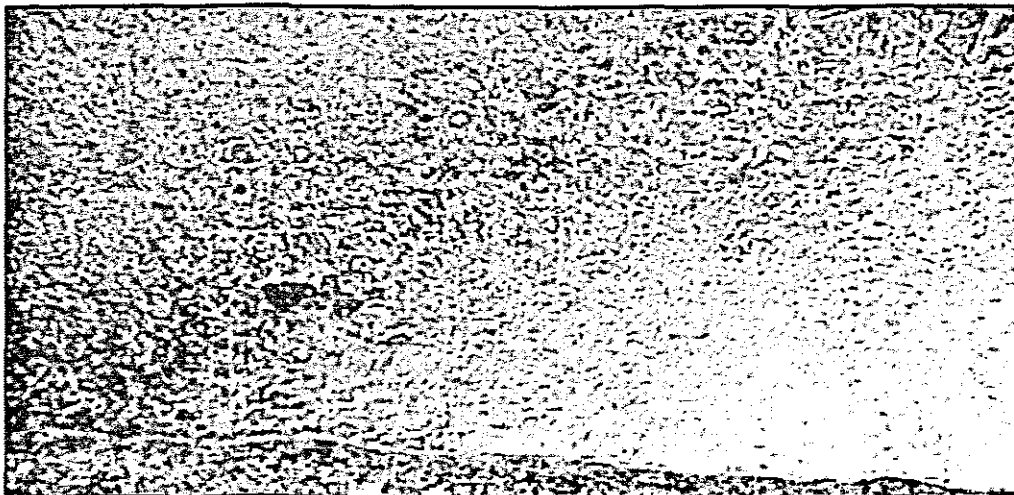


Figure 5.12: Bottom of the laser cladding layer ($\times 200$)

A study of the above Figures indicates that there are different solidification parameters for different positions in the cladding layer. The microstructure at the top of clad layer was the regular pine-tree eutectic crystal structure with the dendrite crystal being the coarser structure. The microstructure at the middle of clad layer was mostly the small cell and columnar crystal structure. The microstructure at the bottom of clad layer was the typical extension growth on a basis plane with small cell crystal structure.

The crystalline anisotropy was a main factor in influencing the crystal growth. Because the components in the micro-zone of the cladding layer are not uniformly distributed, the different elements segregate along the crystalline axes or in inter-dendritic areas resulting in the non-uniform microstructure.

5.3.3 Effect of laser scanning speed variation on microstructure

The effect of the laser scanning speed on the microstructure of clad layer is shown in the following figure 5.13 which shows the microstructure of samples 7-1, 7-2, 7-4 and 7-5. Their scanning speed varied from 0.1m/min to 0.2m/min. The critical grain size gradually decreases from sample 7-1 to 7-5.

For an increase in the laser scanning speed the cooling speed of the liquid metal in the melt pool will increase so there is not enough time for the crystal core to grow sufficiently. So with the increase of scanning speed the crystal grains size obviously decreases.

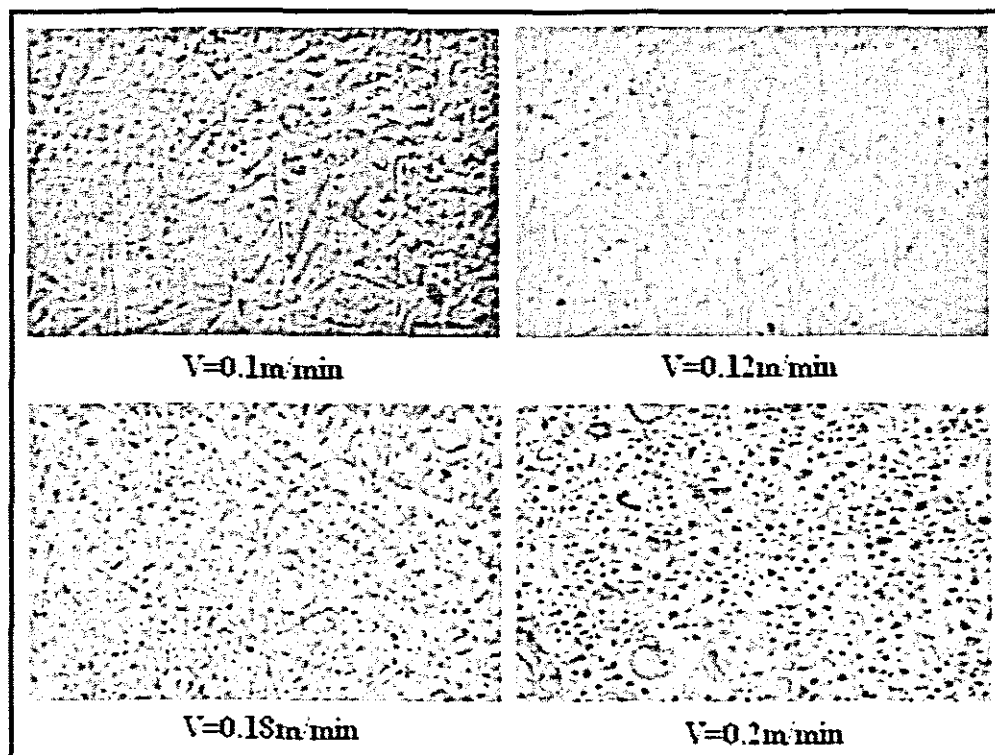


Figure 5.13 Effect of scanning speed on grain size ($\times 200$)
Sample 7-1, 7-2, 7-4, 7-5,

We can conclude that crystal grains size is refined with increasing laser-scanning speed.

5.4 Analysis of microstructure features near the bonding interface

The formation of the complex microstructure near the bonding interface is controlled not only by the melting and mass-transfer properties of the cladding materials and substrate, but also by the solidification conditions. For instance not all the laser energy can reach the surface due to attenuation by the powder cloud. Part of the laser beam penetrates through the powder cloud to arrive at the substrate and makes it melt and churn up and mix the alloy powder. Instability of grain boundary structure of substrate increases the actual melting point on a microscopic level. This will cause unsymmetrical fluctuant solid / liquid interfaces on microscopic scale causing the grains near to edge of melt pool to be in a semi-melted state. These semi-molten grains will be the start of new grains so the nucleation rate is high. The crystal grows from these nucleation sites after solidification.

Solidification kinetics depends mainly on the liquid components of the crystal front, temperature gradients of the crystal growth direction (G_l), and the solidification speed (V_s). The melt size and solidification dynamics limits convection so atoms in the solidification front cannot be discharged which increases the stability of the interface.

The partially melted area is the area, which has the maximal temperature gradient in the crystal growth direction and minimal cooling rate. [Liu Qibing, 2002] The crystal growth parameter G_l / V_s is close to infinity. Because of high dilution in this area, it is characterized by a single-phase solid solution structure γ - (Fe, Cr, Ni, Si).

After a period of solidification the dilution in the front decreases causing the chemical components reach the eutectic level causing the microstructure to change. It should form a lamellar eutectic crystal, but due to the dilution of the substrate material and the high value of G_l / V_s , solidification structure in this area will continue to grow on a plane basis, so a transition layer comes into being. See Figure 5.14.

As the solidification process continues the front of the growing solid - liquid interface is affected by the cooling speed gradually increasing as the temperature gradient (G_l) gradually decreases. Convection also disturbs the liquid alloy and dilution decreases destroying the plane crystal growth causing a convex disturbance. The convex growth parallel to the maximal thermal dissipation direction grows and , engulfs crystals with the wrong tropism. So the crystal morphology of solidification will change from plane crystal to dendrite. Thus the microstructure is affected by the degree of dilution of the substrate and local cooling conditions.

The following figure shows the characteristic microstructure of the bonding interface of laser cladding coating.

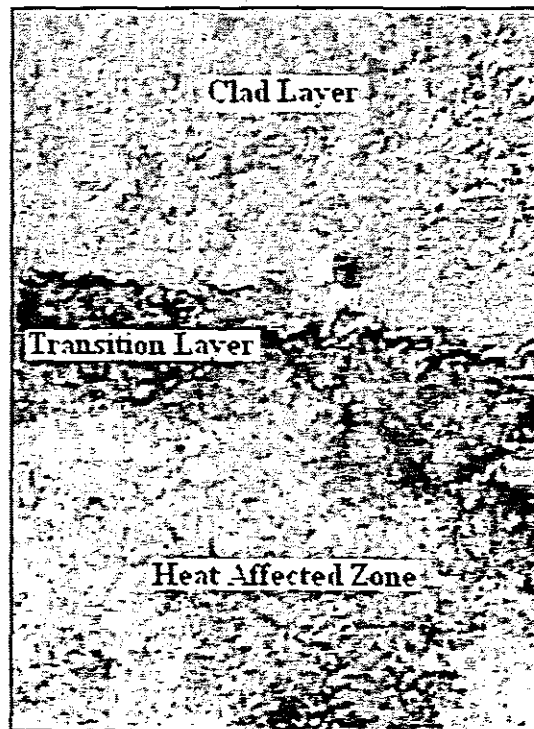


Figure 5.14 characteristic microstructure of the bonding interface of a laser cladding coating, Sample 7-2, high magnification

Carefully observe Figure 5.14; it is found that there is a dark gray transition layer. It has a relatively flat and straight interface. But the transition layer has a relatively zigzag interface with the cladding coating. Near the transition layer are exiguous eutectic microstructures. It tightly grips together with the zigzag interface of the transition layer. This zigzag microstructure acts like nails wedged into the cladding coating helping to enhance the bonding interface between the substrate and the cladding coating.

This shows that a matching between the coating and substrate is generated in the interface layer, which releases the stress concentration and avoids the formation of cracks while realizing better metallurgical bonding between the coating and substrate.

5.5 Effect of Rare-earth element on microstructure and wear resistance of the laser clad layer

As mentioned in chapter 1, the literature shows that rare-earth elements are accepted as the strategic elements in the new-tech revolution, but the study of the effects and mechanisms of rare-earth elements on laser cladding is just beginning.

Rare-earth elements can refine and purify the microstructure of the clad coating, reducing the dilution of the clad material by the substrate, decreasing the lattice constant of the solid solution. The author planned to do laser cladding experiments adding different amounts of a rare-earth element (Cerium oxide) in the nickel alloy powder to study these effects. Unfortunately it was not available.

Wang Kun-lin [Wang Kun-lin, 1999] mixed different amounts of lanthanum oxide (La_2O_3) powder with nickel-based alloy powder, using flame spraying to pre-place the powder mixture onto a C45 steel substrate (thickness 0.5mm). Then a CO_2 laser was used to finish the laser cladding, and by applying several adjacent tracks a varied coating was obtained. The amount of lanthanum oxide was varied (from 0% to 8%). Laser parameters: Power 1.5kW, laser beam: 4mm, scanning speed 5mm/s, overlapping rate 40%. The following figure shows the comparison of the microstructure of the nickel-based alloy coatings without lanthanum oxide (left) and with lanthanum oxide (right).

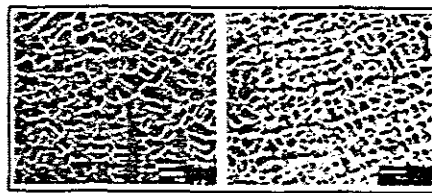


Figure 5.15 Affect of lanthanum oxide on the microstructure of nickel-base alloy coatings (Left: $\text{La}_2\text{O}_3=0\%$, Right: $\text{La}_2\text{O}_3=0.8\%$)

The comparison indicates that with the addition of lanthanum oxide, the microstructure of nickel-based alloy coating is obviously refined and purified. The uniformity of the microstructure obviously improves. In addition, with the addition of lanthanum oxide, the microhardness of the coating obviously increased. This is due to the refined and purified microstructure of the coating, and is also has related to the hard phase formed by the lanthanum compound.

But the investigation also indicates that it is inadvisable to add too much of the additional lanthanum oxide otherwise the microstructure of the coating will be too coarse.

5.6 Conclusions

The goal of the laser cladding experiments was to achieve good quality clad layers. Laser clad layer properties are influenced by the process parameters.

Effect of scanning speed variation on the geometry of the clad layer:

The clad height increases with the laser scanning speed, but in contrast the clad width, clad depth and dilution rate decreased.

Effect of laser power variation on the geometry of the clad layer

Lower power levels will result in the substrate not melting sufficiently or not melting at all. This results in the formation of clad layers that are not smooth, narrow or even winding. It also results in poor metallurgical bonding between the substrate and cladding coating.

Too high a temperature results in undesirable compounds being formed within the clad layer and additional dilution and distortion of the substrate and a large heat affected zone.

The clad width, clad depth and dilution rate increases with the laser power, but the clad height in contrast decreases. It indicates that for higher power the pre-placed powder layer and substrate will absorb more energy, and more fusion will occur.

Effect of beam diameter variation on geometrical dimension of clad layer

With a decrease of the laser beam diameter, the energy density will increase. The pre-placed powder layer and substrate will absorb more energy, and this will cause more fusions of substrate. The dilution rate will increase. The clad layer will flow.

Effect of laser scanning speed variation on microstructure

Increasing the laser scanning speed refines the crystal grains size.

Formation features of solidification microstructure for laser clad layer:

There are different solidification parameters for different position in cladding layer. The microstructure at the top of clad layer was the regular pine-tree eutectic crystal while the dendrite crystals are coarser. The microstructure at the middle of clad layer was mostly the small cell and column crystal. The microstructure at the bottom of clad layer was the typical extension growth in the plane with a small cell crystal structure.

The interface layer provides a matching between coating and substrate, releasing stress concentrations, and preventing the formation of cracks while producing a better metallurgical bonding between coating and substrate.

Chapter 6

Analysis of the microhardness distribution and wear resistance of the laser cladding coating

6.1 Introduction

The purpose of laser cladding is to achieve good quality clad layers, for the enhancement of mechanical properties including micro-hardness and wear-resistance. At present, due to its excellent features, a ceramic wear resistant-cladding layer is one of the most popular cladding coatings.

In this chapter, by using a micro-hardness tester and wear test machine, the micro-hardness and wear resistance of laser cladding coating are studied and investigated. The study yielded some results, figures and conclusions.

6.2 Distribution of microhardness in laser cladding coating

6.2.1 Microhardness test experiments

A microhardness tester (as shown Figure 6.1) was used to measure the micro-hardness

of the laser cladding samples. Before the test, the laser cladding samples were cut, mounted and polished. A 5% concentration of nitric acid ethanol solution (nital) was used to etch them. A 300-gram weight was used in the microhardness tests. Figure 6.2. shows the geometric midline of the clad layer.

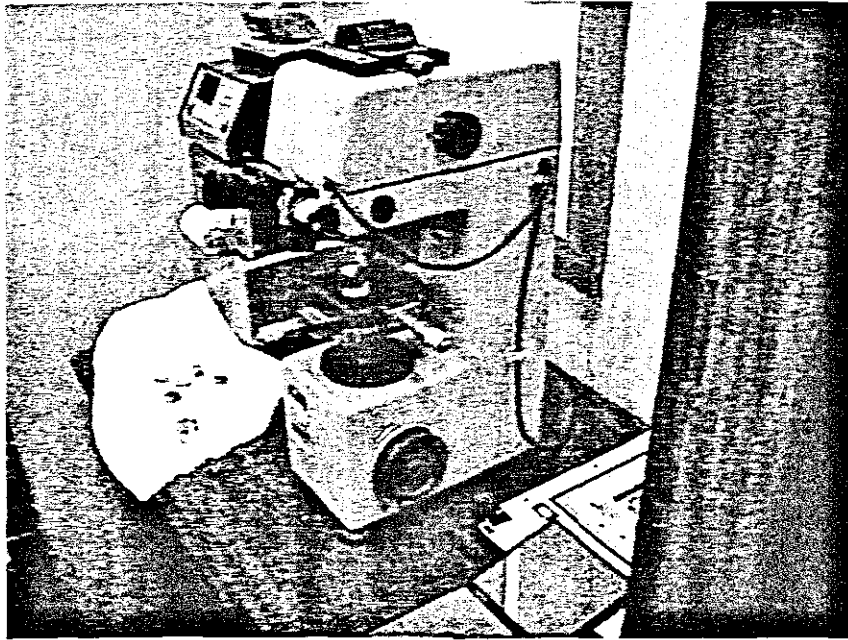


Figure 6. 1 Microhardness tester

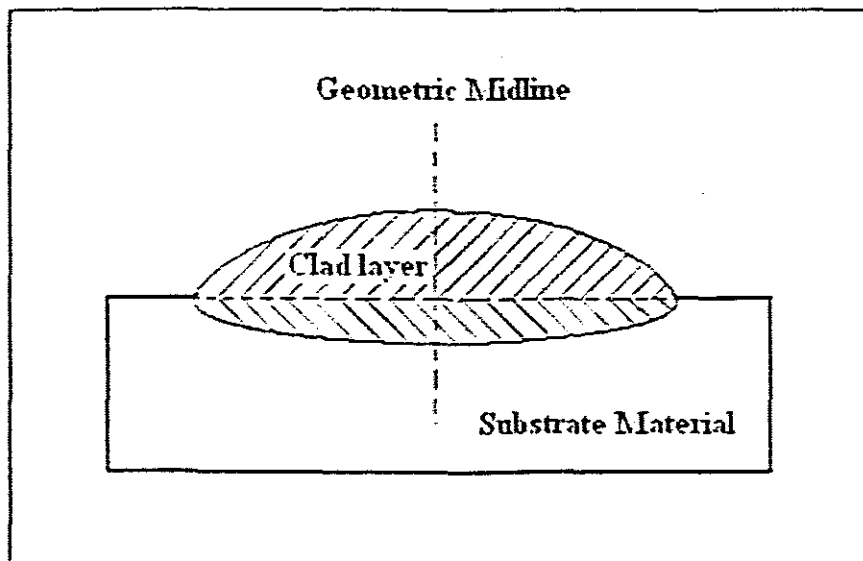


Figure 6. 2 Midline along which hardness calculations are performed

Hardness indentations were made along the midline from the surface of clad layer to the substrate: the interval distance between every indentation was $100\mu\text{m}$. in total, 7-8 indentations were made in every sample.

6.2.2 Micro-hardness test results and analysis

6.2.2 Micro-hardness test results and analysis

The following table 6-1 shows the micro-hardness values of sample 2.1, 2.5 and 3.2. The micro-hardness distribution is also shown in the following figures 6.3, 6.4 and 6.5.

Experimental value of Sample 2.1		
Distance from surface ($\Delta=100\mu\text{m}$)	Microhardness (HV)	Area
$P_1 = 100\mu\text{m}$	$HV_1 = 981.5$	Cladding coating
$P_2 = 200\mu\text{m}$	$HV_2 = 950$	Cladding coating
$P_3 = 300\mu\text{m}$	$HV_3 = 810$	Cladding coating
$P_4 = 400\mu\text{m}$	$HV_4 = 777$	Cladding coating
$P_5 = 500\mu\text{m}$	$HV_5 = 409$	Heat affected zone
$P_6 = 600\mu\text{m}$	$HV_6 = 367$	Substrate
$P_7 = 700\mu\text{m}$	$HV_7 = 370$	Substrate
Experimental value of Sample 2.5		
Distance from surface ($\Delta=100\mu\text{m}$)	Microhardness (HV)	Area
$P_1 = 100\mu\text{m}$	$HV_1 = 997.6$	Cladding coating
$P_2 = 200\mu\text{m}$	$HV_2 = 996.6$	Cladding coating
$P_3 = 300\mu\text{m}$	$HV_3 = 995.5$	Cladding coating
$P_4 = 400\mu\text{m}$	$HV_4 = 790$	Cladding coating
$P_5 = 500\mu\text{m}$	$HV_5 = 458$	Heat affected zone
$P_6 = 600\mu\text{m}$	$HV_6 = 378$	Substrate
$P_7 = 700\mu\text{m}$	$HV_7 = 370$	Substrate
Experimental value of Sample 3.2		
Distance from surface ($\Delta=100\mu\text{m}$)	Microhardness (HV)	Area
$P_1 = 100\mu\text{m}$	$HV_1 = 1187$	Cladding coating
$P_2 = 200\mu\text{m}$	$HV_2 = 1080$	Cladding coating
$P_3 = 300\mu\text{m}$	$HV_3 = 1052$	Cladding coating
$P_4 = 400\mu\text{m}$	$HV_4 = 1012$	Cladding coating
$P_5 = 500\mu\text{m}$	$HV_5 = 1012$	Cladding coating
$P_6 = 600\mu\text{m}$	$HV_6 = 950$	Cladding coating
$P_7 = 700\mu\text{m}$	$HV_7 = 425$	Heat affected zone

Table 6-1 Micro-hardness experimental results

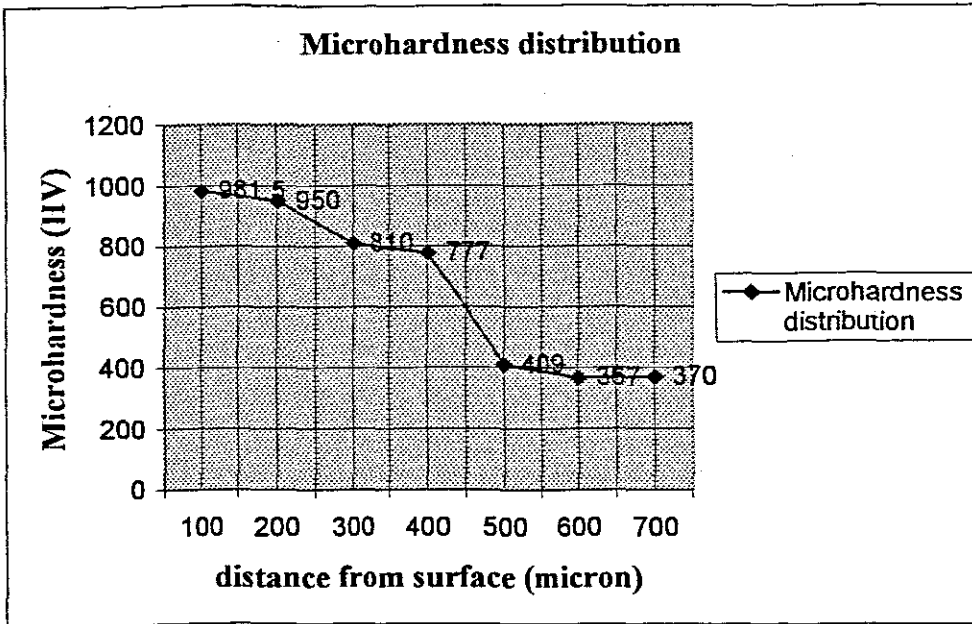


Figure 6.3 Micro-hardness distribution of sample 2.1

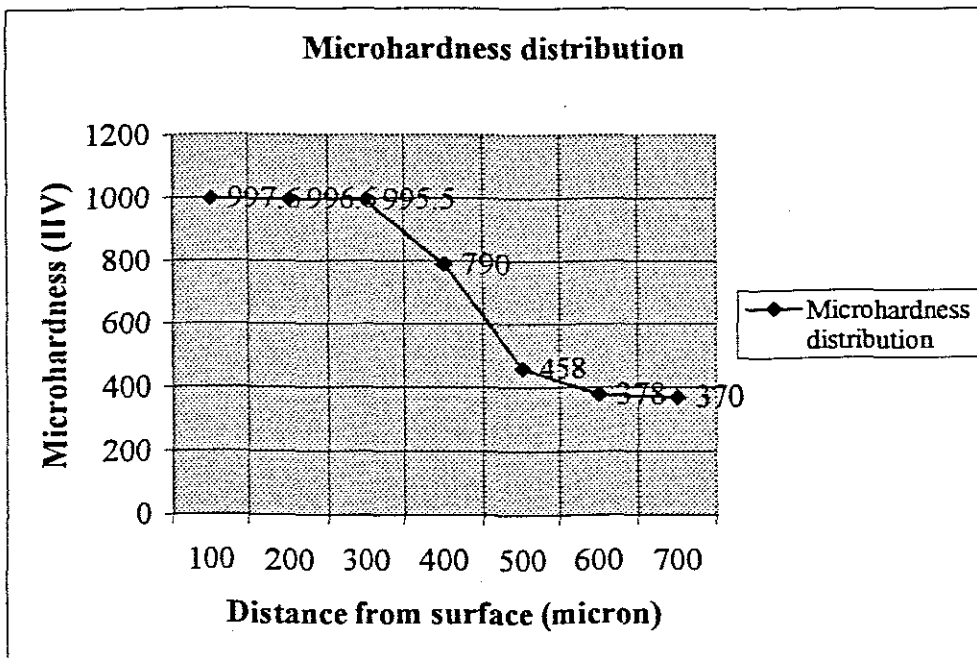


Figure 6.4 Micro-hardness distribution of sample 2.5

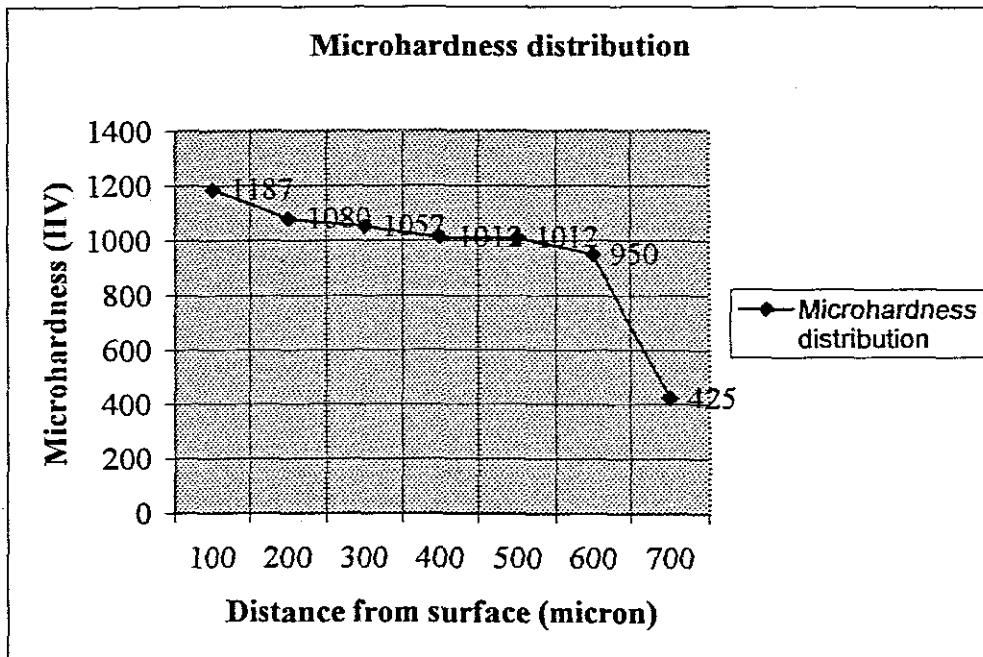


Figure 6.5 Micro-hardness distribution of sample 3.2

Analysis:

After a study of the above data and Figures, the author found that after laser cladding, the micro-hardness of the clad layer was 2-3 times of that of the substrate. The micro-hardness value from the cladding coating to the heat affected zone and substrate follows a gradient which tends to have three steps in the micro-hardness distribution curve as can be seen in figure 6.3. These steps correspond to the cladding coating, heat affected zone and substrate. The results showed that tungsten carbide particles increased the hardness of cladding coating as expected. The gradient distribution of the micro-hardness near the bonding interface improves the matching between the coating and substrate, releasing stress concentration and avoiding the formation of cracks. It also produces a better metallurgical bonding between the coating and substrate as previously described.

6.3 Wear resistance property of laser cladding coating

6.3.1 Wear resistance test experiments

Following the laser cladding experiments, a Struers LaboPol-5 machine and Precisa XT220A analytical balance were used to measure the wear resistance for different widths of clads. Samples were manufactured as 10mm length \times 3mm width \times 10mm thickness slices. The following Figure 6.6 shows the experimental equipment. The wear testing was done on a metallurgical grinding and polishing machine.

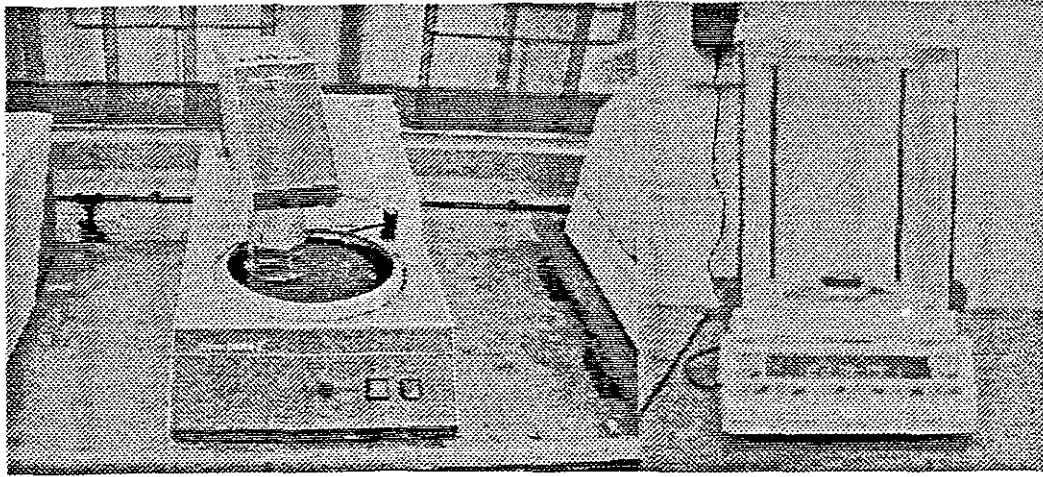


Figure 6.6 Polishing machine used for wear test (Left) and Precisa XT220A analytical balance (Right)

The rotational speed of the machine used for the test was 300rpm using an abrasive disk (struers MD Piano 220 grit) with radius 110mm. The duration of the wear experiments was 2 hours. Before and after the wear test, every tested sample was weighed using an analytical balance. The wear area and weight lost of every sample was calculated and recorded as listed in table 6-2.

The author designed three groups of experiments to study the effect of the laser scanning speed and tungsten carbide percentage on wear resistance. The laser scanning speed varied from 0.1m/min to 0.2m/min, the percentage of tungsten carbide varied from 10% to 40%.

6.3.2 Wear resistance test results and analysis

Cladding Materials	Scanning speed (m/min)	Weight Loss (g)	Wear area (mm ²)	Wear rate (g/h×mm ²)
10% tungsten carbide + 90% Ni-based Alloy (Sample 6)	0.1	0.0148	12.78×3.13	1.85×10 ⁻⁴
	0.12	0.0162	13.18×3.10	1.62×10 ⁻⁴
	0.15	0.0089	10.05×3.09	1.43×10 ⁻⁴
	0.18	0.0111	11.65×3.06	1.55×10 ⁻⁴
	0.2	0.0106	10.02×3.01	1.76×10 ⁻⁴
20% tungsten carbide + 80% Ni-based Alloy (Sample 10)	0.1	0.0103	10.07×3.19	1.60×10 ⁻⁴
	0.12	0.0104	11.21×3.12	1.49×10 ⁻⁴
	0.15	0.0101	12.06×3.11	1.34×10 ⁻⁴
	0.18	0.0091	10.51×3.12	1.39×10 ⁻⁴
	0.2	0.0125	13.76×3.08	1.48×10 ⁻⁴
30% tungsten carbide + 70% Ni-based Alloy	0.1	0.0098	11.68×3.10	1.36×10 ⁻⁴
	0.12	0.0098	12.30×3.05	1.30×10 ⁻⁴
	0.15	0.0074	9.96×3.05	1.22×10 ⁻⁴

(Sample 2)	0.18	0.0073	9.58×3.06	1.25×10 ⁻⁴
	0.2	0.0104	12.16×2.98	1.43×10 ⁻⁴
40% tungsten carbide + 60% Ni-based Alloy (Sample 8)	0.1	0.0083	9.00×2.99	1.55×10 ⁻⁴
	0.12	0.0103	11.58×3.10	1.43×10 ⁻⁴
	0.15	0.0103	12.30×3.02	1.38×10 ⁻⁴
	0.18	0.0079	9.65×2.96	1.39×10 ⁻⁴
	0.2	0.0101	11.88×2.98	1.43×10 ⁻⁴
Substrate material	—	0.0448	12.16×3.08	5.98×10 ⁻⁴

Table 6-2 Data of wear resistance experiments

The following Figure 6.7 shows the wear-rate curves of laser cladding coatings, under the same wear conditions, for different laser scanning speeds and different tungsten carbide percentages.

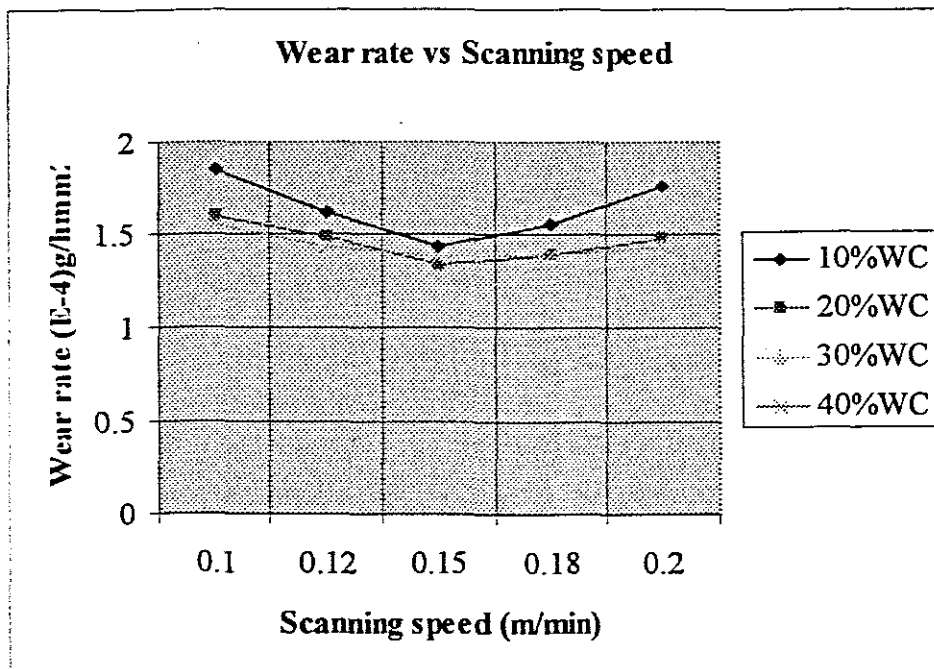


Figure 6.7 Wear resistance compare

The data shown in Table 6-2 and the curves of Figure 6.7 shows that tungsten carbide particles increased the wear resistance. For the same tungsten carbide percentage, with the increase of the laser scanning speed the wear rate at first decreases and then at a certain point starts to increase again. So the wear rate is a minimum for a particular scanning speed between 0.15m/min to 0.18m/min. The wear resistance of the coating is thus a maximum in this range.

With an increase of percentage tungsten carbide of the cladding coating also increased up to a point. At 30% tungsten carbide the wear resistance arrived at a maximum. When the percentage tungsten carbide rose to 40% the wear-resistance of the clad layer

decreased to the level at 20%.

The author also compared the wear rate of the laser cladding coating with that of substrate. The wear resistance of laser cladding coating was found to be 3.5 times that of the substrate.

6.4 Analysis of wear resistance

6.4.1 Wear mechanism analysis

According to the mechanism of wear, wear can be classified into abrasive wear, adhesive wear, fatigue wear, corrosive wear and erosion wear etc. [Wu Xinwei, 1996]. In practice the work piece always experiences multiple kinds of wears. Typically, there should be only one dominant type of wear.

So, in order to enhance the wear resistance of materials, people should solve the dominant wear which affects the working capability and performance of the equipment. For example consider a steel roller used in a rolling mill, [Zhang Guangjun, 2000] after using laser cladding heat treatment to enhance wear-resistance and hardness, the adhesive wear was greatly reduced, and the working life of the laser cladding treated rollers increased by 3-5 times.

The wear test the author did was abrasive wear; abrasive wear is a kind of wear characterized by material transfer caused by hard granules or hard protuberances. It is the most common and ubiquitous wear. Based on the above experiments results, the author analyzed the main factors affecting the wear resistance of the laser cladding coating below.

6.4.2 Effects of micro-hardness distribution on the wear resistance properties of the material:

The experimental results showed that tungsten carbide particles increased the hardness and wear resistance. Generally, the micro-hardness distribution of materials partially reflects the wear resistance of the material. So to enhance the hardness of the material is one method to increase the wear resistance of materials. With the increasing of the scanning speed of the laser beam, the microstructure of the cladding coating is refined while, with an increase in scanning speed, we find a supersaturation of the solid solution of the cladding layer. Additional tungsten carbide, being a kind of independently hard particle, greatly enhances the micro-hardness of the cladding coating. More exiguous and refined dispersive tungsten carbide is produced for a supersaturated solid solution during the cooling process. This also has the function of dispersion aggrandizement.

The wear resistance of the material not only depends on its micro-hardness level.

Increasing scanning speed helps to enhance the microhardness of the material [Wu Xinwei, 1996] but this will result in carbide separating out from the supersaturated solid solution with decreased γ -Ni. The micro-hardness is enhanced to a certain level but the effect on the morphology of the carbide then starts to affect the wear resistance. The refinement and dispersion of the carbide particles in the cladding layer is a crucial factor. The abrasive wear-resistance of the material depends on the space between the hard particles in the laser-cladding layer. The smaller the distance between the hard particles the higher the wear resistance of the material.

6.5 Other methods for enhancement of wear resistance

There are some other methods to enhance the wear resistance of laser cladding coating. Add a small quantity of rare-earth elements in the cladding powder, for example, lanthanum-oxide (La_2O_3) and cerium dioxide (Ce_2O_3). Rare-earth elements, with their excellent performance, are widely used in metallurgy, electron and chemical industry etc. Rare-earth elements that are used in surface engineering have greatly enlarged the area of application.

Wang Kunlin, [Wang Kunlin, 1999] from the Department of Mechanical Engineering, Tsinghua University, China, respectively mixed 0%, 0.4%, 0.8%, 2.0%, 4.0%, and 8.0% of La_2O_3 to Ni-based alloy powder. After the uniform mixing, flame spraying is used to pre-place the mixture onto the steel substrate. The pre-placed powder of thickness 0.5mm is then finished with the laser.

Their experimental results were compared with those of the coatings without La_2O_3 addition. The comparison indicates that the addition of La_2O_3 can refine and purify the microstructure of the clad coating, reducing the dilution of clad material from the substrate, decreasing the lattice constant of the solid solution. Moreover, the friction coefficient of the clad coating with La_2O_3 addition is reduced and the wear resistance of clad coating with the addition of La_2O_3 is enhanced.

6.6 Conclusions

The hardness distribution and wear resistance are important properties of clad layers. Laser cladding is an effective heat treatment method for the enhancement of mechanical properties including micro-hardness and wear-resistance. The results of this chapter indicated that tungsten carbide particles increased the micro-hardness and the wear resistance properties of the laser cladding coating. The comparative test indicated that after laser cladding heat treatment, the micro-hardness value of the clad layer was increased to a level of 2-3 times of that of the substrate; the wear resistances of the laser cladding coating increased to a level of 3.5 times that of substrate.

It was also found that the micro-hardness value followed a gradient from the cladding coating to the heat affected zone and substrate with three steps in the micro-hardness

distribution curve. These steps correspond to the cladding coating, the heat affected zone and substrate, which provides a matching interface between the coating and substrate with benefits to the material properties.

The wear resistance property of cladding layer has a maximum value for 30% tungsten carbide in the cladding material. The laser scanning speed affects the wear-resistance property of the laser cladding layer but the distribution of tungsten carbide is also important so that a critical value exists for laser cladding scanning speed in terms of wear resistance.

Chapter 7

Study of the factors influencing the crack behaviour of the laser clad

7.1 Introduction

The cracking behaviour of the laser-cladding layer is the primary factor influencing the quality of clad layer. Consistent quality of the clad layer is one of the most important reasons preventing large-scale industrialization of laser cladding. The most important defect found in laser cladding is cracking. The other important defects are gas porosity and component asymmetry (the components in micro-zone of the cladding layer are not uniform) especially for thick and large area cladding layers.

In order to allow the cladding of products by non-academic personnel and, an effective transfer of results from laboratory to the production environment research is needed. A study of the quality index of the laser cladding layer and an analysis of reasons for the defects, in order to find an effective control method is therefore undertaken.

In this chapter, the author studied and analysed the relationship between cracking

behaviour and four factors: parameters of the laser system, process parameters, the material of the cladding layer and state of the substrate. For the pre-placed powder and the powder injection method experiments, the author analysed the reasons for cracking and looked at some methods of crack prevention.

7.2 Analysis of the reasons for cracking in metals

Due to the high laser power, the alloy material and substrate melts in a very short time, and only a very thin layer of the substrate material can be melted. Solidification occurs at a high speed within 10^4 - 10^6 K/S. [Gnanamuthu, 1979; Nagarathnam, 1995; Komvopoulos, 1990; Nagarathnam, 1993;].

There are three kinds of cracks, the first one is the clad coating crack; the second one is the interface-substrate crack, and the third one is the crack in the overlap area. Crack behaviour is affected by mechanical factors, metallurgical factors and especially by inherent defects in the substrate materials.

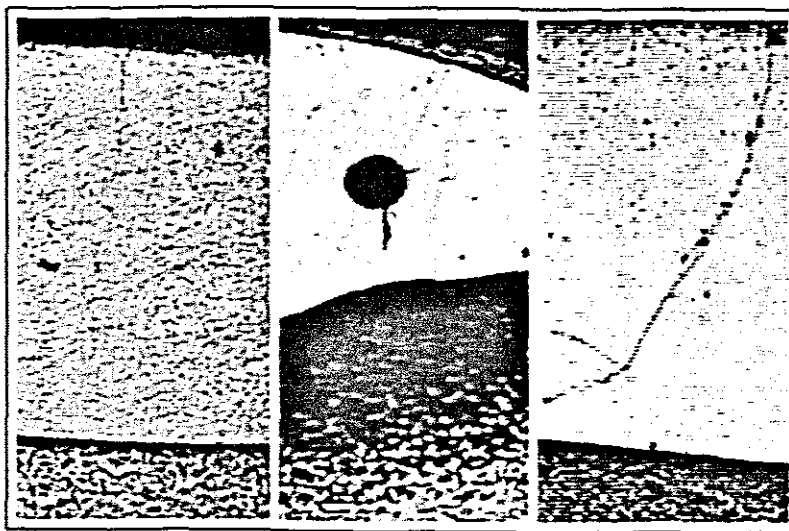


Figure 7.1 Some crack samples (17), (4-2) and (14), (50 \times).

Zhang Guangjun found the existence of tensile stress in the melt-solidification layer. When the local tensile stress exceeds the limit of the material, clad cracks come into being. Cracks appear mostly at the interface of dendrites, at gas porosity or at impurities or other areas of weakness. [Zhang Guangjun, 2000].

The following figure 7.2 shows two samples, which have serious cracks, caused by impurities and gas porosity. The author found that cracks, as shown in the left side of the figure, stem from an impurity in the cladding material. The figure shows that during the laser cladding process, due to the high power laser and the resulting temperature, the impurities in the cladding material explode and consequently cause serious cracks during the cooling stage. In this figure, a crack extends to the substrate. The crack

shown in right figure stems from two sites of gas porosity: a large site and a small one. The figure indicates that cracks appear around the sites of gas porosity.

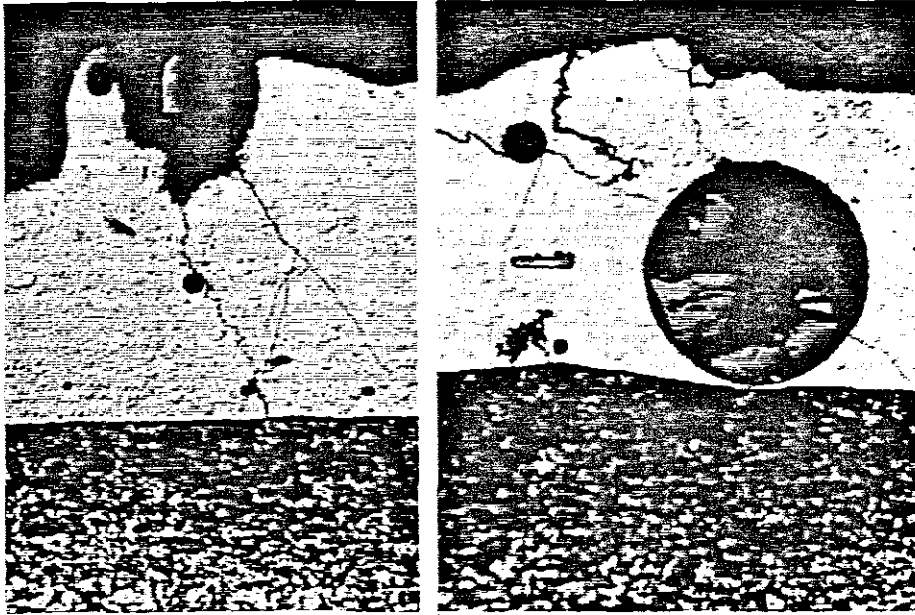


Figure 7.2 Cracked samples caused by impurities and gas porosity (50×).

The formation of cracks in the clad layer is mainly caused by the thermal stress created by the high thermal gradient built up during the cooling stage and the difference between the thermal expansion coefficients [Frenk, 1991, 1993; Li, 1992; Pilloz, 1990; Vasauskas, 1996; Zhang, 1994; Zhou, 1991]. Especially layers that are characterized by the presence of hard and brittle particles, such as carbides, are prone to cracking [Luft, 1995]. Ceramic layers are also vulnerable to cracking, because of their limited ductility combined with the difference in thermal expansion coefficients compared with metals [VandeHaar, 1988].

If we further analyse the effect of the difference between the expansion coefficient of the clad layer alloy and the substrate material we find that during the process of solidification and contraction, when the difference of the expansion coefficient is big enough, it will create tensile stress. When the tensile stress exceeds the utmost limit of tensile yielding at a given temperature then a crack immediately appears [Li Biwen, 2000]. Because of the rapid heating and cooling in the laser cladding layer ($10^4 \sim 10^6$ K/s), the life of melt pool is very short. This means that it is possible that oxides, sulfides and other impurities do not have enough time to discharge from the solidifying structure. These defects exist in the cladding layer and can easily become the crack fountainhead.

In addition, after the laser beam moves away, instantaneous solidification and crystallization happens and a cladding layer is formed, it is easy to cause a disturbance of the crystal interface, increasing the crystal vacancy. In addition hot-shortness (red

brittleness) increases while ductility (Plasticity and Toughness degree) decrease so that the crack sensitivity increases. The thicker the cladding layer the more the above-mentioned situation becomes observable.

Thermal stress of Ceramic (Tungsten Carbide, etc.) depends on the following formula [Wu Weiwen, 1994].

$$\sigma_c = \frac{E_c \cdot \Delta T \cdot (\alpha_c - \alpha_s)}{1 + 2((E_c / E_s) \cdot (T_c / T_s))} \quad (7.1)$$

In the above formula:

σ_c is the thermal stress,

E_c is the elastic modulus of laser cladding coating,

ΔT , is the temperature difference between Ceramic melting point and substrate.

α_c is thermal expansion coefficient of Ceramic cladding coating.

α_s is thermal expansion coefficient of substrate.

T_c is clad thickness of laser cladding coating.

T_s is thickness of substrate.

For the above formula, we can find that the thermal stress depends on the thermal physics and mechanistic performance of the ceramic and substrate. Differences in melting point, thermal expansion coefficient, thermal conductivity and elastic modulus between the ceramic and substrate are very big. That is why the thermal stress in the cladding coating is always large. It is also easy for cracks and porosities to occur in the laser cladding coating due to the stress and impurities resulting from the process of applying the coating. We need to look at ways of controlling cracking and porosity to make laser cladding more popular in industry.

Porosity is a very important reason for the formation of cracks. We thus need to study the cause of porosity formation and ways of preventing it. Powell [Powell, 1981] indicated the presence of holes in the clad layer as being referred to as porosity. Porosity can be caused by several reasons. Porosity may be the result of the formation of gas bubbles that are trapped in the solidifying melt pool. This phenomenon can be decreased by a method of vibration of the work piece (Frequency: 25 Hz; Amplitude: 20 mm).

Secondly, if solidification proceeds in different directions, some regions in the melt can be enclosed. A contraction occurs upon solidification of these enclosed regions. That contraction causes tensile stress in the layer and may even lead to the formation of holes. These two kinds of porosity are to be found in the clad layers.

Two other kinds of porosity are confined to the substrate-clad interface. The first one is caused by the presence of minor flaws, such as grease which influences the surface

tension and thereby the bonding of the coating material to the substrate.

The last type of porosity appears when overlapping tracks are applied. This so-called 'inter-run porosity' can occur when too much powder is supplied. This can be avoided with a width-height ratio of more than five [Steen, 1987].

7.3 Effect of laser system parameters on laser cladding coating crack

7.3.1 Effect of beam diameters on cracking of laser cladding coating

During the laser cladding process, when the output of the laser is constant, the power density has an inverse relation with the laser beam diameter. With the increase of laser beam spot diameter, the power density will decrease. Laser beam diameter is one of the important parameter that affects cladding quality. Laser beam diameter directly affects the geometry of the cladding coating, namely width and depth [Wang Liuying, 1999].

In chapter 5, the author already showed the dependence between the clad width (W_C) and the laser beam spot size. In this chapter, the author found that the laser beam diameter affects not only the geometry of the cladding layer, but also has an obvious effect on the microstructure. An increase of laser beam diameter leads to crystal grains becoming finer and smoother. The microstructure mainly consists of dendrites and cellular pine-tree crystal. With the decrease of the laser beam spot diameter, the crystal grains became coarser. Their microstructure mainly consists of cellular crystal or a small quantity of cellular shaped dendrite crystal. The following Figure 7.3 shows the microstructure of sample series 12, which was produced with different diameters of laser beam: 2.0mm, 2.5mm and 3.0mm. Their microstructures are quite different.

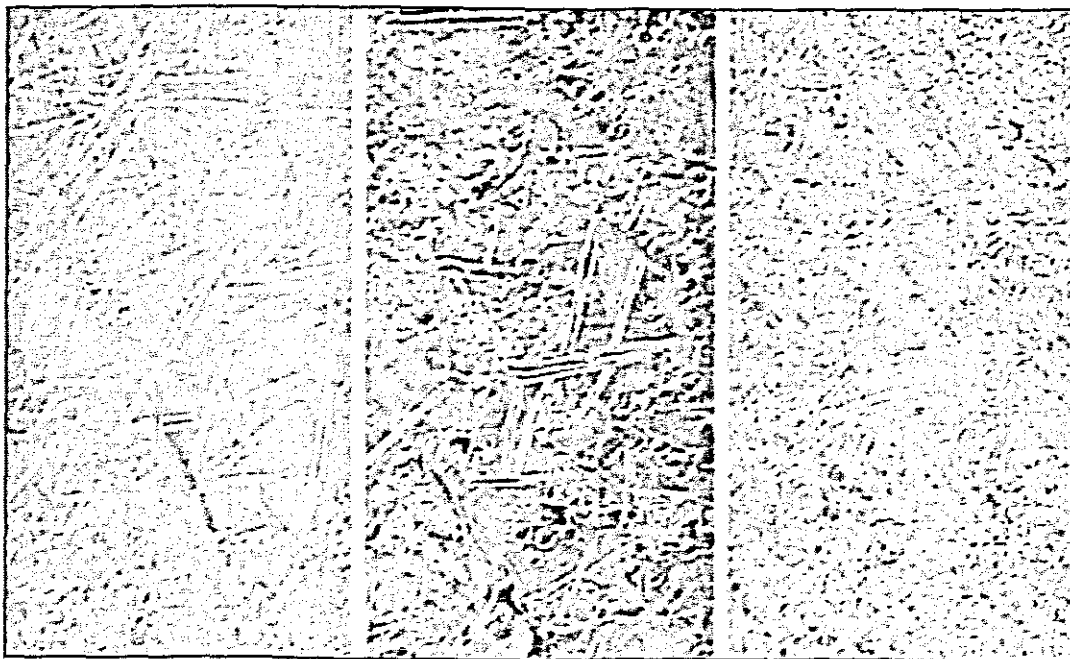


Figure 7.3 Sample12, Beam spot =2.0mm, 2.5mm, 3.0mm (200×)

7.3.2 Effect of laser scanning speed on crack behaviour

In chapter 5, the author already studied the effect of laser scanning speed on the size and shape of the laser cladding coating. During the laser cladding process, scanning speed also greatly affects the microstructure and quality of the laser cladding coating.

The following Figure 7.4 shows the effects of scanning speed on crack behaviour. From left to right are Samples 10-2, 10-3 and 10-5. They were produced with increasing scanning speed from 0.12m/min, 0.15m/min to 0.2m/min.

For a constant laser power, too low or too high a scanning speed will cause different crack degrees. Only when we use moderate scanning speed are fine metallurgical compounds produced between the cladding layer and substrate with no cracks and gas porosity in the coating.

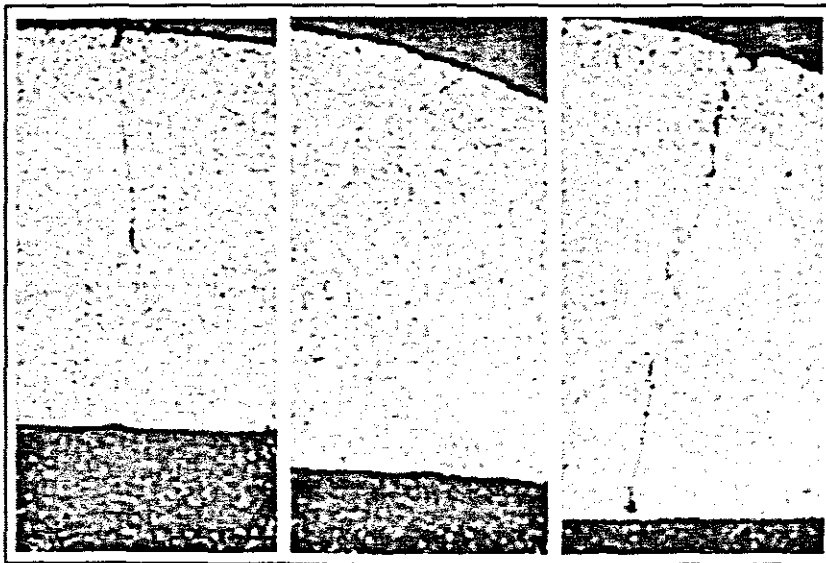


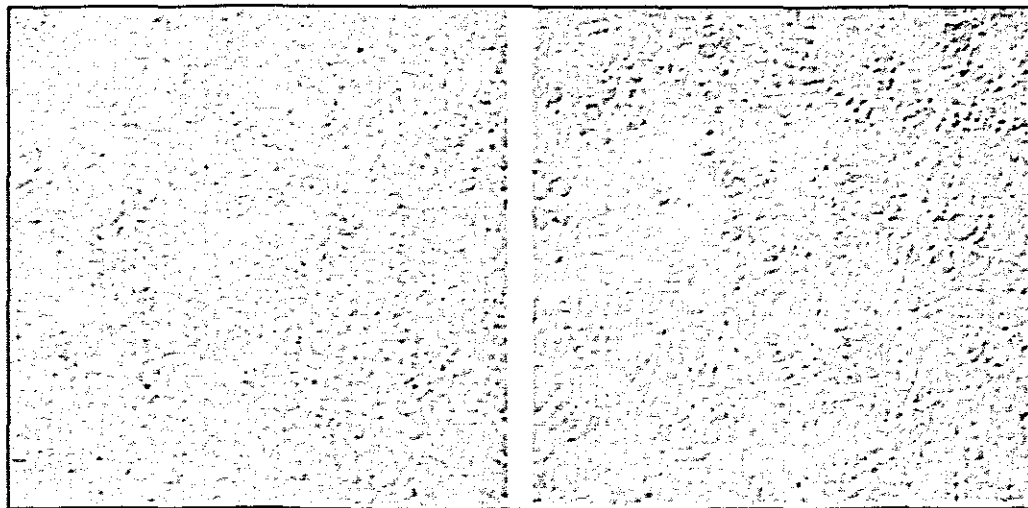
Figure 7.4 Effects of scanning speed on crack behaviour, (50 \times). From left to right are Samples 10-2 ($V=0.12\text{m/min}$), 10-3 ($V=0.15\text{m/min}$), 10-5 ($V=0.2\text{m/min}$).

Analysis: Because of the rapid heating and fast cooling, very big temperature gradient appear between cladding coating and substrate material. With the increase of scanning speed, temperature gradient will increase as well. The corresponding internal stress increased. When the scanning speed reaches a certain numerical value the internal stress in the cladding exceeds the ultimate yield and a crack appears. The scanning speed at this moment is the critical scanning speed for crack formation. Crack phenomena will more obvious and visible cracks as this scanning speed is exceeded.

7.4 Effect of conditions of laser technological treatment on laser cladding layer

Laser power, beam diameter and scanning speed are the key parameters to control how much energy can be absorbed by alloy layer. In chapter 1, the author introduced the specific energy formula (1.1): $E=P/DV$. Generally, the thicker the layer, the more energy is needed. The author already described how these parameters affect the quality of the laser-cladding layer.

In order to prolong the life of the melt pool and in order to increase the energy input the author performed some experiments to increase the laser power density and decrease the scanning speed. These actions have some good effects but must be control within limits. Generally, higher power and slower scanning speed helps the powder layer to adequately melt; helps to prolong the life of melt pool; helps impurities to float up to the surface of melt pool; helps the combining of the cladding layer and substrate; decreases the probability of cracking and crack fountainheads. However, with the increase of specific energy input, the dilution rate of the cladding layer will also increase, microhardness will decrease, crystal grain size will be bigger and coarser. The burning loss rate of the elements will increase. Thus the benefits of the laser cladding treatment will be lost. Figure 7.4 show two samples 3-4 and sample 3-1, it can be found, that with the increase of laser power, the crystal grain size becomes coarser than that of the lower power.



Sample 3-4: P=1kW

Sample 3-1: P=1.3kW

Figure 7.5 Effect of laser power on crystal grain size. Sample 3-4 (P=1kW, V=0.2m/min) and Sample 3-1 (P=1.3kW, V=0.2m/min) (200×)

Conclusion: So, according to the above investigation, when we choose practical parameters for cladding we should base our choice on the following factors: thickness of the cladding layer, melting point of the powder material, absorption coefficient, matching of properties with the substrate material, wettability, etc. It is necessary to

determine these parameters by experiment. Only when we have optimal technology parameters, will we be able to control the energy density and time of action. Then will be able to avoid cracks and obtain an optimum quality of the layer.

Re-melting method: We also adopted the so-called laser re-melting treatment method on sample 19, 23 and 24 to investigate the so-called re-melting technology. After the first laser-cladding operation is performed, then the laser beam is used to scan the clad layer again. The author found using this method also have some other effects, it helps to produce a uniform microstructure, to eliminate impurities, smooth the surface and eliminate defects. It was found that after using the re-melting technology, some of the cracks formed in the first cladding process disappeared but for deep penetrating cracks and those crack extending to the substrate surface, re-melting is of no use.

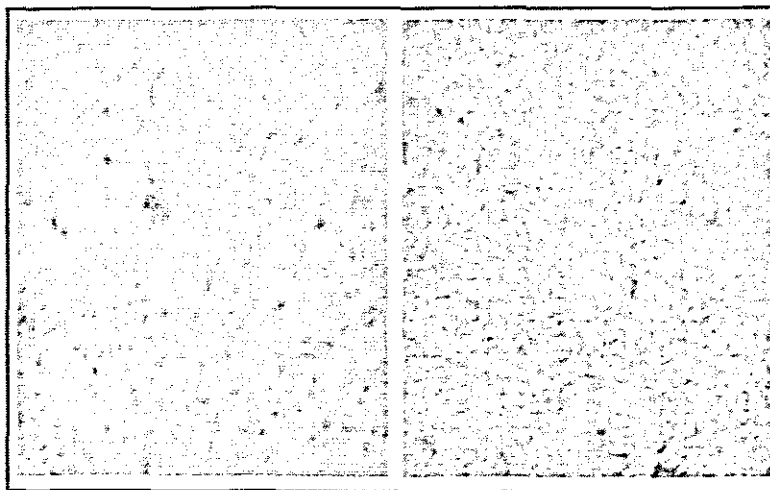


Figure 7.6 Effect of Re-melting, Sample 21 and 19 (500 \times)

Different laser scanning method: We also used some un-conventional laser scanning method. As shown in Figure 7.7 EN8 mild steel was clad with a Nickel Tungsten carbide layer using a rectangular-spiral scan to minimize distortion.

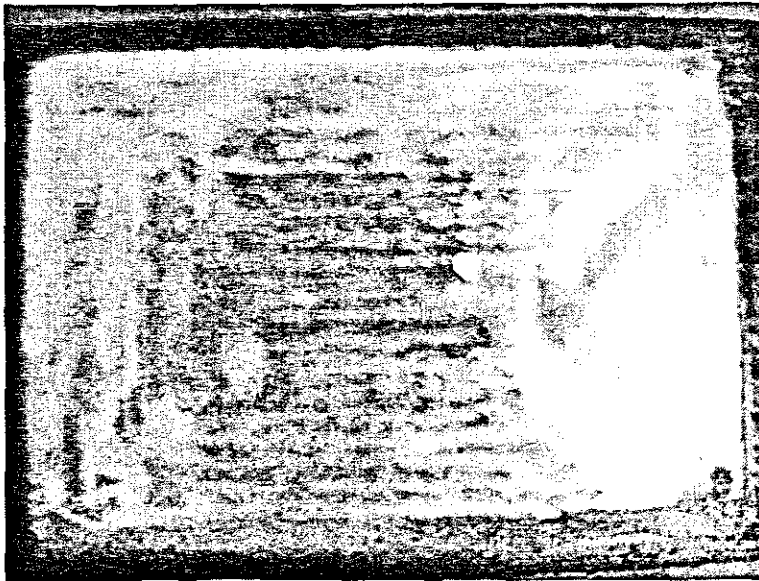


Figure 7.7: Sample 22, Mild steel EN8 clad with a Nickel Tungsten carbide layer using a spiral scan to minimize distortion and crack.

The author found that sample 22, after being treated with the rectangular-spiral scanning method, the distortion of the substrate noticeably decreased and improved and the crack numbers in clad layer also decreased compared with sample 21, which used the same laser treatment parameters as sample 22, but with a conventional laser scanning method.

Some of the cracks were formed by tensile stress in the clad layer caused by the cooling and contracting stage. After adopting a rectangular-spiral scanning method the distortion obviously decreased and improved as a result of the improvement of tensile stress in clad layer which reduced the crack opportunities.

7.5 Effect of cladding material on laser cladding crack

Commonly, as mentioned in chapter 1, lasers cladding applied powders are the same as those used in flame and plasma spraying because the intended functional properties are the same. Most of the research experiments use thermal or plasma spray powder. Usually a Ni-base alloy or a Co-based alloy is used as the main constituent of the powder.

In flame and plasma spraying all the powders, contain boron and silicon. Boron and silicon have benefits in terms of deoxidising; slagging; wetting and to restrain gas porosity. These elements help to create a hard phase, increasing the hardness of the cladding layer, but with the increase in the hardness of the cladding layer, the crack opportunity will also increase. Boron is very soluble in Fe and Ni which makes it easy to separate out and centralize at the crystal interface of causing cracks.

In a high Nickel content alloy, Si can form low-fusing eutectic impurities, which have a great effect on crystal cracking [Zhang Wenyue, 1984]. Due to the short life of the laser cladding, melt pool, chemical combination happen between Silicon oxide and boron oxide, resulting in the chemical borosilicate which has no time to adequately float up to melt pool surface. This is especially true for thick cladding layers where some of the low melting point borosilicate remains in the cladding layer. This layer becomes a liquid membrane during the cooling process and with the tensile stress in the layer caused by the cooling and contracting stage, cracks appear. So it is better to decrease boron and Si content.

According to metal theory, high carbon content can increase hardness. The increase of hardness and brittleness always goes with an increase of the carbon content while the crack probability increases also. On the other hand, it is possible that carbon and chromium elements become a chemical compound, Chromium Carbide. This will cause the chromium content in the cladding layer to decrease so the corrosion resistance of the laser-cladding layer decreases.

In fact, the high-energy laser heat resource has a special function to produce various strengthen effects. Some researchers have shown that for the same powder, the laser cladding layer hardness is 20%-40% better than compared to plasma spraying.[Shi Shihong, 1995]. Therefore, there are various benefits on suitably decreasing the carbon content in the cladding powder.

Intermediate Layer: Another method to control cladding cracking, is to adopt the intermediate layer technology [Zha Ying, 1999]. Namely to pre-place a higher crack-resistant powder layer onto the substrate surface the physical character of must be compatible with the substrate. The intermediate layer is a very thin layer. After the intermediate layer is clad onto the substrate, we proceed to clad using the required powder on the surface of the pre-clad intermediate layer as before. This is more complex and more expensive than the normal method and the powder utilization ratio is decreased. Nevertheless, in order to enhance the suitability of the powder for the substrate material for a thick clad layer, this technology still has practical significance.

7.6 Effect of substrate materials condition on laser cladding layer crack

7.6.1 Effect of substrate materials on crack

The effect of the expansion coefficient of the substrate material: During the laser cladding process, a pool of molten metal is formed with the surface of the bonding zone melting. A temperature gradient comes in to being from the melt pool to the substrate and different degrees of thermal expansion occur. After the laser beam moves on, the molten pool quickly cools down and contracts.

The heat-affected zone within the substrate also begins to cool down and contract. The

bigger the difference between the expansion coefficient of the substrate and the clad layer the more serious the effect of the cooling contraction will be in causing compressive stress in the cladding layer if the contraction of the substrate is larger than the clad layer. In contrast, if the cooling contraction of the substrate-bonding zone is weaker than that of cladding layer, the cladding layer will suffer tensile stress. If the tensile stress exceeds the stress limit at that temperature a crack will appear. It is preferable for the clad layer to experience compressive rather than tensile stress, as this tends to close cracks rather than open them.

On the other hand, when the heat-affected zone contracts, it also limited by the substrate and surrounding metal block. When the resulting tensile stress exceeds the stress limit, the surface layer of substrate may crack. This kind of crack may extend to the cladding surface. A substrate with good plasticity is more resistant to cracking than a brittle one.

7.6.2 Effect of substrate surface condition on laser cladding crack

The best condition of the substrate surface is smooth, glossy, with uniform microstructure, without defect and without residual stress to prevent cracking. Generally, it is not necessary to remove the old cladding layer to do re-cladding because after the last cladding, the microstructure of the heat-affected zone has already changed. However, residual stress, remaining defects such as a slight crack may become the source of new cracks in the next clad.

7.6.3 Effect of thermal capacity of the substrate on cracking

A very important characteristic of laser cladding is that temperature rises quickly to the melting point of the material and after the laser beam moves away, the melt pool cools down rapidly. Most of heat in the layer dissipates into the substrate material in a process known as self-quenching. So, the bigger the thermal capacity of the substrate the higher the cooling rate of the clad layer with a higher tendency for cracking. That is why sometimes, no crack occurs in experimental samples, but the same cladding process on machine parts might have cracks. An important reason is that most of the lab-samples have a small volume, so their thermal capacity is also small but machine parts have a larger volume with a larger thermal capacity and hence higher cooling rates producing cracks.

Pre-heating and heat preservation

The author also used a kiln to pre-heat some samples to 200-300°C for 1-2 hours before laser cladding. After laser cladding the samples were kept in the kiln for a further 1-2 hours for heat preservation. It was confirmed this method has some effect because it reduces the temperature gradient. Heat preservation can retard the cooling rate of the clad layer possibly reducing the crack opportunity. Pre-heating and heat preservation

also has the effects of eliminating residual stress and restraining crack growth. However, if the heat preservation temperature is too high or if the heat preservation time is too long, it will result in the clad layer's microstructure being coarser and as grain size increases, hardness decreases.

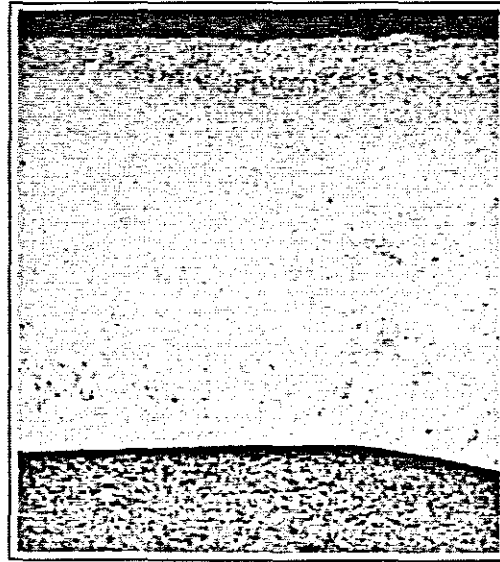


Figure 7.8 Pre-heated and heat preservation sample 21, (50×)

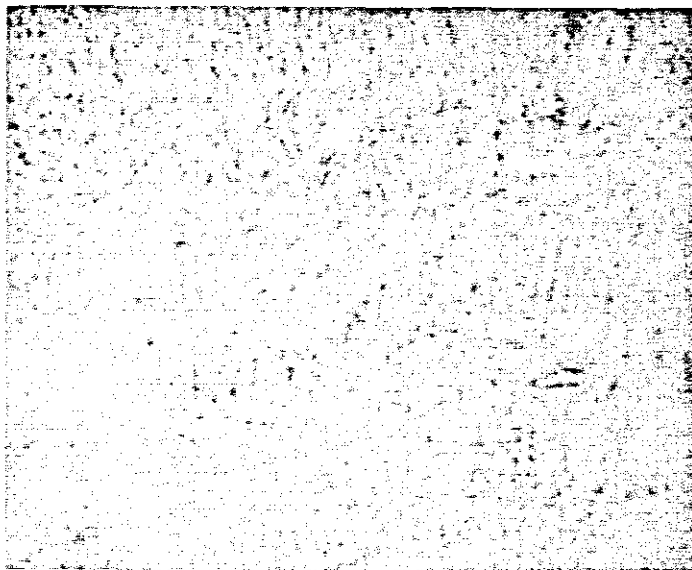


Figure 7.9 Microstructure of Pre-heating and heat preservation sample 24, (500×)

7.6.4 Effect of shape and structure on laser cladding crack

The shape and structure of the substrate also affects cladding quality. It is quite easy to produce a crack in an un-symmetrical sample. During the laser cladding process, the thermal stress distribution in a uniform sample is relatively symmetric; so the crack probability is quite small. The probability of cracking is higher for unsymmetrical

workpieces which experience complex thermal stresses. The asymmetry of the tensile stress will increase the crack opportunity. So some researchers excavate a groove around the cladding layer [Li Biwen, 2000]. This is an effective measure to cut off tensile stress around the cladding layer. In addition, pre-heating, heat preservation post treatment and the use of intermediate layer technology can decrease the crack opportunity.

7.7 Conclusions

Reasons for the cracking of the laser cladding layer:

The formation of cracks in the clad layer is mainly caused by the thermal stress created by the *high thermal gradient built up during the cooling stage and the difference between the thermal expansion coefficients*. When the local tensile stress exceeds the limit of stress intensity, a crack will occur. The position of the crack is mostly at the *interface of dendrites, at gas porosity and at impurities*. Crack formation is affected by mechanical factor, metallurgical factors and especially inherent defects of the substrate material.

Crack classification:

According to the positions the crack occurs at we can describe three kinds of cracks: *clad coating cracks, interface-substrate cracks and overlap area cracks*.

Methods of eliminate and prevent cracks:

Optimise the chemical composition of the powder. Reduce impurities mixed in the powder, and enhance the obdurability of the alloy powder. On the other hand the substrate should be without any defects and without residual stress. In addition control the laser parameters, use pre-heating and heat preservation, use an intermediate layer, the re-melting method and consider the thermal capacity of the substrate.

Chapter 8

Conclusions and recommendations

8.1 Conclusions

The purpose of this work was to study and investigate laser cladding surface treatment technology for the enhancement of mechanical properties including micro-hardness and wear-resistance.

The study mainly included: design of the composition of the cladding materials, the choice of the sticking agent, finding the optimal laser processing parameters, and by means of an optical microscope, micro-hardness tester and wear-resistance testing machine, to analyse the shape of the cladding coating, the microstructure, the distribution of the micro-hardness, properties of wear-resistance, the integration of the interface between the cladding layer and substrate and the dilution of the alloying elements. The formation mechanism of crack behavior and preventive control methods were analysed. Some features in solidification process of pool under laser were also analysed.

The literature survey showed that laser cladding is predominantly performed by powder injection, because that method is more flexible and easier to control. The literature

survey also revealed that laser cladding is not a mature technique yet.

Laser cladding experiments were performed using a mixture of a Nickel base alloy powder and tungsten carbide powder on a mild steel substrate using the pre-placed powder method and powder injection method. It indicated that with a reasonable matching of the processing parameters a result can be obtained with no cracking, no gas porosity and clad layer with a good finish. Metallurgical bonding between the cladding layer and substrate material was realized.

The Finite Element Method for calculating the surface temperature distribution was used to help predict the temperature distribution of the laser cladding results. The composition of cladding materials was designed; the sticking agent was chosen for the pre-place powder method. Clad coatings were obtained by changing the processing parameters of the laser cladding, and a detailed study has been carried out.

The effect of laser parameter variation on clad geometry was studied. It was found that, on the condition that other laser parameters remain unchanged, the clad height, clad width, clad depth and dilution rate are a function of the laser scanning speed. The clad height increases with the laser scanning speed, but in contrast the clad width, clad depth and dilution rate decrease.

It was also found that the clad height, clad width, clad depth and dilution rate are a function of the laser power. The clad width, clad depth and dilution rate increase with the laser power, but the clad height in contrast decreases.

Similarly, the clad height, clad width, clad depth and dilution rate are a function of the laser beam diameter. The clad height and clad width increase with the laser beam diameter, but in contrast, the clad depth and dilution rate decrease.

During the laser cladding process, the laser scanning speed affects not only the size and shape of laser cladding coating but also greatly affects the microstructure and quality of the laser cladding coating. With constant laser power, too low or too high a scanning speed will cause different degrees of cracks. Only under the suitable scanning speed will the required metallurgical compounds between the coating and substrate be realized.

The author also found that the laser beam diameter affects not only the size of the cladding layer, but it also has an obvious effect on the microstructure. Assuming all the other parameters remain unchanged, with an increase in laser beam diameter, the crystal grains become finer and smoother. The microstructure mainly consists of dendrites and cellular pine-trees crystal. With a decrease of the laser beam spot diameter, the crystal grains become coarser. In this case their microstructure mainly consists of cellular crystal or a small quantity of cellular shape dendrite crystal.

The results show that microstructure of clad layers comprise three zones: the cladding layer, bonding zone and heat-affected zone. The results showed that tungsten carbide particles increased the hardness and wear resistance. The wear resistance of the laser cladding coating is 3.5 times than that of substrate. The micro-hardness range of the cladding layer is from HV 981.5 to HV 1187, which is 2-3 times than that of substrate. The micro-hardness value from the cladding coating to the transition layer then to the substrate follows a gradient. The gradient distribution of the micro-hardness near the bonding interface improves the matching between the coating and the substrate, releasing stress concentrations and avoiding the formation of cracks while realizing a better metallurgical bonding between the coating and substrate.

The study and investigation of the solidification features and the formation law of the microstructure for the laser cladding layer has been carried out. This showed that there are different solidification parameters for different positions in the cladding layer. The microstructure at the bottom of the cladding was the typical extension growth on a plane. The microstructure at the top and middle was the regular pine-tree eutectic crystal and small cell and column crystal respectively. And the crystalline anisotropy was a main factor in influencing the form of crystal growth.

Cracks: According to the appearance and positions we identify three types, clad coating cracks; interface-substrate cracks and overlap area cracks

The effect of laser scanning speed on cracks: There is an optimal scanning speed for the prevention of cracking. A very high scanning speed will cause serious cracking between the cladding layer and substrate. A moderate scanning speed will produce fine metallurgical compounds between the cladding layer and substrate and no cracks and gas porosity will exist in the coating.

Reasons for cracks: The formation of cracks in the clad layer is mainly caused by the thermal stress created by the high thermal gradient built up during the cooling stage and the difference between the thermal expansion coefficients. When the local tensile stress exceeds the intensity limit, a crack will occur. Cracks appear mostly are at the interface of dendrites, at gas porosity, at impurities and other areas of weakness. Cracks are affected by stress, metallurgy and the condition of the substrate.

Crack prevention methods: Increasing of the laser power density, and the decreasing of the scanning speed helps to prevent cracks. The higher power and slower scanning speed helps the powder layer to adequately melt and prolongs the life of the melt pool allowing impurities to float up to the surface so that the cladding layer and substrate combines well. We can also use re-melting to remove surface cracks and improve the uniformity of the microstructure.

8.2 Recommendations for future work

Laser cladding technology is a new surface strengthening and surface modification technology, which has only existed for decades. Compared to other surface technologies, this technology can yield superior properties such as purity, homogeneity, hardness, superior bonding and microstructure. Laser cladding is also considered as a strategic technology. But laser cladding technology is not a mature technique yet. The present application fields of laser cladding technology are still limited and conservative indicating a great need for further research work.

The rapid solidification theory and research on the structure of the interface needs to still be developed. More cladding materials need to be developed to satisfy various requests. Research applications of rare-earth elements in the laser cladding field need to be developed because rare-earth elements can improve the performance of the metal materials.

To realize the large-scale industrial application of laser cladding technology, an intelligent control system will be required. Quality monitoring and defect control is one of the most important issues of laser cladding that still needs to be developed.

References

1. Abbas G West D R F. wear. 1991, 143 (3): 353-363.
2. Abbas, G., West, D.R.F., 1989, Laser Produced Composite Metal Cladding, High Power Lasers and Laser Machining Technology, Proc. SPIE, vol. 1132, pp. 232-236.
3. Abboud J.H. Journal of Materials Science Letters, 1992,11(18):1322-1326.
4. Arlt, A.G., Muller, R., 1994, Technology for Wear Resistant Inside Diameter Cladding of Tubes, Proc. ECLAT '94, pp. 203-212.
5. Atamert, S., Bhadeshia, H.K.D.H., 1989, Comparison of the Microstructures and Abrasive Wear Properties of Stellite hardfacing Alloys Deposited by Arc Welding and Laser Cladding, Metall. Trans. A, vol. 20A, no. 6, pp. 1037-1054.
6. Ayers J.D., Abrasive wear with fine diamond particles of carbide-containing aluminum and Titanium alloy surface, wear, 1984,93.
7. Ayers J.D., Modification of metal surface by the laser-melt particle injection process, Thin Solid film, 1981,84.
8. Amende, W., Nowak, G., 1990, Hard Phase Particles in Laser Processed Cobalt Rich Claddings, Proc. ECLAT '90, pp. 417-428.
9. Ariely S, Bamberger M,Hogel H et al. J Mater Science, 1995; 30:1849
10. Bathe K J, 1982, Finite Element Procedures in Engineering Analysis. Prentice-Hall, Inc., Englewood Cliffs, New Jersey. 415-418.
11. Blake, A.G., Eboo, G.M., 1985, Laser Hardfacing Turbine Blades Using Dynamic Powder Feed, Laser Welding and Surface Treatment.
12. Boas M, Bamberger M, Revez G Surf. Coat. Technol. 1990, 42:175-186.
13. Bos, Moes, H., 1993, Frictional Heating of Elliptic Contacts, Proc. of the 20th Leeds-Lyon Symposium on Tribology, Lyon.
14. Brenner, B. Reitzenstein, W., 1996, Laser Hardening of Turbine Blades, Industrial Laser Review, April, pp. 17-20.
15. Bruck, G.J., 1987, High Power Laser Beam Cladding, J. of Metals, vol. 39, no. 2, pp. 10-13.
16. Brandt, A., 1984, Multigrid Techniques: 1984 Guide with Applications to Fluid Dynamics, GMD-studien, No. 85.
17. Choi, J., Mazumder, J., 1994, Non-equilibrium Synthesis of Fe- Cr-C-W Alloy by Laser Cladding, J. of Materials Science, vol. 29, pp. 4460-4476.
18. Chen, X., Tao, Z., 1989, Maximum Thickness of the Laser Cladding, Key Engineering Materials vols 46 & 47, pp. 381-386.
19. Cai, G., Molino, G., 1990, Comparison Between Cladding by Means of Plasma Spray and the More Recent Technologies of Plasma Transferred Arc, Plasma

- Semi-Transferred Arc and Laser on Traditional Filler Material and New Nickel Base Boron-Free Alloys, Proc. Laser-6, pp. 79-90.
20. Carslaw, H.C., Jaeger, J.C., 1959, Conduction of Heat in Solids, Oxford University Press.
 21. Chen J.C. International Journal of heat and Mass Transfer, 1991, 34(3):663-674.
 22. Cooper, K.C., Slebodnick, P., 1989, Recent Developments in Laser Melt/Particle Injection Processing, J. of Laser Applications, October 1989, pp. 21-30.
 23. De Hosson, J.Th.M., 1995, Fundamental and Applied Aspects of Laser Processed Ceramic Coatings of Metals, Proc. Surface Treatment 95, pp. 1-15.
 24. De Hosson, J.Th.M., Mol van Otterloo, L. de, 1996, Microstructural Features of Laser Coatings, Proc. ECLAT '96, pp. 337-348.
 25. Du Ting, Physical and chemistry effect of rare-earth element in metal materials. The Chinese Journal of Nonferrous Metals, 1997, 33 (1): 69-77.
 26. Ding Peidao, Liu Jianglong, Shi Gongqi, Solidification features of melt pool surface with laser. Chemical industry publishing company, June, 1995.
 27. Eiholzer, E., Cusano, C., Mazumder, J., 1985, Wear Properties of Laser Alloyed and Clad Fe-Cr-Mn-C Alloys, Proc. ICALEO'84, pp. 159-167.
 28. Engstrom, H., et al., 1988, Combined Corrosion and Wear Resistance of Laser-Clad Stellite 6B, Proc. ECLAT '88, pp. 164-168.
 29. Elshof, H.L.F., 1994, Heat Fluxes Between Semi-Infinite Solids, Un. of Twente, Graduate Thesis, Dept. of Mech. Eng.
 30. Ellis, M., et al., 1995, Processing Aspects of Laser Cladding an Aluminum Alloy onto Steel, J. of Materials Processing Technology, vol. 52, pp. 55-67.
 31. Fishman, M., Sherbaum, N., Zahavi, J., 1995, Laser Cladding and Alloying for Refurbishing Worn Machine Parts and Improving their Surface Properties, SPIE, vol. 2426, pp. 181-188.
 32. Fouquet, F., et al., 1993, Microstructural and Electrochemical Characterization of Laser Deposited 18-10 Austenitic Stainless Steel Clad Layers, J. de Physique IV, Colloque C7, pp. 991-995.
 33. Fu Geyan, Laser Cladding Sealing Face of In-outlet Valve Part in Methylamine Pump, Heat Treatment of Metals, 2000, Vol.01.
 34. Fouquet, F., et al., 1994, Austenitic Stainless Steels Layers Deposited by Laser Cladding on a Mild Steel: Realization and Characterization, J. de Physique IV, Colloque C4, pp. 89-92.
 35. Gasser, A., et al., 1996, Oberflächenbehandlung mit Zusatzwerkstoffen, Proc. ECLAT '96, pp. 287-298.
 36. Gassmann, R., et al., 1992, Laser Cladding of Hard Particles Rich Alloy, Proc. ICALEO '92, pp. 288-300.
 37. Grunenwald, B., et al., 1992, Laser Surface Alloying of Case Hardening Steel with Tungsten Carbide and Carbon, Materials Science and Technology, July 1992, vol. 8, pp. 637-643.
 38. Grunenwald, B., et al., 1996, Laserbeschichten mit CO₂- und Nd:YAG-Lasern, Proc. ECLAT '96, pp. 299-306.
 39. Gnanamuthu, D.S., Laser surface treatment. [C]. Application of Laser in

- Materials Processing, ASM, 1979.177-211.
40. Hegge, H.J., Boetje, J., De Hosson, J.Th.M., 1990, Oxidation Effects During Laser Cladding of Aluminium With SiC/Al Powders, *J. of Materials Science*, vol. 25, no. 5, pp. 2335-2338.
 41. He. Guanhu, 1987,3, Physics properties of metal materials and measure method, Beijing, Metallurgy Industry publishing company, pp.58-62.
 42. Hu C, Barnard L, Mridha S. et al. *J Mater Processing Tech*, 1996; 58:87.
 43. Huang, C.-C., Tsai, W.-T., Lee, J.-T., 1995, Microstructure and Electrochemical Behavior of Laser Cladded Fe-Cr-Mo-Si-N Surface Alloys on Carbon Steel, *Materials Science and Engineering*, vol. A 196, pp. 243-248.
 44. Jiang Yongqiu, 1993, Rupture of coating materials. *Chinese journal of materials research*.26, (1), 73-79.
 45. Jasim, K.M., West, D.R.F., 1989, Laser Cladding of Carbon Steel with a Ceramic Metallic Composite, *High Power Lasers and Laser Machining Technology*, Proc. SPIE, vol. 1132, pp. 237-245.
 46. Jasim, K.M., Rawlings, R.D., West, D.R.F., 1993, Metal-Ceramic Functionally Gradient Material Produced by Laser Processing, *J. of Materials Science*, vol. 28, pp. 2820-2826.
 47. Kar, A., Mazumder, J., 1988, One-Dimensional Finite-Medium Diffusion Model for Extended Solid Solution in Laser Cladding of Hf on Nickel, *Acta Metall.*, vol. 36, no. 3, pp. 701-712.
 48. Kar, A., Mazumder, J., 1989, Extended Solid Solution and Nonequilibrium Phase Diagram for Ni-Al Alloy Formed During Laser Cladding, *Metall. Trans. A*, vol. 20A, pp. 363-371.
 49. Komvopoulos, K., Nagarathnam, K., 1990, Processing and Characterization of Laser-Cladded Coating Materials, *J. of Engineering Materials and Technology*, vol. 112, pp. 131-143.
 50. Komvopoulos, K., 1994, Effect of Process Parameters on the Microstructure, Geometry and Microhardness of Laser-Clad Coating Materials, *Mat. Sci. Forum*, vols. 163-165, pp. 417-422.
 51. Konig, W., et al., 1989, Surface Treatment with the Laser Beam: A Discussion of Various Machining Methods, *Annual Industrial Laser Handbook 1989*, pp. 117-121.
 52. Kreutz, E.W., et al., 1995, Rapid Prototyping with CO₂ Laser Radiation, *Applied Surface Science*, 86, pp. 310-315.
 53. Komvopoulos, K., Nagarathnam, K., 1990, Processing and Characterization of Laser-Cladded Coating Materials, *Journal of Engineering Materials and Technology*, vol. 112, pp. 131-143.
 54. Kurz W, Fisher J. *Fundamentals of Solidification*. Aedermannsdors, Switzerland: Transations Technical Publications, 1989: 67.
 55. Kupper, F., et al., 1990, Cladding of Valves with CO₂ Laser Radiation, *Proc. ECLAT '90*, pp. 461-468.
 56. Lubrecht, A.A., Ioannides, E., 1989, A Fast Solution of the Dry Contact Problem and the Associated Sub-Surface Stress Field, *J. of Tribology*, vol. 113, pp.

- 128-133.
57. Li, Y., Steen, W.M., 1992, Laser Cladding of Stellite and Silicon on Aluminum Substrate, Proc. ICLOE '92, SPIE, vol. 1979, pp. 602- 608.
 58. Leach P W. Journal of Materials science letters. 1992,11(16): 1131-1123.
 59. Liu Qibing, Microstructure characteristics of bonding interface of cast WC_p /Ni based alloy composite coating by wide-band laser cladding, Laser technology, 2002, Vol.26. No.3.
 60. Li Qiang, Lei Tingquan et al. Chinese Journal of Lasers. 1999, 26 (1): 80-84.
 61. Liu, Y., Mazumder, J., Shibata, K., 1992, Laser Cladding of Ni-Al Bronze on Cast Al Alloy AA333, Proc. ECLAT '92, pp. 381-386.
 62. Li Guohua, Study on Slurry Abrasive Characteristics of Laser Cladding Coating and Its Application, Journal of Iron and Steel Research, 1999, Vol. 05.
 63. Lugscheider E. Surface engineering 1991, 7(4):341-344.
 64. Li Biwen, Shi Shihong, Wang Xinlin. Quality Control on Laser Cladding Chemical Industry Valve. Hot Working Technology. 2000.1.
 65. Liu, Y., et al., 1994, Processing, Microstructure, and Properties of Laser-Clad Ni Alloy FP-5 on Al Alloy AA333, Metallurgical and Mat. Trans. B, vol. 25B, pp. 425-434.
 66. Li Chunhua, Effect of Laser Cladding Technology on Quality of Cladding Layer on Exhaust Valve Surface, Heat Treatment of Metals, 2000, Vol.7.
 67. Li Hengde, Xiao Jimei, Surface and interface of Material, Beijing, Tsinghua University Publishing Company, 1990, June. pp. 28-32.
 68. Li, J., Yuan, L., 1994, Mathematical Method for Optimizing the Process of Heat Treatment with Powerful Lasers, Lasers in Engineering, vol. 2, pp. 239-245.
 69. Lang, A., Waldmann, H., Bergmann, H.W., 1994, Cladding of Metallic Substrates with Diamonds and Cubic Boron Nitride, Proc. ECLAT '94, pp. 456-460.
 70. Liu Renqing, Cellulose Chemistry Fundamental, Science and Technology publishing company, Beijing, September 1985, pp.85-88.
 71. Li Biwen, Shi Shihong, Wang Xinling, Quality Control on Laser Cladding Chemical Industry Valve, Hot Working Technology. 2000,1.
 72. Liu Ximing, Lian Jianshe, A study on the factors influencing the effective utility rate of cladding heat and coating material in powder feeding type laser cladding. China Surface Engineering, 2000, 13,3,
 73. Molian, P.A., 1988, Principles and Applications of Lasers for Wear-Resistant Coatings, 1st International Conference on Surface Modification Technology, pp. 237-265.
 74. Monson, P.J.E., Steen, W.M., 1990, Comparison of Laser Hardfacing with Conventional Processes, Surface Engineering, vol. 6, no. 3, pp. 185-193.
 75. Marsden, C.F., et al., 1990, Characterisation of the Laser Cladding Process, Proc. ECLAT '90, vol. 1, pp. 543-553.
 76. Nowotny, S., et al., 1994, Influences on the Wear Resistance of Carbide Laser Claddings, Proc. ECLAT '94, pp. 252-259.
 77. Nagarathnam, K, Komvopoulos K. Microstructural characterization and in suit

- transmission electron microscopy analysis of laser-processed and thermally treated Fe-Cr-W-C clad coatings [J]. *Metallurgical Transaction A*, 1993, 24A(7):1621-1629.
78. Nagarathnam, K; Komvopoulos, K, Microstructural and microhardness characteristics of laser-synthesized Fe-Cr-W-C coatings,[J]. *Metallurgical and Materials Transaction A*, 1995, 26A(8):2131-2139.
 79. Oberlander, B.C., Lugscheider, E., 1992, Comparison of Properties of Coatings Produced by Laser Cladding and Conventional Methods, *Materials Science and Technology*, vol. 8, pp. 657-665.
 80. Oberlander, B.C., Lugscheider, E., 1992, Comparison of Properties of Coatings Produced by Laser Cladding and Conventional Methods, *Materials Science and Technology*, vol. 8, pp. 657-665.
 81. Pei, Yutao, et al., 1995, Microstructure of Laser Cladding SiC-Ni Alloy Composite Coating, *Mat. Sci. and Eng. A*, vol. A194, pp. 219-224.
 82. Pei, Y.T., Ouyang, J.H., Lei, T.C., 1996, Microstructure of Bonding Zones in Laser-Clad Ni-Alloy-Based Composite Coatings Reinforced with Various Ceramic Powders, *Metall. and Mat. Trans. A*, vol. 27A, pp. 391-400.
 83. Pei Yutao, Ouyang Jiahu, Lei Tingquan, Research on Laser Cladding Complex Coating, *Journal of Harbin Institute of Technology*. 1994 (2): 73-79.
 84. Powell, J., Steen, W.M., 1981, Vibro Laser Cladding, *Proc. Lasers in Metallurgy*, pp. 93-104.
 85. Ready, J.F., 1971, *Effects of High Power Laser Radiation*, Academic Press, New York.
 86. Pelletier, J.M., Sallamand, P., Criqui, B., 1994, Microstructure and Mechanical Properties of Some Metal Matrix Composites Produced on Different Materials by Laser Cladding, *Lasers in Engineering*, vol. 3, pp. 15-27.
 87. Pelletier, J.M., et al., 1996, Hadfield Steel Layers Manufactured by Laser Cladding: Mechanical and Tribological Properties, *Proc. ECLAT '96*, pp. 329-336.
 88. Shafristien G *Surface and coating Technology*, 1991,45(1-3):417-423.
 89. Shi shihong, *The Application of Laser Cladding Technology on Valve Parts*, [J] *China Mechanical Engineering*.1999 (5).
 90. Steen, W.M., 1987, *Surface Engineering with Lasers*, *Applied Laser Tooling*, pp. 131-181.
 91. Shi shihong, *The Application of Laser Cladding Technology on Valve Parts*, [Journal] *China Mechanical Engineering*.1999 (5).
 92. Steen, W.M., et al., 1992, *Alloy System Analysis by Laser Cladding*, *Proc. ICALEO '92*, pp. 278-288.
 93. Singh, J., Mazumder, J., 1985, Microstructure and Wear Properties of Laser Clad Fe-Cr-Mn-C-alloys, *Proc. ICALEO '85*, pp. 179-185.
 94. Singh, J., Mazumder, J., 1987, Microstructure and Wear Properties of Laser Clad Fe-Cr-Mn-C Alloys, *Metall. Trans. A*, vol. 18A, pp. 313-322.
 95. Tan Wen, et al., *Research on Laser Cladding Fe-C-Si-B, Heat Treatment of Metals*, 2000, Vol.01.

96. Venner, C.H., 1991, Multilevel Solutions of the EHL Line and Point Contact Problems, Ph.D. Thesis, Enschede.
97. VandeHaar, et al., 1988, Effect of Process Variables on the Laser Cladding of Zirconia, Proc. ICALEO '87, pp. 189-193.
98. Wu Weiwen, et al. Laser cladding ceramic coating, Inorganic material transaction, 1994, 9(2).
99. Wolf, S., et al., 1994, Laserstrahlbeschichten nach der Einstufigen Prozeßführung am Beispiel "Beschichten von Gußeisen", Laser und Optoelektronik, vol. 26, no. 4, pp. 63-68.
100. Wolf, S., Volz, R., 1995, Einsatz des Laserstrahlbeschichtens beim Bau von Kunststoffverarbeitungsmaschinen, Laser und Optoelektronik, vol. 27, no. 2, pp. 47-53.
101. Wang Liuying, Wang Hangong, et al. Effect of Processing Parameters on Microstructure of Ni-Cr-B-Si coating by laser cladding on aluminum alloy surface. Heat treatment of material, No.7, 1999.
102. Wang Kun-lin, Zhang Qing-bo, Wei Xing-guo. Rare earth La_2O_3 modification of laser cladding coatings, Journal of Materials Science, 1998, Vol.,33, 3573-3577.
103. Wang Kun-lin, Zhang Qing-bo, Wei Xing-guo, Zhu Yunming, Effect of La_2O_3 on the microstructure and wear resistance of laser clad nickel-based alloy coatings, Journal of Tsinghua University Science And Technology, Vol.39 No.8 1999.
104. Wang, A.A., Sircar, S., Mazumder, J., 1990, Laser Cladding of Mg-Al Alloys, Proc. ICALEO '90, vol. 71, pp. 502-512.
105. Weerasinghe V. M. and steen W.M., Laser cladding with pneumatic power delivery, Pro.4 the.int. Conf, laser in material processing, ASM, Metals Park, Ohio, USA, 1983.
106. Wang, A.A., Sircar, S., Mazumder, J., 1993, Laser Cladding of Mg-Al Alloys, J. of Materials Science, vol. 28, pp. 5113-5122.
107. Wang Jiajin, Laser machining technology, China metrology publishing company. 1992, 11 pp. 274-279.
108. Webber, T., 1987, Advances in the Applications of Laser Cladding of Multi-Dimensional Part Geometries, Lasers in Motion for Industrial Applications, vol. 744, pp. 137-143.
109. Wang Kunlin et al. Effect of La_2O_3 on the microstructure and wear resistance of laser clad nickel-based alloy coatings, Journal of Tsinghua University Science and Technology. Vol.39, No. 8, 1999.
110. Wu Xinwei, Ceng Xiaoyan, et al. Laser cladding ceramic technology research. Heat Treatment of Metals, 1996, Vol.4, 40-44.
111. Wu Xiaolei, Cheng Guangnan, Metal transaction 1998, Vol.10, 1033-1038.
112. Yan Yuhe, Zhong Mingling, High-power laser machining and application, Tianjing science and technology publishing company, 1994, pp.112-167.
113. Yang, X.C., et al., 1988, Microstructure and Performance of Laser Cladding NiCrSiB Alloy, Proc. ICALEO '87, pp. 209-220.
114. Yang, X.-C., Zhen, T.-X., Zhang, N.-K., 1990, Laser Cladding of WC-Co Powder, Proc. ICALEO '90, pp. 520-524.

115. Yang, X.-C., Zheng, T.-X., Zhang, N.-K., 1991, Research on Convection and Mass Transport in Laser Cladding: FeCrSiB Alloy, Proc. ICALEO '91, pp. 445-452.
116. Zha Ying, et al. Study of Improvement of Properties of Laser Cladding Ni Super alloy and WC Composite Layers. China laser, 1999, Vol. 10.
117. Zhang Chunliang, Study on Process of Laser Cladded Nuclear Valve Parts, Nuclear power engineering, 2000, 21, 3.
118. Zhang Guangjun, Status and Development of Laser Heat Treating in China, Heat Treatment of Metals, 2000, Vol. 1.
119. Zhang Wenyue, Metal Fusion Welding Theory and Technology. [M]. Beijing: Engineering Industry Publishing Company. 1984: 105-108.
120. Zhang, N., Ekambaranathan, G., Willemse, P.F., 1994, Residual Stresses and Cracking in a Laser-Deposited Co-Cr-Ni-Mo Alloy on Steel, Proc. LANE '94, pp. 317-324.
121. Zhang Wenyue, Metal fusion welding theory and technology, [M] Beijing, Engineering Industry Publishing Company. 1984:105-108.
122. Zhu, B., et al., 1993, Coarse Cemented WC Particle Ceramic- Metal Composite Coatings Produced by Laser Cladding, Wear, vol. 170, pp. 161-166.
123. Zhou, X.B., De Hosson, J.Th.M., 1991, Dependence of Surface Residual Stress on Laser Power and Laser Scan Velocity, Scripta Metall. et Mat, vol. 25, pp. 2007-2010.
124. Zhang Guangjun, Status and Development of Laser Heat Treating in China. Heat Treatment of Metals, 2000, Vol. 1.

Appendix 1

Literature of Substrate and cladding materials

Ferrous Substrate		
Cladding materials	Substrate Materials	Information Source
AISI 304, 316	Low carbon steel	Fouquet, 1994
Al-Mn-Fe, Al-Co-Fe, Ni-Co-Fe	Mild steel EN 1A	Steen, 1992
AISI 316	Mild steel EN 3B	Weerasinghe, 1983
Alloy 4815+SiC, Alloy 4815	Mild steel EN 3B	Abbas, 1989
Al-Sn10Si4Cu1 with Ni sandwich	Mild steel EN 3B	Ellis, 1995
Stellite 6	Mild steel EN 3B	Abbas, 1989, 1991
Stellite 6 and SiC mixture	Mild steel EN 3B	Abbas, 1991
AISI 304	Mild steel	Fouquet, 1993
Triballoy T-800	Mild steel	Amende, 1990

Ni-Cr-B-Si, CoC+WC	Mild steel	Oberlander, 1992
Ni-Cr-B-Si	Mild steel ST 37	Sepold, 1989
Stellite 157, F, 6, deloro 40, 22	C40 and C45	Gassmann, 1992
Nicrobor 40, deloro 60	C40 and C45	Brenner, 1996
Stellite 6	C40 and C45	Kreutz, 1995
Hadfield steel	C15/C20/C22	Pelletier, 1996
ZrO ₂ + 8%Y ₂ O ₃ + AISI 316,	C15/C20/C22	Jasim, 1989
Cr-Mn-C, Fe-Cr-Mn-C	AISI 1016	Singh, 1985
Ni-Cr-Al-Hf	AISI 1016	Singh, 1987
Fe-Cr-C-W	AISI 1016	Choi, 1994
Fe-Cr-Mn-C	AISI 1016	Eiholzer, 1985
Nichrome	AISI 1020	Ayers, 1981
Ni-Cr- B - Si	AISI 1020	Yang, 1988
WC and Co	AISI 1020	Yang, 1990
Fe-Cr- B - Si	AISI 1020	Yang, 1991
Fe-Cr-Mn-C, Fe-Cr-C-W	AISI 1020	Komvopoulos, 1994
Fe-Cr-Mo, Fe-Cr-Si ₃ N ₄ , Fe-Cr-Mo-Si ₃ N ₄	AISI 1020	Huang, 1995
Cr ₂ O ₃ and Fe powder	AISI 304	Zhou, 1991
Stellite F, SF6	AISI 304	Giordano
Stellite 6	AISI 316	Bruck, 1988
Stellite F, SF6, 1, 6, CTS 10136	AISI 316	Magrini, 1986
Stellite 6	AISI 410	Liu, 1983
SiC and Ni	AISI 1043/1045	Pei, 1995
Ni-Cr-B-Si +SiC, Ni-Cr-B-Si+TiN	AISI 1043/1045	Pei, 1996
Stellite 6	AISI 1008	Pizurova, 1993
Ni-Cr-B-Si+ZrO ₂	4Cr13 stainless steel	Pei, 1996
Ni-Cr-Fe-Si-B-C and WC	20Ni4Mo steel	Zhu, 1993
Stellite 6, F	X45CrSi9	Kupper, 1990
Cu and Ni	Carbon steel	Bruck, 1987
Ni-Cr-Si-B	0.16C 1.2Mn steel	Chen, 1989
Cr ₂ O ₃ and Fe	SAF 2205	Zhou, 1991

SAE 4340	Co-base alloy	Fishman, 1995
Stellite 1, 6	GGG40 cast iron	Wolf, 1994
Ni-base alloy	GGG40 cast iron	Gasser, 1996
Non-Ferrous Substrate		
Cladding materials	Substrate Materials	Information Source
Al+SiC	Al-base	Hegge, 1990
Stellite 6, and Si	AlCu4SiMg (H15)	Li, 1992
Ni-Al bronze (Cu-Al-Ni-Fe)	Al 333	Liu, 1992
TiC	5052 Al	Ayers, 1981
Al+SiC	Inconel 625	Jasim, 1993
Triballoy T-400	Inconel 625	Cooper, 1989
WC/Co	Nicrobor 20	Gassmann, 1992
Al+SiO ₂	Al 6061	De Hosson, 1995
Triballoy T- 400	Ti-6Al-4V	Lang, 1994
Mg-Zr, Mg-Al	Mg-base	Wang, 1990
Mg-Al	Mg-base	Wang, 1993
Ni-base alloy	Cu-Zn-Pb (brass)	Pelletier, 1994
Al	Ni	Kar, 1989
Fe-Cr-P-C	Ni	Marsden, 1990
CuAl-bronze	AlSi12	Grunenwald, 1996

Appendix 2
Performed Pre-placed Powder Experiments Process

Powder Components	Sample Number	Laser Power [kW]	Scanning Speed [m/min]	Beam Spot Diameter D [mm]	Pre-place Thickness T_p [mm]
Sample 1 Series 70%Ni alloy + 30% WC	1-1	1.0 kW	0.1	2.5mm	Powder thickness 0.6mm
	1-2		0.12		
	1-3		0.15		
	1-4		0.18		
	1-5		0.2		
Sample 2 Series 70%Ni alloy + 30% WC	2-1	1.2 kW	0.2	2.5mm	0.6mm
	2-2		0.4		
	2-3		0.6		
	2-4		0.8		
	2-5		1.0		
Sample 3 Series 70%Ni alloy + 30% WC	3-1	1.3 kW	0.2	2.5mm	0.6mm
	3-2		0.4		
	3-3		0.6		
	3-4	1.0 kW	0.2	2.5mm	0.6mm
	3-5		0.1		

Sample 4 Series 70%Ni alloy + 30% WC	4-1	1.5 kW	0.2	2.5mm	0.6mm
	4-2		0.3		
	4-3		0.4		
	4-4		0.5		
	4-5		0.6		
Sample 5 Series 70%Ni alloy + 30% WC	5-1	1.8 kW	0.2	2.5mm	0.6mm
	5-2		0.4		
	5-3		0.6		
	5-4		0.8		
	5-5		1.0		
Sample 6 Series 90%Ni alloy + 10% WC	6-1	1.0 kW	0.1	2.5mm	0.6mm
	6-2		0.12		
	6-3		0.15		
	6-4		0.18		
	6-5		0.2		
Sample 7 Series 90%Ni alloy + 10% WC	7-1	1.2 kW	0.1	2.5mm	0.6mm
	7-2		0.12		
	7-3		0.15		
	7-4		0.18		
	7-5		0.2		
Sample 8 Series 60%Ni alloy + 40% WC	8-1	1.0 kW	0.1	2.5mm	0.6mm
	8-2		0.12		
	8-3		0.15		
	8-4		0.18		
	8-5		0.2		
Sample 9 Series 60%Ni alloy + 40% WC	9-1	1.2 kW	0.1	2.5mm	0.6mm
	9-2		0.12		
	9-3		0.15		
	9-4		0.18		
	9-5		0.2		
Sample 10 Series 80%Ni alloy + 20% WC	10-1	1.0 kW	0.1	2.5mm	0.6mm
	10-2		0.12		
	10-3		0.15		
	10-4		0.18		
	10-5		0.2		
Sample 11 Series 80%Ni alloy + 20% WC	11-1	1.2 kW	0.1	2.5mm	0.6mm
	11-2		0.12		
	11-3		0.15		
	11-4		0.18		
	11-5		0.2		
Sample 12 Series	12-1			1.5	
	12-2			2.0	

80%Ni alloy + 20% WC	12-3	1.0 kW	0.15	2.5	0.6mm
	12-4			3.0	
	12-5			3.5	
Sample 13 Series 60%Ni alloy + 40% WC	13-1	1.2 kW	0.15	1.5	Powder thickness 0.6mm
	13-2			2.0	
	13-3			2.5	
	13-4			3.0	
	13-5			3.5	
Sample 14 60%Ni alloy + 40% WC	Several adjacent tracks	1.2 kW	0.15	3.0mm	Powder thickness 0.6mm Step over 3mm
Sample 15 60%Ni alloy + 40% WC	Several adjacent tracks	1.3 kW	0.15	3.0mm	Thickness 0.6mm Step over 3mm
Sample 16 60%Ni alloy + 40% WC	Several adjacent tracks	1.0 kW	0.15	3.0mm	Thickness 0.7mm Step over 2.5 mm
Sample 17 60%Ni alloy + 40% WC	Several adjacent tracks	1.0 kW	0.13	D=3.0mm	Thickness 0.7mm Step over 2.5 mm
Sample 18 70%Ni alloy + 30% WC	Several adjacent tracks	1.0 kW	0.13	3.0mm	Thickness 0.7mm Step over 2.5 mm
Sample 19 70%Ni alloy + 30% WC Vertically Remelt with Initial-line	Several adjacent tracks,	Initial 1.0 kW	Initial 0.13	Initial 3.0	Initial Step over 2.5
		Remelt 1.0 kW	Remelt 0.2	Remelt 2.5	Remelt Step over 2.0 Thickness 0.7
Sample 20 70%Ni alloy + 30% WC	Several adjacent tracks	1.0 kW	0.3	2.5mm	Thickness 0.7mm Step over 2.0 mm
Sample 21 70%Ni alloy + 30% WC	Several adjacent tracks	1.0 kW	0.2	2.5mm	Thickness 0.7mm Step over 2.0 mm

Sample 22 70%Ni alloy + 30% WC	Several adjacent tracks	1.0 kW	0.2	2.5mm	Clad track were homocentric Rectangle, Step over 2.0 mm
Sample 23 70%Ni alloy + 30% WC	Several adjacent tracks Remelt	1.0 kW Remelt same as Initial	0.2 Remelt same as Initial	2.5mm Remelt same as Initial	Clad and Remelt track were homocentric Rectangle, Step over 2.0 mm
Sample 24 70%Ni alloy + 30% WC	Several adjacent tracks Remelt	Initial 1.0 kW	Initial 0.13	Initial 3.0	Initial Step over 2.5
		Remelt 1.0 kW	Remelt 0.2	Remelt 2.5	Remelt Step over 2.0

Appendix 3

Geometrical Properties of single Track Samples (Pre-placed Powder Method)

Sample Number	Clad Width (W_c)	Total clad height (T_c)	Clad Height (H_c)	Clad depth (D_c) $D_c = T_c - H_c$	Geometrical Dilution	Special Energy $E = P/DV$	
	[mm]	[mm]	[mm]	[mm]	[%]	[Jm^{-2}]	
2	2-1	2.56	0.66	0.51	0.15	22.7	144
	2-2	2.53	0.61	0.54	0.07	11.5	72
	2-3	2.54	0.65	0.6	0.05	7.7	48
	2-4	2.50	0.66	0.61	0.05	7.6	36
	2-5	2.45	0.69	0.65	0.04	5.8	28.8
3	3-1	2.60	0.67	0.50	0.17	25.3	156
	3-2	2.57	0.57	0.52	0.05	8.8	78
	3-3	2.55	0.61	0.56	0.05	8.2	52
	3-4	2.58	0.68	0.61	0.07	10.3	240
	3-5	2.60	0.8	0.6	0.2	25	120
	4-1	2.73	0.7	0.48	0.22	31.4	180

4	4-2	2.66	0.68	0.51	0.17	25	120
	4-3	2.66	-	-	-	-	90
	4-4	2.62	0.6	0.56	0.04	6.7	72
	4-5	2.6	0.61	0.58	0.03	4.9	60
5	5-1	2.76	0.68	0.45	0.23	33.8	216
	5-2	2.74	0.42	0.32	0.10	23.8	108
	5-3	-	-	-	-	-	72
	5-4	-	-	-	-	-	54
	5-5	2.7	0.58	0.55	0.03	5.5	43.2
6	6-1	2.6	0.88	0.8	0.08	9.1	240
	6-2	2.59	0.89	0.82	0.07	8	200
	6-3	2.57	0.91	0.85	0.06	7.1	160
	6-4	2.58	0.88	0.84	0.04	4.5	133.3
	6-5	2.52	0.91	0.87	0.04	4.0	120
7	7-1	2.63	0.88	0.79	0.09	10.2	288
	7-2	2.7	0.92	0.84	0.08	8.7	240
	7-3	2.74	0.75	0.69	0.06	8.0	192
	7-4	2.60	0.94	0.87	0.07	7.4	160
	7-5	2.57	0.95	0.89	0.05	5.3	144
8	8-1	2.63	0.6	0.52	0.08	13.3	240
	8-2	2.6	0.6	0.54	0.06	10	200
	8-3	2.6	0.62	0.58	0.04	6.5	160
	8-4	2.54	0.61	0.57	0.04	6.6	133.3
	8-5	2.51	0.64	0.61	0.03	4.7	120
9	9-1	2.64	0.63	0.50	0.13	21	288
	9-2	2.63	0.62	0.52	0.10	16.1	240
	9-3	2.63	0.63	0.55	0.08	12.7	192
	9-4	2.60	0.61	0.56	0.05	8.2	160
	9-5	2.52	0.64	0.6	0.04	6.3	144
10	10-1	2.55	0.53	0.4	0.13	24.5	240
	10-2	2.53	0.62	0.55	0.07	11.2	200
	10-3	2.54	0.57	0.53	0.04	7.01	160
	10-4	2.51	0.57	0.54	0.03	5.3	133.3
	10-5	2.5	0.62	0.59	0.03	4.8	120
11	11-1	2.58	0.45	0.38	0.07	15.6	288
	11-2	2.53	0.61	0.50	0.11	18	240
	11-3	2.54	0.57	0.54	0.03	5.3	192
	11-4	2.54	0.58	0.55	0.03	5.2	160
	11-5	2.52	0.63	0.60	0.03	4.8	144
12	12-1	1.58	0.67	0.55	0.12	17.9	266.7
	12-2	2.08	0.63	0.57	0.06	9.5	200
	12-3	2.52	0.63	0.58	0.05	7.01	160
	12-4	3.0	0.66	0.62	0.04	6.1	133.3

	12-5	3.52	0.65	0.62	0.03	4.6	114.3
13	13-1	1.59	0.67	0.5	0.17	25.4	320
	13-2	2.10	0.62	0.54	0.08	12.9	240
	13-3	2.53	0.67	0.59	0.08	11.9	192
	13-4	3.05	0.68	0.60	0.08	11.7	160
	13-5	3.54	0.71	0.61	0.1	14.08	137.1
21	-	-	0.61	0.48	0.13	21.3	240